The Mouse Nervous System

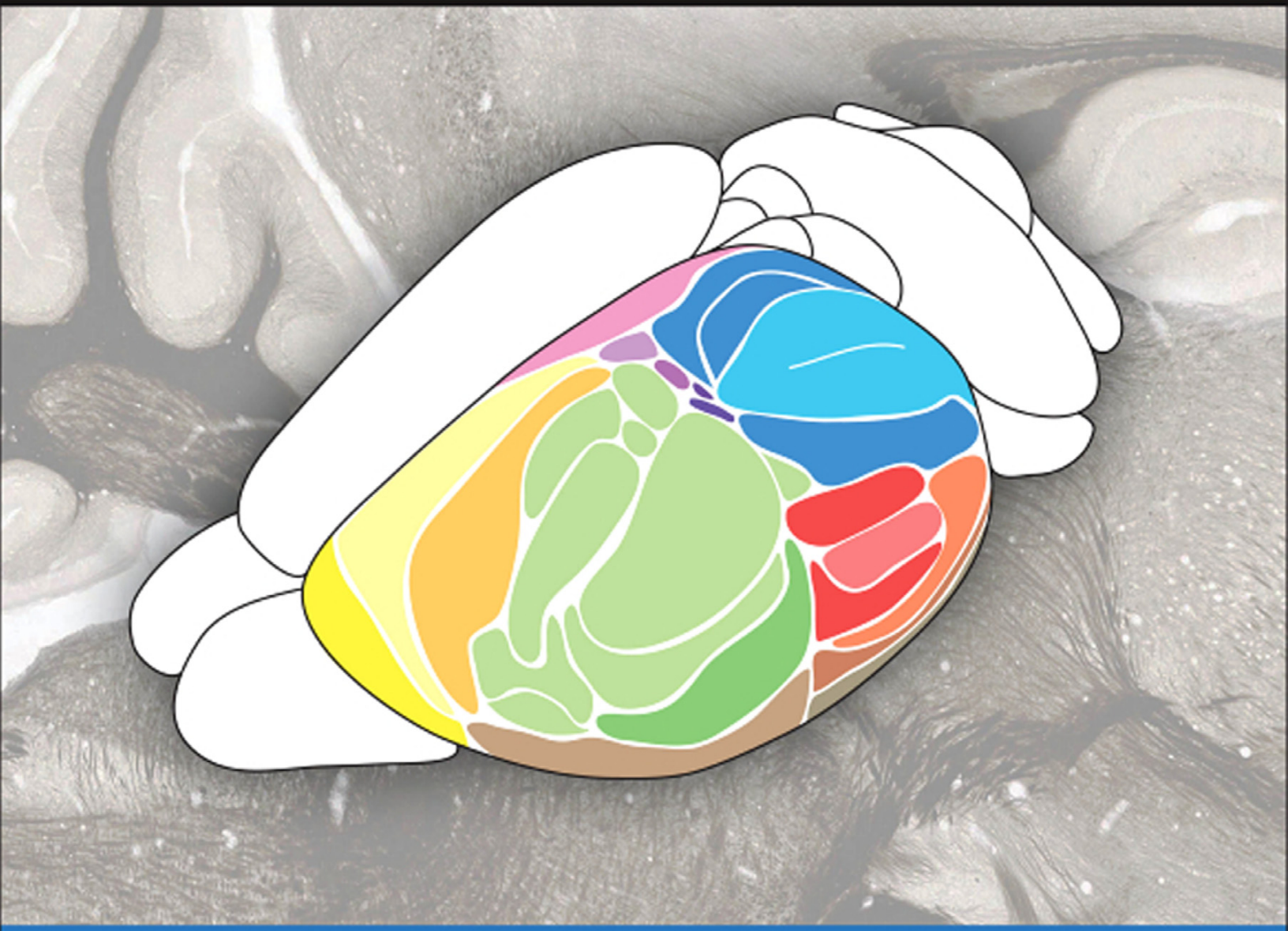

Edited by
Charles Watson • George Paxinos
Luis Puelles

CHAPTER

24

Auditory System

Manuel S. Malmierca[*], *David K. Ryugo*[†]

[*]Auditory Neurophysiology Unit, Institute for Neuroscience of Castilla y León, Salamanca, Spain and Faculty of Medicine, University of Salamanca, Salamanca, Spain, [†]The Garvan Institute of Medical Research, Darlinghurst, NSW, Australia

OUTLINE

INTRODUCTION

Advances in gene targeting have led to a renaissance in the use of the mouse as a model for investigation of human disease mechanisms. Until recently, the most commonly used experimental animal for auditory research and many other fields in neuroscience was the cat; other species used to a lesser extent include the rat, guinea pig, chinchilla, gerbil, and ferret. More than one hundred years ago, the mouse was used by Ramón y Cajal (1909; 1904) to study the neuroanatomy of the brain. The reason for this was two-fold; neurons in neonatal and juvenile mice could be well impregnated by the Golgi method and, perhaps more importantly, the small size of the mouse brain facilitated the study and tracing of axonal and dendritic processes more easily than the longer and more tortuous distances traveled in brains of larger mammals. Thus, Ramón y Cajal based many of his classical studies on the mouse brain. Special mention should also be made of Lorente de Nó, (1933; 1981), Cajal's final student, who made extensive use of the mouse in his

influential studies of the auditory nerve and cochlear nucleus.

The availability of strains of mice that carry specific genetic abnormalities affecting the brain, including the auditory system, has also proven useful to researchers. Mice are now widely used for producing gene-manipulated animal models (Willott et al., 2001). For example, the C57 strain of mice is a model for studying aging related, progressive, high-frequency, hearing loss (Mikaelian, 1979). Humans suffering from presbycusis share this same hearing loss pattern (Willott, 1986). The mouse has become a favorite source for '*in vitro*' brain slice preparations because of the ease with which bloodless recordings of single cells using sharp and/or patch electrodes can be conducted (Oertel, Wu and their associates). Thus, the mouse is a popular research animal for anatomical, physiological, and behavioral studies of the auditory system (e.g., Amann et al., 2009; Berglund et al., 1996; Berglund and Brown, 1994; Brown et al., 1988; 1991; Brown and Benson, 1992; Brown and Ledwith, III, 1990; Brown and Levine, 2008; Brown and Liu, 1995; Egorova et al., 2001; 2002; 2006; Egorova and Ehret, 2008; Ehret, 1976a,b; 1978; 2002; Ehret and Schmid, 2009; Ehrlichman et al., 2009; Fichtel and Ehret, 1999; Galindo-Leon et al., 2009; Hage and Ehret, 2003; Heffner et al., 2001; Hofstetter and Ehret, 1992; Koay et al., 2002; Maison et al., 2007; May et al., 2002; Prosen et al., 2000; Reetz and Ehret, 1999; Stiebler and Ehret, 1985; Taranda et al., 2009; Yan and Ehret, 2001; Yan and Ehret, 2002; Yan and Zhang, 2005) and a wealth of complementary data now exists.

Understanding the diseases of the human auditory system and the underpinning cellular and molecular mechanisms is of primary interest in current hearing research. Comparative hearing research is important, because animal models can be developed, evaluated and eventually applied to clinical problems. The investigation of mouse mutants with hearing impairments is useful for elucidating the pathological processes underlying auditory defects, as well as for understanding the normal process of auditory development and sensory transduction. Deaf mouse mutants are also valuable for identifying the responsible genes by positional cloning, and are being used in the search for genes involved in human deafness (Steel, 1995). It should be stated, however, that the study of species other than mice is crucial because

(1) strain differences can be as large as species differences;
(2) the mouse is mostly sensitive to high frequency sounds, whereas humans are mostly sensitive to low frequency sounds;
(3) the mouse is lissencephalic, compared to the gyrencephalic nature of human cerebral cortex and has a relatively limited behavioral repertoire;
(4) the anesthetic dose for mice is near the lethal dose;
(5) the mouse is small and can cannot endure the physical demands of long electrophysiological recording sessions.

Due to these inherent differences between the mouse and man, data from many species of the animal kingdom are required to form concepts that could be applicable to humans.

In summary, the mouse auditory system (Fig. 24.1) has proven valuable for exploring some general features of the central nervous system. The publication of the *Auditory Psychobiology of the Mouse* (Willott, 1983), provided valuable insight for its day. Today, 25 years on, it is timely to revisit the progress made on the mouse auditory system and explore the possibilities modern research techniques and technology offer. The purpose of the current review is to highlight the functional organization of the mouse auditory system and to focus on mouse as a useful and economical animal model for hearing research. Thus, this review is based largely on studies of the mouse auditory system, and citations refer to the mouse unless stated otherwise. When complementing the description with data from other species, we should refer mostly to the rat, a small rodent and relatively similar to mouse (Malmierca, 2003; Malmierca and Merchan, 2004). Other species will be referred to for

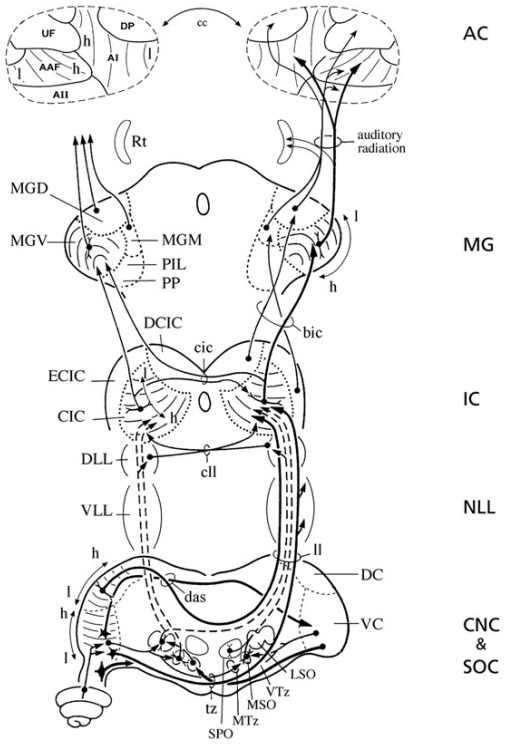

FIGURE 24.1 Ascending auditory pathways of the mouse. (Modified after Brodal, 1981; AC is from Stiebler et al., 1997.) For abbreviations see list.

comparative purposes or if particular data are not available.

The specific stimulus for the ear is air pressure waves within a certain range of frequencies. The range of frequencies to which the ear responds varies between species. In mouse (Fig. 24.2B) the frequency range is from 2–100 kHz (Ehret, 1976a; Heffner et al., 2001; Koay et al., 2002) while it is about 1–80 kHz in rat, 0.2–50 kHz in guinea pig and 0.125–60 kHz in cat. In humans the range is 0.02–20 kHz.

Traditionally, the auditory system has been considered as groups of neurons that are directly or indirectly connected by axons to the auditory part of the inner ear. Sound waves are transmitted mechanically through the outer and middle ear to the sensory hair cells of the organ of Corti, in the cochlear partition of the inner ear. Receptor potentials set up in the sensory hair cells cause action potentials to be initiated in the innervating cochlear nerve fibers. These fibers transmit the auditory signals to the brainstem by way of the auditory or cochlear nerve (Fig. 24.1). All fibers of the auditory nerves undergo obligatory synaptic interruption by terminating as synaptic endings in the cochlear nucleus (Fig. 24.1). Individual fibers branch and ramify throughout the nucleus and give rise to between 50–100 terminal endings (Brown and Ledwith, III, 1990; Fekete et al., 1984). These endings contact different cell populations, where the signals are distributed, processed, and then shipped out along a number of parallel ascending tracts (Osen, 1969).

The ascending auditory tracts converge in the auditory midbrain and the inferior colliculus, which is a major relay nucleus along the route to the auditory cortex (Fig. 24.1). There can be as few as four synaptic interruptions in this ascending trajectory, but there is another key pathway which has additional synaptic stations in the superior olivary nuclei. Moreover, there are multiple stages of convergence in the auditory pathways, including pathways from other neuronal systems. In addition, there are at least seven commissures that add to the complexity of organization of the central auditory system.

SOUND TRANSDUCTION IN THE EAR

In the mouse, as in other terrestrial mammals, the pinna collects the sound waves and funnels them via the external acoustic meatus to the tympanic membrane. The chain of three small ossicles, the malleus, incus and stapes, transfer the sound vibrations of the tympanic membrane through the air-filled middle ear to the footplate of the stapes, which inserts in the oval window and rests on the fluid-filled inner ear. The area of the footplate is considerably smaller than that of the tympanic membrane, so that the increased force/cm^2 at the footplate serves to match impedance of air to that of fluid. In the inner ear, the endolymph-filled membranous labyrinth, also known as the cochlear duct or scala media, is suspended in the perilymph-containing osseous labyrinth. The auditory part of the mammalian osseous labyrinth is the cochlea, and the membranous labyrinth consists of the cochlear duct (Fig. 24.2A). The basilar membrane is an elastic membrane, situated in the middle of the cochlear duct, and acts as a hydromechanical frequency analyzer.

The structure of the mouse cochlea (Fig. 24.2C) corresponds to the basic mammalian plan (Ehret, 1979; Francis et al., 2004). The outer form of the mouse cochlea is cylindrical and the spiral is made up of 2.25 turns. Fig. 24.2A shows a mid-modiolar section through the cochlea in the mouse. The cochlear duct divides the bony cochlea into three fluid-filled compartments: the scala media, scala vestibuli, and scala tympani.

The scala tympani is separated from the scala vestibuli by the osseous spiral lamina. The scala media is separated from the scala vestibuli and scala tympani by the vestibular (Reissner's) membrane above and the basilar membrane below, respectively. At the lateral wall, the scala media is limited by the stria vascularis. The outer scala tympani and scala vestibuli are joined at the apex by an opening called the helicotrema. These outer scalae (scala tympani and scala vestibuli) are filled with a fluid known as perilymph, which contains a high concentration of Na^+ (140 mM) and a low concentration of K^+ (4 mM; Johnstone and Sellick, 1972), similar to the extracellular ionic composition. By contrast, the scala media contains endolymph, which is similar to the intracellular fluid, as it has a high concentration of K^+ (120 mM) and a low concentration of Na^+ (1 mM; Bosher and Warren, 1968).

The endolymph and perilymph are separated by the vestibular membrane; a thin sheet of connective tissue covered on both sides by epithelial cells joined by tight junctions.

The stria vascularis, a three-layered epithelium surrounding a dense network of capillaries, regulates the ionic composition of the endolymph and provides a physical seal between the bony and membranous labyrinths.

THE ORGAN OF CORTI

The organ of Corti (Fig. 24.2C), the sensory epithelium resting upon the basilar membrane (for a review see Slepecky, 1996), senses mechanical vibration of incoming sound and converts it to action potentials. It is made up of two types of sensory cells (Fig. 24.2C–G): *outer hair cells* (OHCs) and *inner hair cells* (IHCs) and several

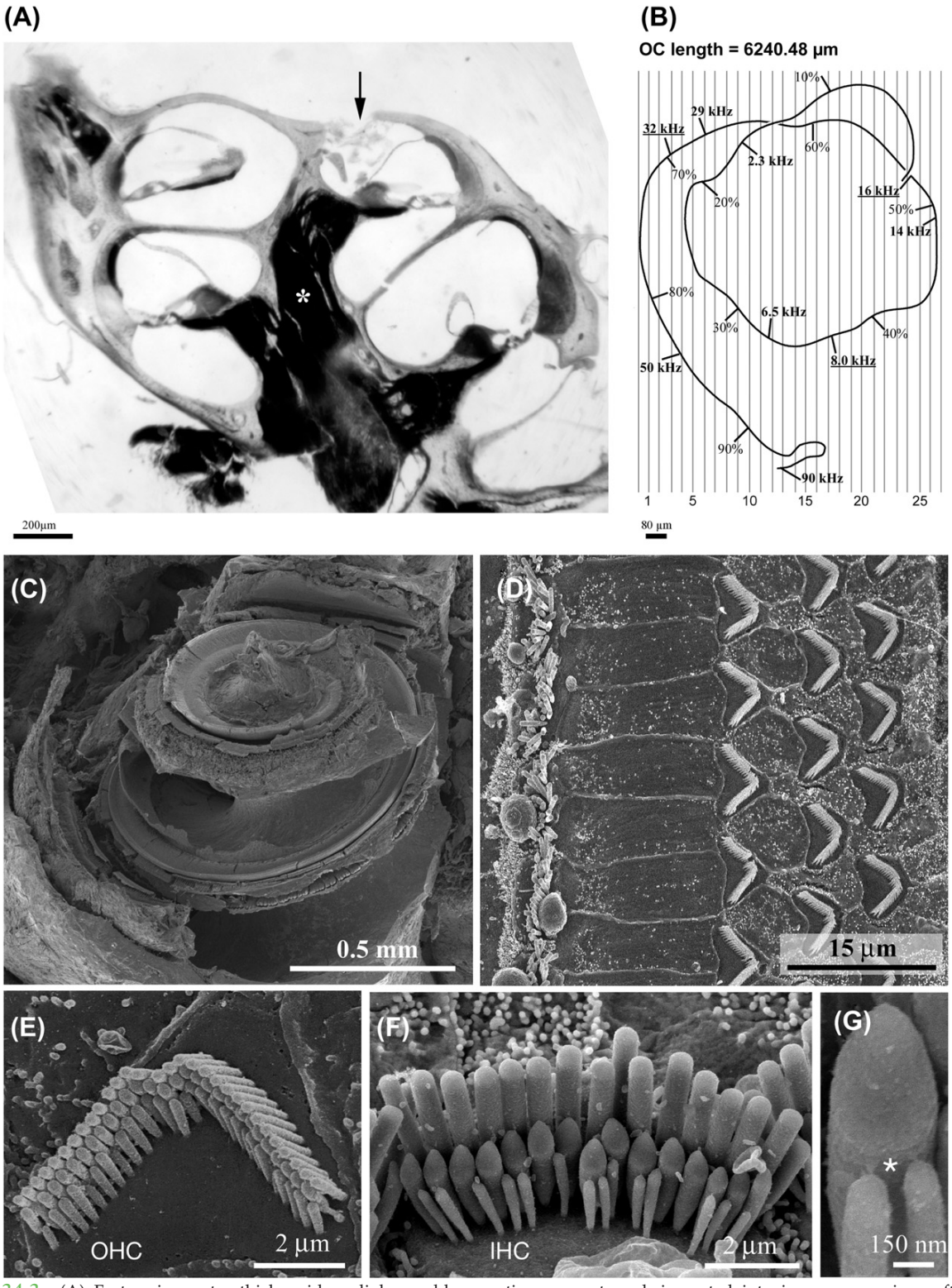

FIGURE 24.2 (A) Forty-micrometer thick, mid-modiolar cochlear sections were traced, imported into image-processing software, and aligned. The modiolus (asterisk) represents the core of the cochlea and contains the central axons of spiral ganglion cells. Note the apical fenestration (arrow) made to facilitate intracochlear perfusion of reagents. (B) Apical view of three-dimensional reconstruction of the basilar membrane. Frequency location was assigned using a cochlear frequency map estimated for mouse (from Ehret, 1979) based on percent distance from the apex. OC, organ of Corti. (C) a whole cochlea; (D) organ of Corti with outer and inner hair cells, (E) an outer hair cell, (F) is an inner hair cell and (G) is inner hair cell stereocilia in close up showing tip links. (*A-B)* from Francis et al., 2004. (*C-G)* Scanning electron micrographs of the mouse cochlea kindly provided by Dr. David Furness.

types of supporting cells (Fig. 24.2D). The OHCs are arranged in three parallel rows (Fig. 24.2D, F), whereas the IHCs are in a single row (Fig. 24.2D, F, G). At their apical end, the hair cells are provided with stereocilia in a typical 'W' pattern. The organ of Corti is overlain by the gel-like tectorial membrane, which is indirectly connected to the osseous spiral lamina through the spiral limbus. Only the stereocilia of the OHCs appear to be in contact with the tectorial membrane. Shearing movements between the basilar membrane with the sensory epithelium and the tectorial membrane cause receptor potentials to be produced in the hair cells, by means of deflections of their stereocilia (reviewed in Nobili et al., 1998). Sensory transduction in the cochlea has been studied for many years, and over the last 30 years it has been recognized that the IHCs (Fig. 24.2G) act as the primary receptor cell (Markin and Hudspeth, 1995; Russell, 1983), whereas the OHCs act as motor cells that can convert membrane potential into a mechanical force (reviewed in Nobili et al., 1998).

The IHCs are flask-shaped with a globular cell soma tapering into a thinner elongated neck. Their nucleus is rounded and located halfway along the length of the cells, so dividing them into two topographic domains. At the basal end are found synaptic contacts from afferent cochlear nerve fibers, hence this pole is also referred to as the neural pole. The neural pole receives about 90–95% of all afferent contacts with cochlear nerve fibers (Fig. 24.3; reviewed in Ryugo, 1992). The apical pole is characterized by a bundle of stereocilia in nearly straight rows and is synapse free (Fig. 24.2).

The OHCs rest on the supporting cells (called Deiter's cells) that comprise 75–80% of all hair cells. The OHCs are cylindrically shaped and possess a large spherical nucleus located at the neural pole. OHCs are characterized by having several cisterns of endoplasmic reticulum distinctly located under the cellular membrane in a laminar fashion extending from the nucleus up to the apical pole (Slepecky, 1996). At the cuticular end, three rows of stereocilia arise forming a typical W-shaped configuration (Fig. 24.2). As opposed to the IHCs, OHCs only receive 5–10% of the afferent innervation from the cochlear nerve, but are contacted by a large number of efferent nerve terminals originating in the olivocochlear bundle discussed below (Fig. 24.3; Warr, 1992).

The most conspicuous supporting cells in the organ of Corti are the inner and outer pillar cells. They form the tunnel of Corti between the IHCs and OHCs. These cells rest upon the basilar membrane.

The frequency components of a sound are mapped along the length of the basilar membrane and its overlying organ of Corti (von Bèkèsy, 1960). The cochlear frequency map (Fig. 24.2B) is determined by the progressive increase in the stiffness of the basilar membrane that is correlated with the decreasing basilar membrane width and increasing thickness from the apex to the base (e.g., Dallos, 1992; Echteler, 1994; von Bèkèsy, 1960). The frequency selectivity and sensitivity however, depends on the physiological integrity of the cochlea (Rhode, 1984).

The pioneering studies of Rasmussen (1940; 1946), Engström (1958) and others (for an extensive review see Slepecky, 1996) on the innervation of the cochlea identified two types of nerve fibers connecting to the organ of Corti: *afferent* and *efferent* fibers (Fig. 24.3). The afferent fibers convey impulses to the cochlear nuclear complex, whereas the efferent fibers convey impulses from the superior olivary complex to the organ of Corti (*v.i.*). More recent studies have detailed the fine structure and organization of the innervation in several species (Kimura, 1975; Spoendlin, 1967; Warr et al., 1997; Warr and Guinan, Jr., 1979) including the mouse (Brown et al., 1988; 1991; Brown and Ledwith, III, 1990; Brown and Levine, 2008; Ehret, 1979; Maison et al., 2007).

There are two subtypes of afferent fibers (Fig. 24.3). The thick myelinated fibers arising from the bipolar type I spiral ganglion cells innervating the IHCs, and the thin unmyelinated fibers arising from monopolar type II spiral ganglion cells innervating OHCs (Berglund and Ryugo, 1987; Brown and Ledwith, III, 1990; Rosenbluth, 1962).

Early studies on the cat demonstrated that 90–95% of type I fibers contacting only IHCs are unbranched and each fiber terminates on a single IHC (Kiang et al., 1982). Each IHC contacts about 20 different fibers (Spoendlin, 1972). The unmyelinated type II fibers arise from small unipolar ganglion cells and constitute about

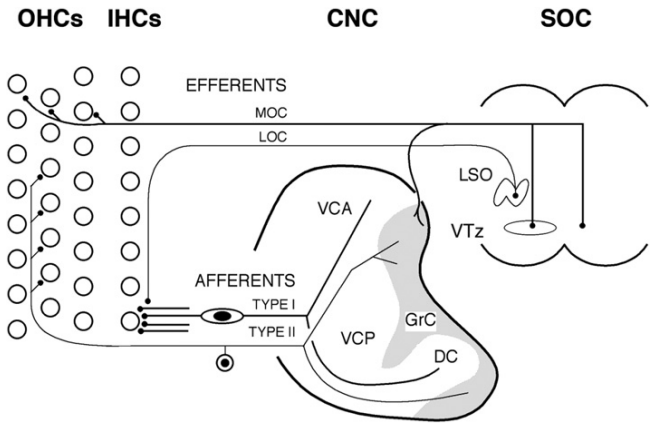

FIGURE 24.3 **Afferent and efferent innervation of the cochlear epithelium.** Note that several type I afferent fibers converge onto single IHCs, whereas a single type II afferent fibers terminate onto several OHCs. Type I fibers terminate in the VCA, VCP and DC. Type II fibers terminate on the GrC, and marginal shell areas of the VC and DC. The efferent MOCs innervate the OHCs and the efferent LOCs innervate IHCs. For abbreviations see list. *Modified after Brown et al., 1988b.*

5% of all ganglion cells. In contrast to type I fibers, type II fibers are highly branched and a single fiber synapses onto multiple OHCs (Fig. 24.3; Berglund and Ryugo, 1987; Kiang et al., 1982).

There are also two systems of efferent fibers: the lateral efferent system (lateral olivocochlear system; LOC) that innervates afferent fibers under the IHCs and the medial efferent system (medial olivocochlear system; MOC) that innervates the OHCs (White and Warr, 1983). They belong to the olivocochlear system (Figs. 24.3, 24.16, 24.19–20) and will be treated in detail in the descending auditory pathway section.

THE COCHLEAR NUCLEAR COMPLEX (CNC)

The CNC is the site of termination of all auditory nerve (AN) fibers (Figs. 24.1, 24.3–5) and thus is the first synaptic center of the ascending auditory pathway (Cant and Benson, 2003; Ryugo, 1992). The axons of CNC projection neurons use three primary pathways to reach higher auditory structures (Fig. 24.5): the dorsal-, intermediate- and ventral acoustic striae (DAS, IAS, and VAS respectively; the VAS is also referred to as the trapezoid body (Tz)). The CNC receives descending projections from the auditory brainstem, midbrain and cortex as well as other non-auditory brain structures (for review see Malmierca, 2003).

In the mouse, the CNC is located on the lateral surface of the brain at the pontine-medullary junction (Fig. 24.4C). The CNC consists of a ventral cochlear nucleus (VC) and a dorsal cochlear nucleus (DC, Fig. 24.4). The VC is divided by the cochlear nerve root into an anteroventral (VCA) and a posteroventral (VCP) nucleus. The DC and VC divisions that are visible externally are marked by a slight depression along the lateral surface. The DC curves around the restiform body along the floor of the lateral recess of the fourth ventricle.

Primary Afferents

In the mouse, as in other mammals, the anatomical distribution of the primary fibers (Fig. 24.4A) forms the basis for the laminar tonotopic organization of the three cochlear subnuclei (Lorente de Nó, 1933; 1981; Ramón y Cajal, 1904; 1909). This tonotopic organization has been demonstrated electrophysiologically and also by c-*fos* immunocytochemistry. Each fiber bifurcates into an ascending branch, which supplies the VCA, and a descending branch, which supplies the VCP and DC (Fig. 24.4A).

There are two types of primary afferents: myelinated type I fibers and unmyelinated type II fibers. These fibers follow similar bifurcation patterns (Figs. 24.3, 24.4A, B), but the terminal targets and modes of termination differ. While type I fibers supply all parts of the CNC except the superficial granule cell areas, the type II fibers innervate areas rich in granule cells and appear to supply the marginal shell of the VC (Fig. 24.3; for review see Ryugo and Parks, 2003). Two basic types of terminals are found: large, axosomatic endings called 'endbulbs of Held' (type I, Fig. 24.4B) and small boutons (type II, Fig. 24.4B). The endbulbs of Held arise mainly from the ascending branches, whereas the small boutons arise from loosely ramifying collaterals of both ascending and descending branches.

Ventral Cochlear Nucleus

On the basis of cytoarchitectural criteria, five main neuronal types are recognized across species (Fig. 24.5), including the mouse (Oertel et al., 1990; Oertel and Wu, 1989; Oertel and Young, 2004; Webster and Trune, 1982; Wickesberg and Oertel, 1988; Willard and Ryugo, 1983). These comprise spherical bushy, globular bushy, octopus, multipolar and small cells (Figs. 24.4C and 24.5; Osen, 1969; Webster and Trune, 1982). The spherical bushy cells are found rostrally in the VCA, the globular bushy cells lie centrally on both sides of the nerve root in the caudal VCA and the rostral VCP, and the octopus cells are located caudally in the VCP. In contrast, the multipolar and small cells are found throughout the VC and constitute a heterogeneous class. The small cells are most abundant around the peripheral margins of the nucleus, just deep to the superficial granule cell layer. A concentration of small cells, located dorsolaterally in a superficial location, forms the *small cell cap* of the VC (Osen, 1969). In the mouse, as in other rodents, there is another principal neuron type scattered within the cochlear root nerve and located just peripheral to the Schwann-glia border. These are called cochlear root neurons (Harrison et al., 1962; Harrison and Warr, 1962; Merchan et al., 1988; Osen et al., 1991). The last major cell class is the granule cell (Mugnaini et al., 1980a, b). These microneurons are sparsely scattered throughout the core of the cochlear nucleus, and form a dense rind over the dorsal, medial, and lateral surface of the VC. An incomplete layer of granule cells forms a border between the VC and the DC, and a sheet of granule cells projects into the DC to form layer II – which is also known as the granule cell layer (Ramón y Cajal, 1909). Granule cells give rise to the parallel fibers that course through layer I of the DC (Mugnaini et al., 1980a, b).

The Spherical Bushy, Globular Bushy and Octopus Neurons

These cells (Fig. 24.5) are characterized by the terminal arborization of their dendrites that resembles

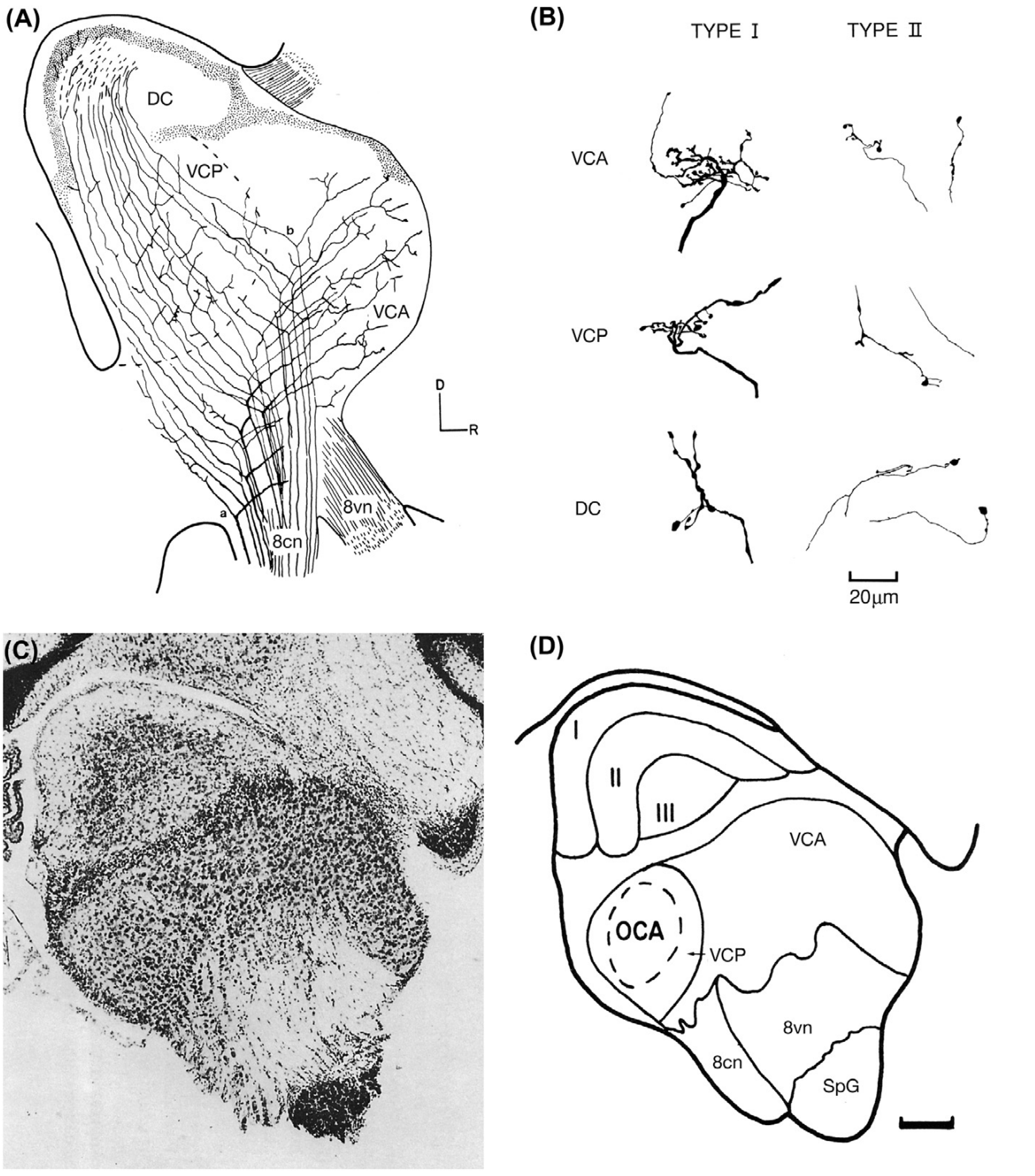

FIGURE 24.4 (A) Modification of parasagittal drawing by Ramón y Cajal (Fig. 24.329, 1909) illustrating the anatomical relationship between the auditory nerve fibers and the cochlear nucleus. (From Willard and Ryugo, 1983.) (B) Representative endings from type I and type II auditory nerve fibers in the mouse with respect to their divisional termination (from Brown et al., 1988a). (C) Cytoarchitectural appearance of the cochlear nucleus of the mouse, shown in the sagittal plane. The drawing in (D) illustrates the changes in cell density that help define nuclear subdivisions. (From Willard and Ryugo, 1983.)

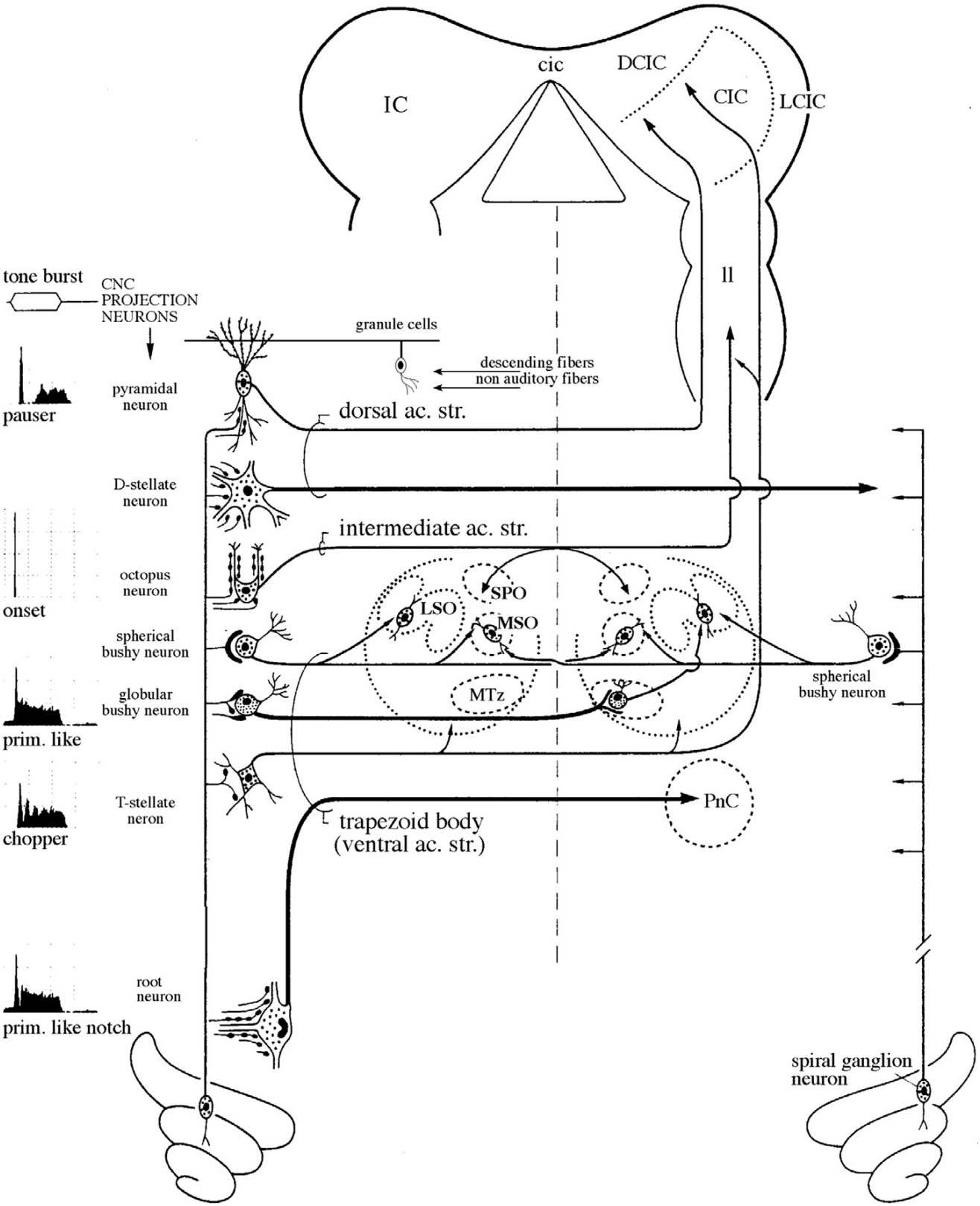

FIGURE 24.5 Main projecting cell types of the CNC in rat with their corresponding physiological responses. For abbreviations see list. *Modified after Moore and Osen, 1979b.*

apical palm fronds (Fig. 24.5). Secondary dendrites tend to originate from a single point, much like the tentacles of a squid. These cell types are further distinguished on the basis of differences in the relative length of the primary dendrites and the shape and size of their terminal bushes. Spherical bushy cells have short dendrites, whereas globular bushy cells have relatively long, wavy dendrites. The cell bodies are also relatively distinct in appearance when stained by basic dyes. Spherical bushy neurons exhibit a central, pale-staining nucleus that is typically associated with a perinuclear cap of Nissl. Nissl bodies are also scattered throughout the cytoplasm. In contrast, globular bushy cells have pear-shaped somata with an eccentric, pale-staining nucleus. The cytoplasm does not exhibit Nissl bodies, but instead is finely granular in appearance due to the presence of free ribosomes and polysomes. In addition, each cell type receives different numbers of afferent cochlear fibers and projects to different targets (Fig. 24.5). Both spherical and globular cells receive a small number of large axosomatic terminals (see review by Ryugo and Parks, 2003), the endbulbs of Held, and have so-called primary-like responses to pure tone stimulation (Fig. 24.5), similar to those of the auditory nerve fibers (Young et al., 1988a). The spherical bushy cells project bilaterally to the medial superior olive and to the ipsilateral lateral superior olive (Cant and Benson, 2003). Like the somatic surface of the spherical bushy cells, that of the globular cells is almost completely covered by synaptic terminals, and the fine structure of these terminals is very similar to that described for spherical cells, although they are not as large as the endbulbs that contact spherical cells. The globular bushy cells project to the contralateral medial nucleus of the trapezoid body (Fig. 24.5). Their axons course ventrally in the trapezoid body. Many of the unique properties of bushy cell membranes and AN input make these cells capable of transmitting the precise temporal information necessary for both high and low frequency sound localization (Young et al., 1988a; Babalian et al., 2003).

The octopus cells are so named because they resemble their namesakes (Fig. 24.5). These cells are relatively large and contain dark-staining, evenly dispersed Nissl in the cytoplasm. The nucleus is round and eccentrically placed. A prominent cap of Nissl substance overlies the nucleus and is located around the nucleus facing the center of the cell body. Nissl substance fills the primary dendrite for a short distance, revealing stout, straight dendrites that emerge from one side of the cell body. These dendrites appear to trail behind the somata, much like the arms of an octopus (Osen, 1969). Octopus cells receive small boutons from collaterals arising from the descending branch of a number of primary fibers (Fig. 24.5). They receive very few GABAergic and glycinergic afferents, and are the only VC cells not receiving inhibitory input from the DC. Their main projection is to the superior paraolivary nucleus on both sides and to the contralateral ventral complex of the lateral lemniscus (for review see Cant and Benson, 2003). Their axons course dorsally, above the restiform body in the IAS (Fig. 24.5). They respond to a tone burst with a single spike and so have been called onset units (Young et al., 1988b).

The Multipolar Cells

These cells (Fig. 24.5) have tapering and moderately branched dendrites and receive primary afferents by means of small boutons from many fibers, mainly on their dendrites, which are moderately tapering and branched. Two types of multipolar cell have been described in mammals (Cant, 1981; 1982). Type I cells have few axosomatic terminals and project to the contralateral inferior colliculus; in contrast, type II cells have many axosomatic terminals and project to the contralateral cochlear nucleus. In the mouse, T-stellate and D-stellate cell types (Fig. 24.5) have been described (Wickesberg and Oertel, 1988), and in the rat planar and radiate cells have been identified (Doucet and Ryugo, 1997), and these correspond respectively to the type I cells and type II cells of cats.

The *Multipolar T-stellate* cells (Fig. 24.5) have oriented dendritic arbors and project to the periolivary region of the superior olivary complex via the trapezoid body, the nuclei of the lateral lemniscus and the central nucleus of the inferior colliculus through the lateral lemniscus (Adams, 1979; Cant and Benson, 2003; Malmierca et al., 2005b). They give off frequency-specific collaterals to both the VC and DC (Lorente de Nó, 1981). They exhibit 'chopper' responses (with regular interspike intervals) to best frequency tone bursts, and they may be specialized for conveying frequency-specific excitatory information about complex acoustic stimuli, including conspecific communication signals.

Multipolar D-stellate cells (Fig. 24.5) have non-oriented dendritic arbors and project to the contralateral CNC, so they are also referred to as commissural neurons (Oertel et al., 1990). The axons give off widely dispersed collaterals to the ipsilateral VC and DC as they course in the dorsal acoustic stria (Oertel et al., 1990; Smith and Rhode, 1989) and terminate in the contralateral CN (Palmer et al., 2003). The D-stellate cells are glycinergic (Doucet et al., 1999; Osen et al., 1991). Thus, they are the best known inhibitory projection neurons of the CNC. They respond to pure tone stimulation with an 'on-chop' pattern characterized by 2–3 regular onset peaks followed by little or no sustained activity (Arnott et al., 2004; Palmer et al., 2003) and often respond over a very large frequency range. A few examples of type II multipolar units show a slightly different form of

PSTH (O_L, single onset peak followed by a pause and then a low level of sustained activity), but it is not yet clear where these cells project and whether they constitute a separate subpopulation. It is also unclear what features of these various forms of multipolar cells cause them to display different PSTH patterns (sustained chopper, onset-chopper or O_L).

The Small Cells

These are abundant in the marginal shell of the VC which is composed of the 'cap area' and adjacent 'granule cell layer'. The granule cell layer is continuous over the free surface of the CNC and forms a lamina partly separating the VC and DC (Mugnaini et al., 1980a, b). In the DC, the granule cell layer co-exists with pyramidal neurons and is covered superficially by a molecular layer. The granule cell axons are distributed as parallel fibers within the molecular layer, running perpendicular to the isofrequency laminae (Mugnaini et al., 1980a, b). The granule cell domain consists primarily of granule cells, but other microneurons are also present, including Golgi cells, unipolar brush cells, and chestnut cells (Mugnaini et al., 1980a; Weedman et al., 1996). The granule cell domain is a region of multimodal convergence where inputs from auditory cortex (Meltzer and Ryugo, 2006; Weedman and Ryugo, 1996), dorsal column nuclei (Wright and Ryugo, 1996), spinal trigeminal nucleus (Haenggeli et al., 2005; Wright and Ryugo, 1996; Zhou et al., 2007), pontine nuclei (Ohlrogge et al., 2001), vestibular nerve (Newlands and Perachio, 2003), and lateral reticular nucleus (Zhan and Ryugo, 2007) are found. This complex neuronal network remains one of the many parts of the auditory system about which more must be learned.

The cap area is distinguishable by its contingent of small cells, many of which show glycine-like and/or GABA-like immunoreactivity (for review see Cant and Benson, 2003). The cap receives input from both type I and type II afferent fibers. Some of the cells in the marginal shell project to the inferior colliculus (Adams, 1979; Malmierca et al., 2005b), whereas others project to the medial olivocochlear system bilaterally, the lateral olivocochlear system ipsilaterally (Ye et al., 2000) and the medial geniculate body (Malmierca et al., 2002). Little information is available on their functional properties (Ye et al., 2000) but the input from high threshold type I auditory nerve fibers (Ryugo, 2008) and connections with OC systems imply a role in gating loud sounds.

Cochlear Root Neurons

These cells (Fig. 24.5) are the largest in the mouse auditory system with an extraordinarily thick axon (5–7 μm). They possess dendrites oriented orthogonal to the AN fibers, which receive small boutons from axon collaterals of AN fibers. These neurons are wedged between the main body of the VC and the glial Schwann-cell border of the AN (Harrison et al., 1962; Harrison and Warr, 1962). They resemble globular bushy cells in a number of respects. They show ovoid somata like globular neurons, respond with a short latency and show primary-like with notch PSTHs to best frequency tones. The CRN have been most studied in rat where they have been shown to project to the contralateral reticular pontine nucleus (Harrison et al., 1962; Harrison and Warr, 1962; Lopez et al., 1999; Nodal and Lopez, 2003). Studies have also suggested that root neurons participate in the acoustic startle reflex (Sinex et al., 2001).

Dorsal Cochlear Nucleus (DC)

The DC shows interspecies variations. In rodents (Fig. 24.4C, D) and carnivores it is distinctly laminated, and resembles a folium of the cerebellar cortex, in humans it is less laminated, and in some cetacea it is virtually absent (Moore et al., 1996; Moore and Osen, 1979). It should be emphasized, however, that the conclusion that primates lose lamination as a phylogenetic process was made on the basis of cytoarchitectonic analysis in tissue stained only by basic dyes. The utilization of cellular and molecular markers along with higher resolution imaging methods revealed that lamination that was not evident in the cytoarchitectonic study (Rubio et al., 2008). In mouse, four layers are discernible in the DC (Mugnaini et al., 1980a, b). Whilst there are a large number of inhibitory (both GABA and/or glycinergic) interneurons, the main cell type is the pyramidal or fusiform cell (Fig. 24.5) and the three superficial layers of DC are related to these. The apical dendritic arbor occupies layer 1, the cell bodies of pyramidal and granule cells occupy layer 2, and the basal dendritic arbor of pyramidal cells resides in layer 3. At the base of the DC lies layer 4, which contains the somata of so-called giant cells and smaller interneurons. Pyramidal cell dendritic arbors are flattened and parallel along the frequency axis of the DC (Blackstad et al., 1984; Spirou et al., 1993). The highest degree of orientation is found in the basal arbor, which is supplied by primary auditory afferents in a strictly tonotopic manner (Ryugo and May, 1993). The spiny apical dendritic arbor of pyramidal cells occupies layer 1 together with granule cell axons and several other types of inhibitory interneurons (Golgi, stellate, and cartwheel cells). Pyramidal and giant neurons are the main projection neurons and supply fibers to the contralateral inferior colliculus via the dorsal acoustic stria (Ryugo et al., 1981; Ryugo and Willard, 1985). In addition, they have a direct projection to the medial division of the medial geniculate body (Malmierca et al., 2002).

The DC is populated by a large number of interneurons that form two systems: the granule cell system,

related to the apical dendritic arbors throughout layer 1 and the cell bodies of pyramidal cells, and the tuberculoventral system, related to the basal dendritic arbors of the pyramidal cells (Fig. 24.5).

The *granule cell system* includes the excitatory granule cells (Osen et al., 1995), chestnut cells (Weedman et al., 1996), the unipolar brush cells (Floris et al., 1994), and three types of inhibitory cells – the GABAergic Golgi and stellate cells and the glycinergic cartwheel cells (Osen et al., 1990). The granule cells receive direct excitatory input from many sources including the somatosensory system and pontine nuclei (Ohlrogge et al., 2001; Wright and Ryugo, 1996) and indirect inhibitory input from these same sources via the Golgi cells. The granule cells contribute parallel fibers to layer 1, where they form asymmetric contacts en passant with the dendritic spines of both pyramidal cells and cartwheel cells and the smooth dendrites of the stellate cells. Such terminals show synaptic plasticity. The unipolar brush cells may represent a unique device for feedforward excitation to links along the mossy fiber pathways. The stellate cells and cartwheel cells provide feed-forward inhibition to the pyramidal cells. Very little is known about the responses of cells in the granular cell system to auditory stimuli. Cartwheel cells show complex spikes (2 or 3 action potentials riding on a depolarization) and complicated responses to auditory stimuli that are difficult to classify (Portfors and Roberts, 2007).

The *tuberculoventral system* reciprocally interconnects the DC and VC. It contains both diffuse and frequency specific projections (Cant and Benson, 2003; Malmierca, 2003). The frequency specific projection from the DC to the VC originates from the glycinergic 'vertical cells'. These cells are located among the basal dendrites of pyramidal cells in layer 3. The dendritic arbors of vertical cells that project to the VC are flattened and parallel to basal dendrites of the pyramidal cell in the isofrequency planes (Rhode, 1999). A separate set of vertical cells with only local collaterals contain both GABA and glycine, the relative amounts of which vary among species (Moore et al., 1996). They receive primary afferents and project to the VC via the tuberculoventral tract after giving off recurrent collaterals to the DC, which terminate on pyramidal cells (Oertel and Young, 2004). Thus, the vertical cells of the DC provide tonotopically organized inhibition in both the DC and VC.

The tonotopic, excitatory projection from the VC to the DC is made up of the collaterals of T-stellate multipolar cells described above. The inhibitory projection from the VC to DC is composed of axons of the glycinergic D-stellate or commissural radiate cells. It has been speculated that off-CF or wideband inhibition from these cells might allow these cells to function as 'spectral contrast detectors' (Doucet et al., 1999). Some small cells of the marginal shell surrounding the VCA also project to the DC. They receive ascending inputs from type II auditory nerve fibers and descending cholinergic inputs (Ye et al., 2000). Thus, these cells may play a role in the integration of neural activity in ascending and descending systems. Yet another type of neuron referred to as adendritic (Friedland et al., 2003) has been found to participate in the VC to DC projection.

Pyramidal cell excitatory responses have been classified as 'pauser' and 'buildup' types in anesthetized preparations as a result of the envelope of the poststimulus time histogram (Fig. 24.5). This same cell is called a type IV unit in decerebrate preparations based on their frequency response area characterized by inhibition at high sound levels of their best frequency, the presence of spontaneous activity, and excitatory responses to broadband noise (Oertel and Young, 2004). Much of the inhibition in pyramidal cells is thought to arise from three cell types: vertical cells and cartwheel cells of the DC and the glycinergic type D-stellate cells in the VC. Vertical and cartwheel cells provide inhibition over a narrow frequency range, whereas the onset-chopper units, also known as D-stellate cells, generate inhibition over a wide frequency range. Behavioral studies suggest that the DC plays some role in directing attention to sound. The type IV units have been found to be sensitive to spectral notches created by the pinna, a feature that may provide important cues for localizing sounds. DC projection neurons receive and respond not only to auditory information but also to somatosensory inputs from muscle proprioceptors in and around the pinna (Kanold and Young, 2001). Such evidence has led to speculation that the DC output may be involved in coordinating pinna orientation with localization cues found in the different spectra of sounds located at different points in space. In fact, bilateral lesions of the dorsal acoustic stria in cats result in reduced accuracy in head orientation responses to broadband sounds, particularly in elevation.

The DC may perform other sophisticated tasks. As previously mentioned, the DC projects directly to the medial geniculate body. The latter in turn projects to the caudate-putamen and amygdala. Behavioral studies indicate that these pathways mediate the conditioned coupling of emotional responses to an acoustic stimulus (LeDoux et al., 1985).

Connections of the Cochlear Nuclear Complex

The ascending projections of the CNC (Fig. 24.1) have already been briefly mentioned and will be discussed in detail when the target nuclei are described. Here it suffices to emphasize that in addition to ascending projection to higher center, the right and left CNC are interconnected by the fibers commissural neurons and the CNC also receives descending projections from

auditory cortex, the inferior colliculus, the ventral complex of the lateral lemniscus, and the superior olivary complex.

THE SUPERIOR OLIVARY COMPLEX (SOC)

The SOC comprises a collection of neuronal groups located in the ventral tegmentum of the caudal pons (Figs. 24.1, 24.5, 24.6). The neurons of the SOC are embedded in a dense matrix of neuronal neuropil, and delimited from the surrounding tissue by a thin fiber capsule (Ollo and Schwartz, 1979). This complex shows considerable variation among species (Osen et al., 1984). Three main nuclei are most consistently identified across species: the lateral superior olive (LSO), medial superior olive (MSO), and the medial nucleus of the trapezoid body (MTz). These three nuclei are surrounded by a diffuse collection of neurons referred to as the periolivary nuclei (PON; Osen et al., 1984).

A consistent feature of the SOC is the relationship of the LSO-MTz and the MSO (Osen et al., 1984). This relationship is evident from the relative sizes of these structures, predictable with respect to the animal's audiogram and natural history. The LSO and MTz are well developed in species that have high frequency hearing, such as rodents and carnivores, whereas they are relatively small in animals with low frequency hearing – such as the human and naked mole rat. The MSO is diminutive in mouse, whereas it is well developed in both the cat and humans. The differences appear

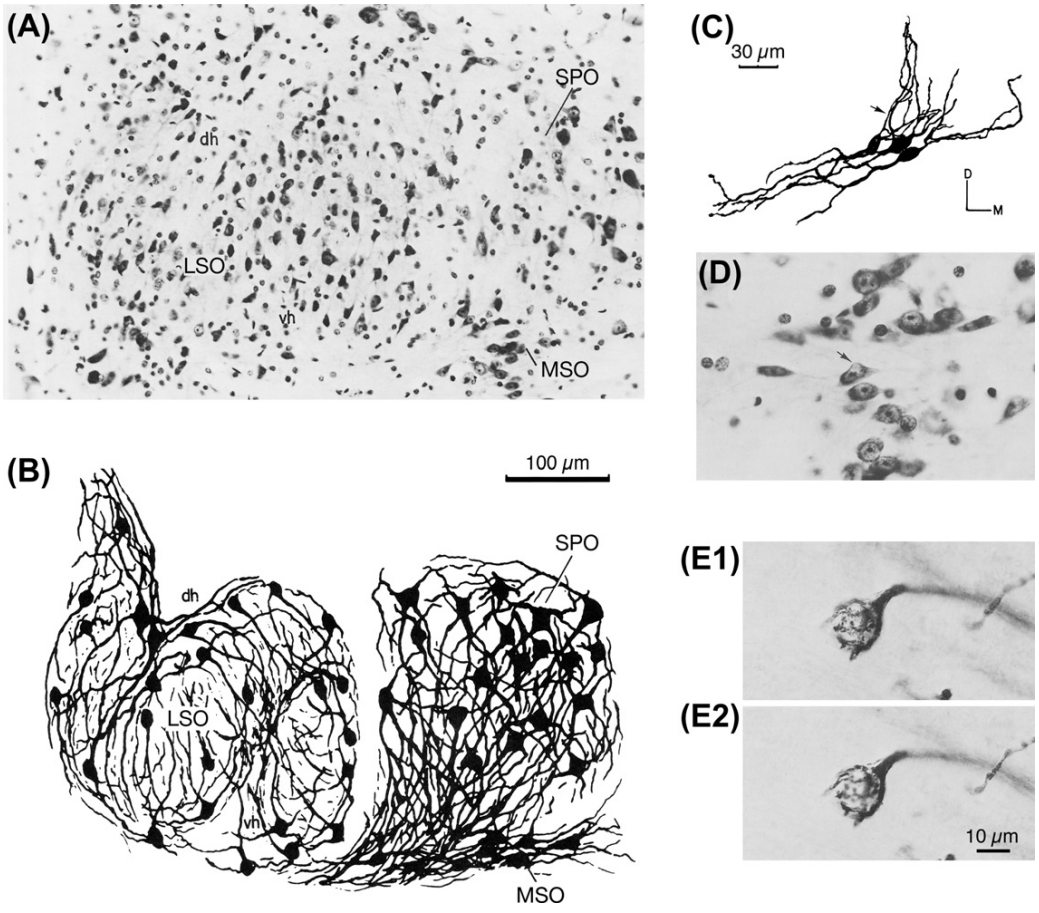

FIGURE 24.6 (A) The cytoarchitecture of the three main nuclei of the superior olivary complex: the lateral superior olive (LSO), medial superior olive (MSO), and superior paraolivary nucleus (SPO). (B) Drawing from a Golgi-stained preparation illustrating the dendritic architecture of the same three nuclei (modified from Lorente de Nó, 1947). Scale bar equals 100 μm for A and B. (From Willard and Ryugo, 1983.) (C) Drawing tube reconstructions of three bipolar (principal) cells of the MSO. Note the predominant horizontal orientation of the dendrites with an occasional vertical dendrite (arrow). (D) Photomicrograph of Nissl-stained somata of the MSO. Faintly stained dendrites reveal the bipolar nature of these neurons with an occasional dorsally directed dendrite (arrow). C and D are matched in magnification. (From Willard and Ryugo, 1983.) (E1 and E2) Photomicrographs of the large calycine endings in the medial nucleus of the trapezoid body in two focal planes. The calyx arises from the end of a thick axon (5 μm in diameter). Each calyx is composed of several thick, gnarled processes that surround the cell body of a principal neuron. The main processes are linked together by a more delicate network of fine fibers and varicosities. Scale bar equals 10 μm. (From Willard and Ryugo, 1983.) For abbreviations see list.

to be correlated to the frequency hearing range in the audiogram. Thus, it is inferred that the MSO is more important for the localization of low-frequency sounds, whereas the LSO-MTz may code all frequencies (Masterton et al., 1975).

In the mouse, as in other rodents, there is an additional, conspicuous and well-defined nucleus; the superior paraolivary nucleus (SPO; Figs. 24.1 and 24.6), located in the dorsomedial part of the complex (Osen et al., 1984; Willard and Ryugo, 1983). It projects to the ipsilateral inferior colliculus (Schofield, 1991) and may represent a hyperdevelopment of homologous periolivary cells that are present in smaller numbers in other mammals. All these four main nuclei are tonotopically organized (Brown and Liu, 1995).

Lateral Superior Olive (LSO)

The LSO occupies the lateral portion within the SOC and appears as a S-shaped row of bipolar neurons (Figs. 24.6A, 24.B), with dendrites oriented approximately perpendicular to the long axis (Ollo and Schwartz, 1979; Ramón y Cajal, 1904; 1909). The S-shaped axis is also the tonotopic axis of the nucleus: low frequencies are represented laterally and progressively higher frequencies are represented more medially (Brown and Liu, 1995; Guinan et al., 1972). When sectioned in other planes, the cells prove to be multipolar with flattened dendritic arbors forming rostrocaudally oriented laminae, which match the orientation of the afferent fiber plexus (Scheibel and Scheibel, 1974; Dovcet and Ryugo, 2003).

The LSO receives input from the VCA on both sides (Fig. 24.5). The ipsilateral input originates from spherical bushy cells, is direct, and is excitatory; multipolar cells from the VCA innervate the LSO as well (Doucet and Ryugo, 2003). Input from the contralateral VC originates from globular bushy cells, which project across the midline to the MTz (Fig. 24.5; Cant and Benson, 2003; Malmierca, 2003). The MTz in turn has a glycinergic inhibitory projection to the LSO on the same side (Fig. 24.5; Spangler et al., 1985). Consequently, LSO neurons are excited by ipsilateral sounds and inhibited by contralateral sounds (EI units) while faithfully encoding interaural intensity differences in the high frequency hearing range (Wu and Kelly, 1992a, b, c; 1994).

The LSO projects bilaterally to the central nucleus of the inferior colliculus (Shneiderman and Henkel, 1987). The ipsi- and contralateral projections are provided by different cell classes (Fig. 24.1). Most of the ipsilaterally projecting cells are glycinergic. The contralaterally projecting cells are glycine-negative and probably excitatory (Saint Marie et al., 1989; Saint Marie and Baker, 1990). The LSO also projects to the dorsal nucleus of the lateral lemniscus bilaterally (Fig. 24.1) and contributes to the lateral olivocochlear system.

Medial Superior Olive (MSO)

The MSO is situated between the LSO and the MTz (Figs. 24.1 and 24.6). The MSO is small in the mouse, and contains only about 200 neurons (Fig. 24.6B–D). It is composed of a row of transversely oriented 'principal cells' with dendrites extending in the medial and lateral directions and oriented rostrocaudally in a series of horizontal laminae. It is tonotopically organized with low frequency tones represented dorsally and high frequency tones ventrally (Brown and Liu, 1995), with most of the nucleus devoted to low frequency tones (Brown and Liu, 1995). In other species, such as the rat, a small population of non-principal cells has been described. The MSO receives input from the VCA bilaterally where fibers arise from low frequency spherical bushy cells. In contrast to the LSO, the MSO receives direct and excitatory input from both sides, but the inputs remain segregated (Fig. 24.5): the lateral dendrites receive input from the ipsilateral side, whereas the medial dendrites receive input from the contralateral side (Smith, 1995; Stotler, 1953). This organization is reminiscent of the required input configuration in the Jeffress model for coincidence detection and sound localization (Jeffress, 1948). The direct bilateral input suggests that the MSO neurons, at least in the cat, are ideally suited to measure interaural phase or time differences (Joris et al., 1998). The MSO projects mainly to the ipsilateral dorsal nucleus of the lateral lemniscus and the central nucleus of the inferior colliculus and their projections are excitatory (Fig. 24.1; Malmierca, 2003).

Medial Nucleus of the Trapezoid Body (MTz)

The MTz is located at the most medial part of the SOC (Figs. 24.1 and 24.19). It possesses two types of cells: principal and stellate. The principal type has the light microscopic appearance of globular bushy cells of the VCA and is situated in between fascicles of fibers in the trapezoid body. The MTz neurons, their axons and their terminal endings show strong glycine immunoreactivity (Saint Marie and Baker, 1990), thus providing an inhibitory influence on their targets.

The MTz receives input from the VCA (Cant and Benson, 2003). The fibers arise from globular bushy cells (Figs. 24.1 and 24.5), which have thick axons that terminate as large axosomatic calyces of Held (1893) in a one-to-one relationship (Fig. 24.6E). The calyces constitute the largest synaptic terminals in the mammalian brain (Morest, 1973) and provide a fast and secure relay of information from the globular bushy cells to the LSO (Guinan and Li, 1990).

The MTz has extensive projections within the ipsilateral SOC (Figs. 24.1 and 24.5), involving the LSO, MSO,

SPO, and ventral (VTz) and lateral (LTz) nuclei of the trapezoid body as well as the ventral and intermediate nuclei of the lateral lemniscus (Thompson and Schofield, 2000). The MTz has been shown to have a strong inhibitory effect on LSO neurons (Moore and Caspary, 1983). Since MTz neurons possess many collateral projections, its neurons exert extensive inhibitory effects on the SOC in response to stimulation of the contralateral ear. In particular, the principal cells convert excitatory inputs from the contralateral cochlear nucleus to inhibitory projections onto principal cells in the ipsilateral LSO. There is a wealth of experiments that have confirmed that MTz cells are specialized to convey signals with minimal jitter or synaptic delay (Wu and Kelly, 1993; Kopp-Scheinpflug et al., 2003, 2008).

Superior Paraolivary Nucleus (SPO)

The SPO is a conspicuous nucleus in rodents such as the mouse (Figs. 24.1, 24.6 and 24.19), gerbil and guinea pig. It consists of several subtypes of multipolar cells, which are the largest in the SOC. The SPO receives inputs from octopus and multipolar cells in the contralateral VC, from multipolar cells in the ipsilateral VCP, and a substantial glycinergic input from the MTz on the same side (Figs. 24.1 and 24.5; Banks and Smith, 1992). The SPO has topographic projections that sustain tonotopy. Its main target is the ipsilateral inferior colliculus (Willard and Ryugo, 1983). A recent study in rats demonstrated that the SPO contains a homogeneous population of GABAergic neurons (Kulesza et al., 2007). The precise function of the SPO is still unknown, but electrophysiological studies in the rat and gerbil reveal surprisingly heterogeneous properties, and suggest that the SPO may serve to encode complex sounds (Dehmel et al., 2002; Kulesza et al., 2007).

Periolivary Nuclei (PON)

The PON contains several groups of neurons with different projection patterns (Fig. 24.1). Although there is some interspecies variation, the various cell types all appear to have specific sites of location within the superior olivary complex (Adams, 1983; Osen et al., 1984). Detailed studies of these regions in the mouse are pending.

The PON receives input from VC bilaterally, the lateral part from the ipsilateral side and the medial part from both sides. These afferents arise mainly from T-stellate cells and perhaps from octopus cells and are probably excitatory. Certain parts of the PON also receive input from the ipsilateral MTz and descending projections from the ipsilateral inferior colliculus and dorsal nucleus of the lateral lemniscus (Bajo et al., 1993). PON cells project to the cochlea, the CNC, and the inferior colliculus (Adams, 1983; Warr and Beck, 1996).

Special mention should be made of the ventral nucleus of the trapezoid body (VTz). The VTz is situated ventral to the MTz and medial to LSO, and represents a heterogeneous group of cells (Figs. 24.1, 24.3 and 24.19) that receives ascending projections from globular bushy cells, octopus and multipolar cells in contralateral VCA, multipolar cells in the ipsilateral VCP, and marginal shell neurons in the VC from both sides (Ye et al., 2000). It also receives descending projections from the inferior colliculus. The VTz projects to the cochlea on both sides, the contralateral CNC, the ipsilateral inferior colliculus, and the nuclei of the lateral lemniscus (Warr and Beck, 1996).

THE NUCLEI OF THE LATERAL LEMNISCUS (NLL)

Over the past decade, extraordinary progress has been made in understanding the anatomy and physiology of the nuclei of the lateral lemniscus (NLL), in particular using the bat and rat animal models (for review see Covey, 1993; Malmierca, 2003). The NLL constitute two main neuronal groups (Fig. 24.7); a ventral nucleus (VLL) and a dorsal nucleus (DLL), although some researchers have also identified an intermediate nucleus (for a detailed discussion on the different cytoarchitectonic schemes see review by Kelly et al., 2009). This organization has been reported for different species by different authors. The division into two components is consistent with the concept of two distinct functional systems; a monaural ventral system and a binaural dorsal system (Covey, 1993; Malmierca, 2003), although there is not universal agreement on this division (Nayagam et al., 2006). There are connectional, neurochemical and physiological properties which are unique to each system. The VLL receives inputs mainly from the contralateral ear, as opposed to the DLL, which receives inputs from both ears.

The Ventral Nucleus of the Lateral Lemniscus (VLL); The Monaural System

The VLL consists of groups of neurons embedded within the lateral lemniscus (Figs. 24.1 and 24.7A), located rostral to SOC. Recent studies on the rat VLL have shown that the cells exhibit a variety of shapes and sizes in Nissl stained sections (Merchan and Berbel, 1996; Wu, 1999; Zhao and Wu, 2001). The majority of cells in the rat VLL are glycine and/or GABA immunoreactive (Riquelme et al., 2001). The idea that neurons of the VLL are organized in a tonotopic fashion is also contentious:

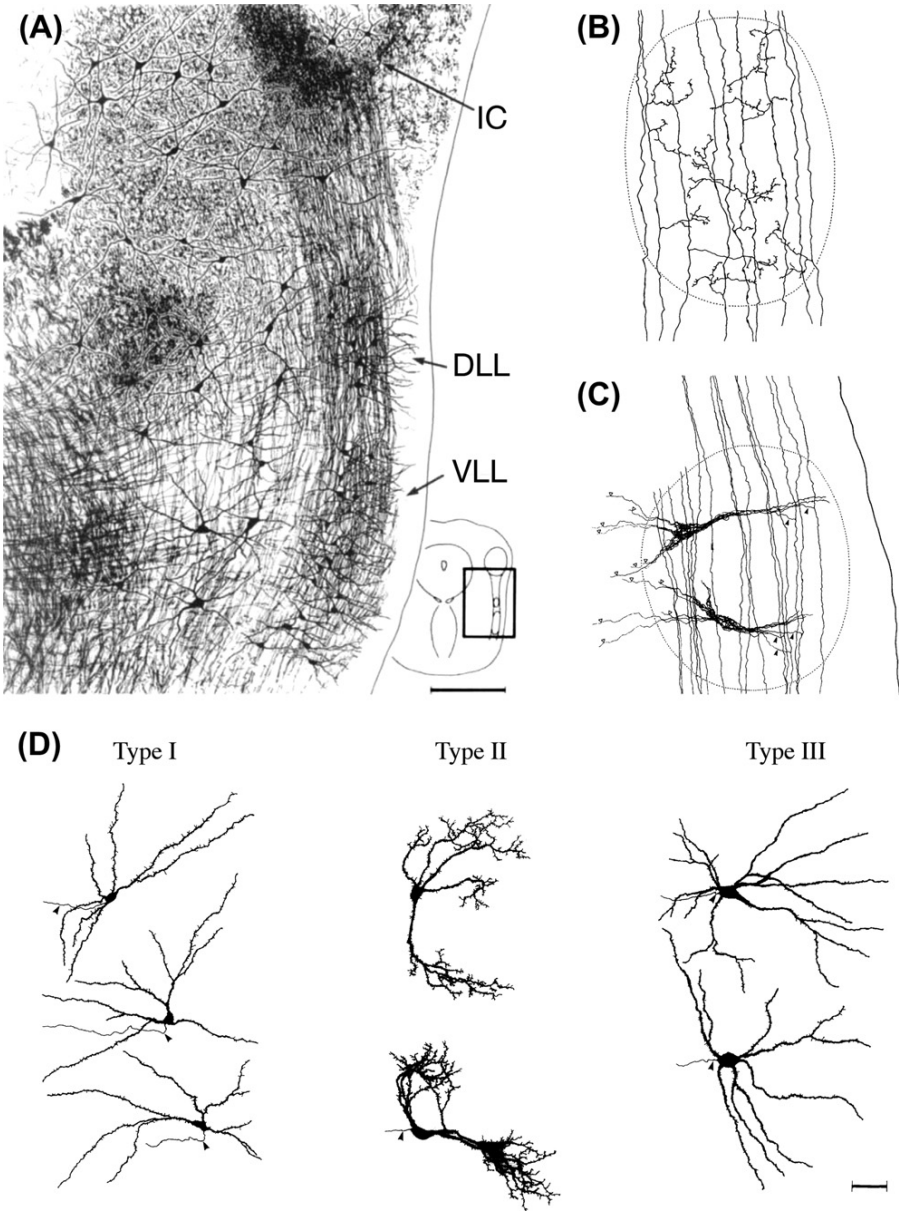

FIGURE 24.7 (A) General view of the ventral (VLL) and dorsal nucleus of the lateral lemniscus (DLL) and adjacent region, in the frontal sections of mice. (B) Thick ascending afferents to the DLL seen in the frontal sections. Rapid Golgi method; (C) Pericellular baskets (A, B) composed of collaterals of lemniscal fibers (closed arrowheads) and afferents from the medial aspect (open arrowheads). (D) Type I, II and III neurons from the mouse DLL. *(Adapted from Iwahori, 1986.)*

the VLL appears to show topographic projections to frequency representations in the central nucleus of the inferior colliculus (Fig. 24.1), which implies a tonotopic organization (Merchan and Berbel, 1996). However, others report that the mapping of physiologically-determined best frequencies using electrophysiological techniques is inconsistent with a tonotopic organization (Nayagam et al., 2006).

Other studies, also carried out in the rat, have correlated the morphological cell types, intrinsic membrane properties and postsynaptic responses in the VLL neuron (Wu, 1999; Zhao and Wu, 2001) using whole-cell patch-clamp recordings combined with intracellular labeling. Afferent projections to the VLL arise mainly from the contralateral VC and ipsilateral MTz. The specific cell types that contribute input arising from the VC include octopus, stellate and globular cells. Large terminals resembling the calyces of Held of the MTz have been shown in the ventral portion of the complex (Malmierca, 2003), and most probably originate from octopus cells. Thus, it seems that these cells would be suited to convey precise and secure temporal information.

The Dorsal Nucleus of the Lateral Lemniscus (DLL); The Binaural System

The DLL is a distinctive group of neurons embedded within the dorsal part of the lateral lemniscus and

projects bilaterally to the inferior colliculus (Fig. 24.7). In contrast to the VLL, the DLL receives input from both ears, and projects in turn to both inferior colliculi (Fig. 24.1). It also projects to the opposite DLL through the commissure of the lateral lemniscus (cll) or Probst's commissure (Bajo et al., 1993; Chen et al., 1999; Zhang et al., 1998). In this way, DLL cells are influenced binaurally.

Using the rapid Golgi method, three main types of neurons in the DLL of the mouse (Fig. 24.7D) have been described (Iwahori, 1986). Type I cell bodies are piriform or triangular with 3–5 primary dendrites. The cell bodies of type II neurons are spindle-shaped or piriform and exhibit 2–4 primary dendrites, and type III neurons possess polygonal or triangular cell bodies with 4–6 primary dendrites. Additional neuronal types have been proposed in other species. Despite their morphological diversity, most DLL neurons are GABAergic and have similar membrane properties, exemplified by a sustained series of regular action potentials evoked by the injection of positive current (Wu and Kelly, 1995a, b, c; 1996). The injection of negative current produced a hyperpolarization that is proportional to the amplitude of the current. There are two types of after-hyperpolarizations; after the occurrence of a spike, some neurons have a single undershoot, whereas others have a double undershoot (Wu and Kelly, 1995a, b, c; 1996). The significance of this difference is not known.

DLL receives input from both ears (Fig. 24.1). Some projections terminate in DLL and others are collaterals from afferents that continue on to innervate the inferior colliculus, i.e., contralaterally from the VC and DLL, ipsilaterally from the MSO, SPO and VLL, and bilaterally from the, LSO (Malmierca, 2003). The studies by Kelly's group in the rat have shown how the DLL refines the binaural response properties of inferior colliculus neurons and contributes to accurate sound localization as demonstrated by behavioral studies (Ito et al., 1996; Kelly et al., 1996; Kelly and Kidd, 2000; Li and Kelly, 1992). The DLL projection to the inferior colliculus is laminar and bilateral (Fig. 24.1), with a predominant projection to the contralateral inferior colliculus (Bajo et al., 1993; Chen et al., 1999; Zhang et al., 1998).

THE INFERIOR COLLICULUS (IC)

The IC is a prominent midbrain structure that is visible on the dorsal surface of the brain wedged between the cerebral hemispheres and the cerebellum. The IC is characterized by a convergence of ascending inputs that arise from numerous lower auditory centers (Fig. 24.1; Casseday et al., 2002; Malmierca, 2003) as well as descending projections from auditory cortex (Doucet et al., 2003). It also receives nonauditory inputs from the somatosensory system suggesting complex multimodal processing (Aitkin et al., 1981; RoBards, 1979).

CYTOARCHITECTURE OF THE INFERIOR COLLICULUS

Ramón y Cajal (1909) identified three major subdivisions in Golgi-impregnated material from a number of mammals: the nucleus, the internuclear cortex, and the lateral cortex. Some modern authors (mouse: Willard and Ryugo, 1983; rat: Faye-Lund and Osen, 1985) have retained this basic scheme (Figs. 24.1, 24.8 and 24.10) with a central nucleus (CIC) covered by a dorsal cortex (DCIC), a lateral cortex (LCIC) and rostrally placed rostral cortex (RCIC). Morest and Oliver (1984) introduced further subdivisions in the cat on the basis of distinguishable neuropil and neuronal populations in Golgi-impregnated material. The subdivisions of the IC may not be the same size in all species, and some may be absent. For example, in the rat, the external cortex appears to occupy a relatively larger portion of the IC than in the cat (Faye-Lund and Osen, 1985; Loftus et al., 2008; Malmierca et al., 1993, 1995). Moreover, in the bat, the 'dorsoposterior division' of the CIC has a hypertrophic representation for the high tonal frequencies used for echolocation (Zook and Casseday, 1982; 1985; 1987).

A recent study by Loftus et al. (2008) has sought to unify the views on the cytoarchitectural schemes used by different authors. The CIC is defined by the presence of *laminae* distinguishable in Golgi material as a parallel organization of afferent lemniscal fibers and neurons with flattened dendritic arbors usually called disk-shaped cells. The layers formed by the cells and fibers are referred to as 'fibrodendritic laminae' (Oliver and Morest, 1984). This characteristic laminar organization of the CIC has been observed in all species studied, including the mouse (Meininger et al., 1986; Willard and Ryugo, 1983) and constitutes the structural basis for the tonotopic organization of the IC (Reimer, 1993; Stiebler and Ehret, 1985).

Neurons in the mouse CIC correspond to the general plan of the mammalian IC (Loftus et al., 2008; Malmierca et al., 1993; Oliver and Morest, 1984). Two main types of neurons in the IC are described: bipolar and stellate neurons (Meininger et al., 1986), corresponding to the F-disk-shaped (flat) and LF (less flat) described in rat (Loftus et al., 2008; Malmierca et al., 1993; Oliver and Morest, 1984) or as oriented (Fig. 24.9) and non-oriented, respectively (Reetz and Ehret, 1999). Physiologically, there are physiological response types with complex properties but no clear correlation are apparent between neurons having particular physiological properties and

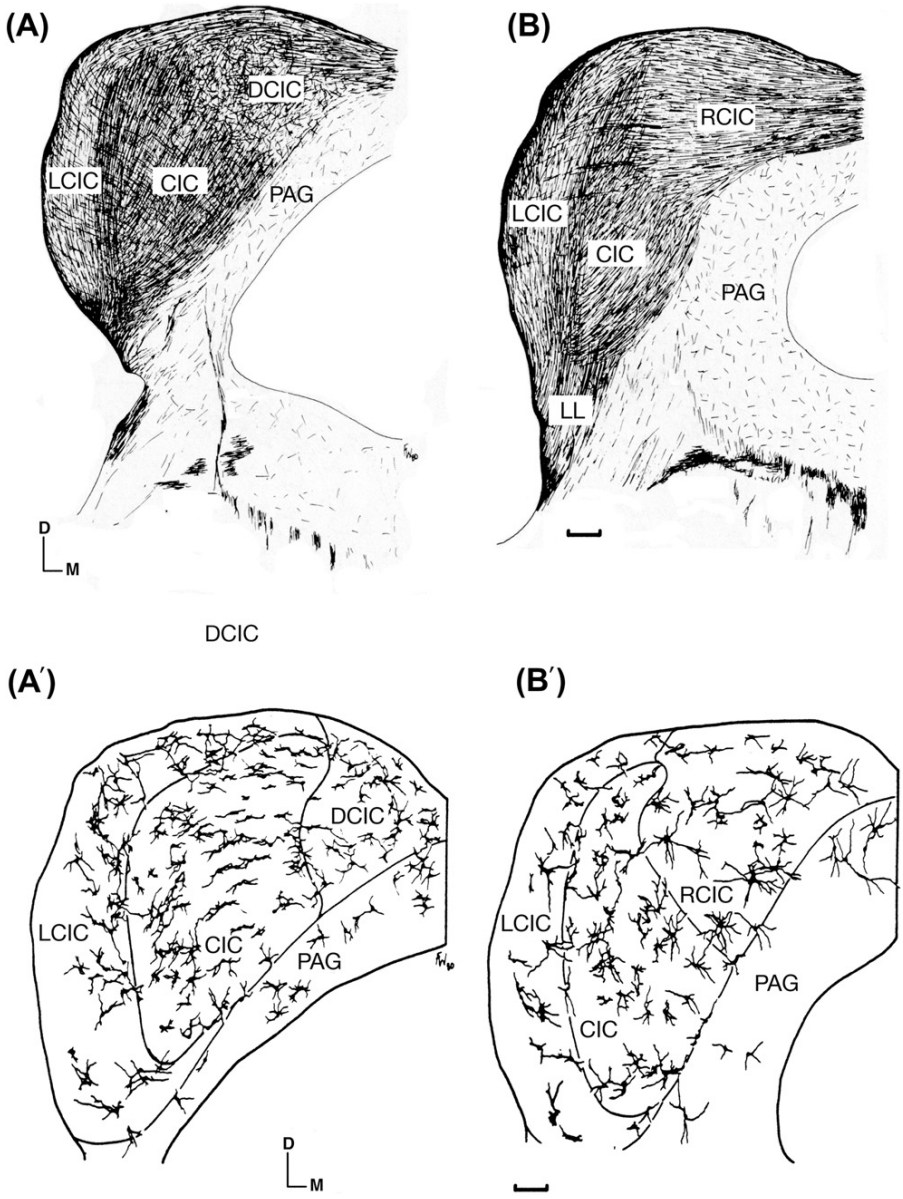

FIGURE 24.8 Drawings that represent the fibroarchitecture and cell types through two sections of the inferior colliculus (IC) (A, B). The central nucleus (CIC) is evident by its dense neuropil, characterized by the innervation from fibers of the lateral lemniscus. There are also efferent fibers that proceed dorsolaterally to penetrate the external cortex before ascending in the brachium of the IC. The lateral cortex (LCIC) is relatively sparse in fibers, whereas the dorsal cortex (DCIC) and rostral cortex (RCIC) is marked by horizontally directed fibers from the commissure. (From Willard and Ryugo, 1983.) A′ and B′, Drawing tube reconstructions through IC sections that illustrate how cell composition helps define subdivisions that correspond to those identified by fibroarchitecture. *From Willard and Ryugo, 1983.*

neurons belonging to specific morphological categories (Sivaramakrishnan and Oliver, 2001; 2006; Tan et al., 2007; Tan and Borst, 2007; Fig. 24.10).

The DCIC covers the dorsomedial and caudal aspects of the CIC (Fig. 24.8 and 24.10). In mice, 4 layers of the DCIC have been defined (Meininger et al., 1986). The most superficial layer (layer 1) is a thin fibrocellular capsule that covers the entire exterior surface of the IC including the LCIC. It contains mostly fibers and some small neurons that are flattened and scattered along the contours of the IC surface. The other layers consist of a mixture of small and medium-sized as well as large multipolar neurons. A distinct feature of the neurons in DCIC (and also LCIC) is the presence of nitric oxide.

The LCIC covers the CIC laterally (Figs. 24.8 and 24.10). Four layers are defined in the LCIC (Meininger et al., 1986). These layers are a continuation of those described in the DCIC. Of particular interest is layer 2, because it is composed of small and medium-sized neurons that are partly aggregated in dense clusters in myelin-rich neuropil. These aggregates are abundant in acetylcholinesterase and GABA. Layers 3 and 4 of the LCIC constitute the largest part and appear contiguous with the non-stratified rostral part (rostral cortex), which is topographically related to the fascicles of the commissural fibers. The neurons located in front of the CIC form the rostral cortex (RCIC; Fig. 24.8 and 10). They include very large multipolar cells, as well as small and medium sized multipolar neurons and thus differ

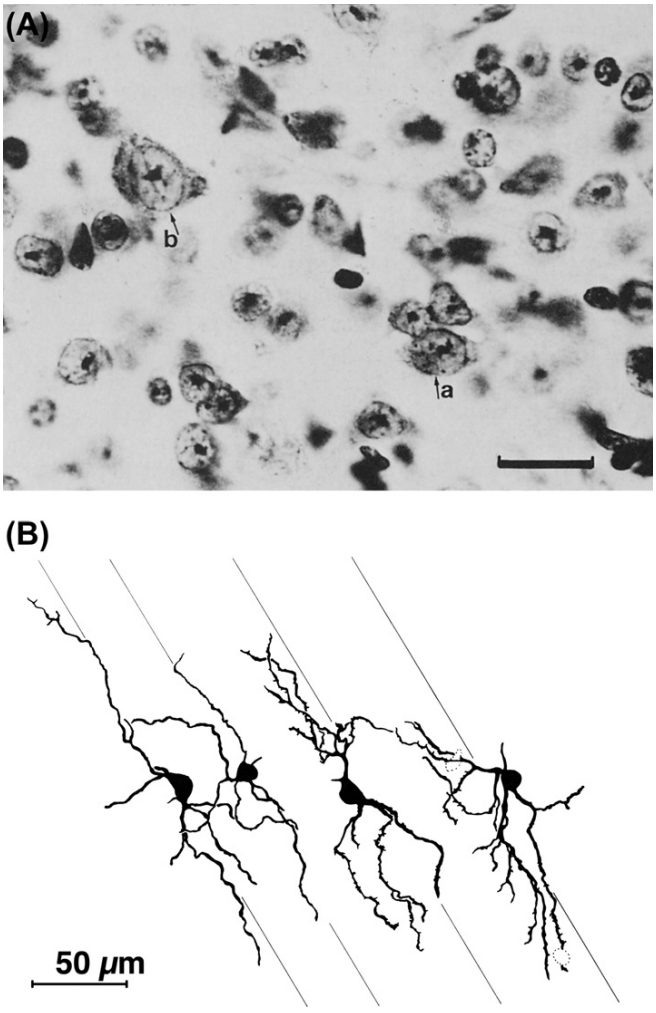

FIGURE 24.9 **Flat neurons of the central nucleus of the inferior colliculus** (A) Photomicrograph of Nissl-stained principal cell (a) and multipolar cell (b). (B) Drawing tube reconstruction of four principal flat cells stained by the Golgi-Kopsch method. Note how the dendritic arbors are rather planar and aligned in parallel with one another and the trajectory of lemniscal fibers (indicated by thin lines). *From Willard and Ryugo, 1983.*

from those of the CIC and LCIC (Faye-Lund and Osen, 1985; Malmierca et al., 1993). Pyramidal-like neurons are also abundant as in the rat (Meininger et al., 1986).

The CIC is chemically heterogeneous. Studies in the cat and rat have shown that about a quarter of the cells in the CIC are GABAergic. IC neurons possess $GABA_A$, $GABA_B$ and glycine receptors (reviewed in Kelly and Caspary, 2005). Other neurons possess NMDA and AMPA receptors.

Connections of the Inferior Colliculus

The CIC receives ascending projections that originate in the VCA, VCP, and DC contralaterally, VLL and MSO ipsilaterally, and DLL and LSO bilaterally (Fig. 24.1) (Cant and Benson, 2003; Malmierca et al., 2005b; Ryugo et al., 1981). Most of the experiments that have studied the afferent input to the IC have been conducted in cats and rats (for reviews, see Malmierca, 2003; Oliver 2005). These experiments have shown that the afferent fibers are tonotopically arranged, and that many of the ascending systems show a 'banded' pattern of projections with dense bands (about 150–200 μm thick) parallel to the isofrequency fibrodendritic laminae.

The DCIC, in particular the deepest layers, receive a similar set of inputs as the CIC, and some of the ascending input from lower auditory centers to the CIC encroaches upon the DCIC, as do the intrinsic projections. The DCIC also receives input from the sagulum. In addition, the DCIC, LCIC, and RCIC receive input from the AC bilaterally, and many non-auditory structures (for review see Malmierca, 2003). The neocortical terminals form a banded pattern similar to that of the ascending projections to the CIC; these descending terminals are tonotopically organized, with their isofrequency contours overlapping and continuous with those of the CIC.

The LCIC and RCIC receive somatosensory input from the spinal cord, dorsal column nuclei, and spinal trigeminal nuclei (RoBards, 1979; Zhou and Shore, 2006). Neurons in the LCIC appear to have relatively broad somatosensory receptive fields in addition to auditory responses, which are also broadly tuned (Aitkin et al., 1978). The multisensory integration in the LCIC mirrors similar types of function at higher levels of the 'extralemniscal' auditory pathway. The DCIC projects to the dorsal division of the MG (Fig. 24.1), whereas the LCIC and RCIC project to the dorsal and medial divisions of the MG (Fig. 24.1). Thus, projections from the three subdivisions of the IC overlap, especially in the medial division of the MG.

The CIC projects to the ventral division of the MG in a tonotopic manner (Fig. 24.1), largely to the ipsilateral side (McMullen et al., 2005) but also with a minor crossed component. The CIC projections originate from both F and LF neurons. The majority of neurons that project from the CIC to the MG use glutamate as a neurotransmitter, but studies in rat and cat have demonstrated there is a population of projecting neurons that contain GABA. The GABA-containing neurons in the IC make short-latency, monosynaptic inputs to the thalamocortical projection neurons in the MG (Bartlett et al., 2000; Peruzzi et al., 1997). This situation is interesting, because in the rat and presumably in other rodents like the mouse, the MG lacks GABAergic cells (Winer and Larue, 1996). Therefore, this monosynaptic inhibitory input to the MG may be important for the regulation of firing patterns in thalamocortical neurons in conjunction with the known GABAergic projection from the auditory sector of the reticular thalamic nucleus.

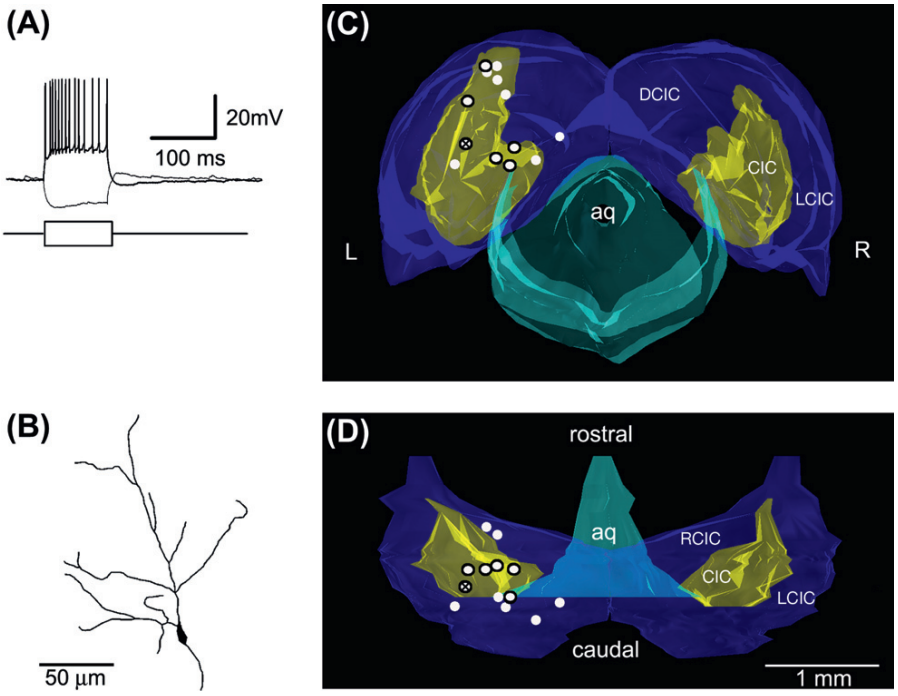

FIGURE 24.10 Localization of biocytin-filled of recorded cells within the mouse inferior colliculus (IC). (A) response to 100-ms, 200-pA hyperpolarizing and depolarizing constant-current injections of the neuron whose morphology is shown in (B) and marked in C and D by a crossed circle. (C) caudal view of a reconstruction of the inferior colliculus. Inferior colliculus is indicated in blue, except for the central nucleus, which is indicated in yellow. Structures outside of the inferior colliculus (periaqueductal gray) are indicated in turquoise. Location of biocytin-filled cells is indicated as white circles. Circles with a black outline were localized within the central nucleus. For abbreviations see list. *Figure kindly provided by Dr. Gerard Borst, adapted from Tan et al., 2007.*

The IC also possesses local and commissural interconnections (Fig. 24.1; Gonzalez Hernandez et al., 1986; Reetz and Ehret, 1999). The ICs from the two sides are interconnected by the commissural fibers. These and the intrinsic or local fibers may represent collaterals of axons with projections to the thalamus or lower brainstem or, alternatively, they may represent the sole projection of a neuron that is truly an interneuron restricted to the IC. The intrinsic fibers form 'sheets' that are parallel to the isofrequency contours of the CIC. The sheets extend into the DCIC, LCIC and RCIC (Malmierca et al., 1995; Saldana and Merchan, 1992). It should be noted that recent studies in rat have shown that the majority of these intrinsic projections may be excitatory and up to at least 25% of the commissural neurons may be GABAergic (Hernandez et al., 2006). Physiological evidence *in vivo* and *in vitro* (reviewed in Malmierca et al., 2003; 2005a) shows that the commissural terminals may have either an excitatory or inhibitory influence on the contralateral IC, and that they affect frequency response areas, binaural properties, and temporal properties.

Physiological Studies of the Inferior Colliculus

Paradoxically, there is a wealth of data on the physiology of the mouse IC, compared to a relatively small number of anatomical studies devoted to the mouse IC. The mouse was used as a model for neurophysiologic studies in the some classical studies conducted by Ehret and colleagues (Egorova et al., 2001; 2002; 2006; Egorova and Ehret, 2008; Ehret et al., 2003; Hage and Ehret, 2003; Stiebler and Ehret, 1985). IC neurons in mouse show a wide variety of response properties to sound stimulation. This complexity is consistent with its intricate, anatomical input-output system.

Neurons in the anaesthetized mouse show a relatively high level of spontaneous activity rate (70 spikes/s). The latency and response patterns of IC neurons depend very much on the type of sound presented; its intensity, and its binaurality (Stiebler and Ehret, 1985; Ehret and Moffatt, 1985a, b). Space limitations prevent a detailed description of these response variables. Mention must be made, however, of the fact that this variety in latency may serve to create variable delay lines. It may also be important in establishing different time constants in response to time-varying signals; such as intensity and frequency modulations and binaural stimuli with various temporal and intensity delays. The response patterns to pure tone stimulation include primary-like, tonic, onset, buildup or inhibitory (if spontaneous activity is present). This diversity of responses reflects the multiple sources of inputs that the IC receives and must integrate (Felix and Portfors, 2005; 2007; Portfors et al., 2009). Other physiological studies have suggested that the laminae of the CIC contain a highly organized representation of both spectral and temporal parameters, i.e., there are different maps of sound response features. These include frequency representation and resolution, sharpness of tuning, threshold response, latency and intensity (see review by Herrnberger et al., 2002).

Studies applying microiontophoresis techniques *in vivo* have demonstrated that both GABA and glycine inhibit IC neurons in several species (LeBeau et al., 2001). Both AMPA and NMDA receptors are involved in the maintenance of the response during stimulation, whereas AMPA receptors seem to be important at response onset. Furthermore, both AMPA and NMDA receptors are involved in maintaining the firing of CIC neurons in response to dynamically changing acoustic stimuli (reviewed in Kelly and Caspary, 2005). The IC shows a variety of frequency response areas in the mouse IC (Egorova et al., 2001, 2006; Egorova and Ehret, 2008) that are both V-shaped and non-V-shaped (LeBeau et al., 2001), as described in other mammals (reviewed in Malmierca, 2003). The iontophoretic application of GABA and glycine antagonists coupled with intracellular recordings (Covey et al., 1996; Kuwada et al., 1997) has shown that neural inhibition contributes to the binaural response of neurons in the IC. Since the basic binaural comparison presumably has already occurred at the SOC (Casseday et al., 2002), it may be that the convergence of binaural pathways and spectral information at the IC could produce a topographic map of auditory space resembling that found in the midbrain of the barn owl (Volman and Konishi, 1990). Studies by Borst and colleagues using *in vivo* patch-clamp recordings in mouse IC neurons have detailed the membrane properties of these midbrain neurons and reported on the intracellular responses to current injections (Fig. 24.10), different sound durations and sinusoidal amplitude tones (Geis and Borst, 2009; Tan et al., 2007; Tan and Borst, 2007).

Although the functions of the collicular cortices are not well known, it is speculated that the LCIC plays an important role in multisensory integration. In agreement with the multitude of inputs, neurons of the LCIC have been shown electrophysiologically to respond not only to auditory stimulation, but also to somatosensory input (Aitkin et al., 1978). The LCIC receives somatosensory input from lower centers (RoBards, 1979; Willard and Ryugo, 1983; Zhou and Shore, 2006), and resident neurons appear to have relatively broad somatosensory and auditory receptive fields (Aitkin et al., 1978). The multisensory integration in the LCIC mirrors similar types of function at higher levels of the 'extralemniscal' auditory pathway. Secondly, the LCIC may have a unique influence on the olivocochlear system. Recent studies show that electrical stimulation of LC has a broadly tuned effect on cochlear responses, in contrast to central nucleus stimulation, which has sharply tuned effects (Ota et al., 2004). Thus, the medial and lateral olivocochlear bundles may be differentially activated by CIC and LCIC, respectively. Thirdly, the LCIC may also have a role in providing auditory input to visual-motor areas that direct head and eye movements involved in gaze initiation. The LCIC may be a major source of binaural cues for gaze control in the superior colliculus (King et al., 1998). Finally, a recent study of RCIC neurons (Malmierca et al., 2009; Perez-Gonzalez et al., 2005) suggests that at least some neurons in this and in other cortical regions may be specialized for detecting novel sounds. It is obvious that there remain many challenges ahead if we are to understand the role of the inferior colliculus in hearing.

THE MEDIAL GENICULATE BODY (MG)

The MG lies on the posterolateral surface of the thalamus as a rounded eminence (Figs. 24.1 and 24.11), lateral and ventral to the superior colliculus and medial to the hippocampus as it transitions from its ventral to dorsal position. It marks the rostral pole of the brachium of the IC. Not only is the MG the main auditory center of the thalamus but also it is the last stage of subcortical auditory processing in the ascending pathway. The structure is commonly divided into three major

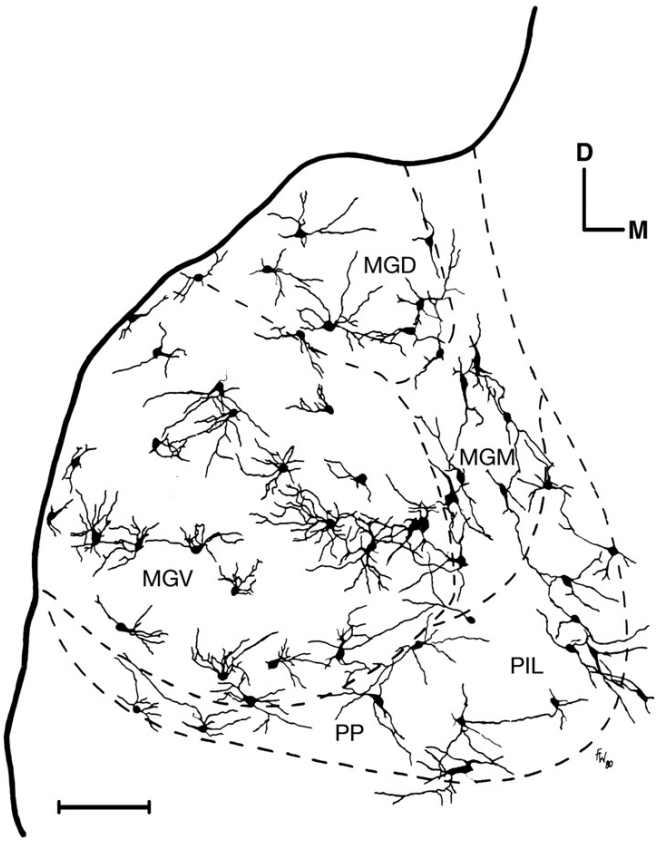

FIGURE 24.11 **Neuronal architecture of the medial geniculate body.** Drawing tube reconstructions of single coronal section stained by the Golgi-Kopsch method. The main subdivisions of the nucleus are illustrated: ventral (MGV), dorsal (MGD) and medial (MGM). *From Willard and Ryugo, 1983.*

divisions named in manner denoting their relative locations within the complex (Fig. 24.11). These include the ventral (MGV), dorsal (MGD), and medial (MGM) or magnocellular divisions.

The auditory thalamus has long been seen as responsible for relaying information to the cerebral cortex, but it has not been until the last decade or so that the functional nature of this structure has attracted significant attention. Whereas earlier views tended to relegate thalamic function to a simple relay process, recent research demonstrates complicated circuitry and a rich array of membrane properties in resident neurons. It is now clear that the MG is not merely a passive conveyor of information to the cortex, but instead is involved in many dynamic processes that significantly alter the nature of the information (Sherman and Guillery, 1998, 2002). The MG is indeed involved in a variety of functions. These include routine auditory processing (Bartlett et al., 2000; Bartlett and Smith, 1999; He, 2003; He and Hu, 2002; Hu, 1995; 2003; Winer et al., 2005; Winer and Larue, 1996) and associated changes involved in learning and memory (Edeline, 1999, 2003). These complementary roles underscore the importance of the thalamus in the hierarchy of sensory processing.

The MG is the last opportunity for auditory signals to be processed before they reach the auditory cortex. Thus, the MG projects to the AC, which in turn sends massive projections back. In addition, the MG receives its major source of ascending inputs from the IC. The MG-AC connections are reciprocal, but non-reciprocal projections also occur (Llano and Sherman, 2008) and they vary such that each subdivision has a particular pattern of connections with other structures. Additional inputs arise from the thalamic reticular nucleus, and to a lesser extent from lower auditory nuclei, including the SOC, NLL, and CNC. Ascending fibers enter the structure medially through the brachium of the IC and terminate among neurons in each subdivision. Connections with auditory cortex pass through the posterior limb of the internal capsule.

A recent study in the mouse MG (Llano and Sherman, 2008, 2009; Lu et al. 2009) using Nissl and immunostaining has revealed cytoarchitectural differences among the subdivisions (Fig. 24.12) consistent with previous descriptions in other species (e.g., Winer et al., 1999). The ventral division of the MG is characterized by the presence of small, densely packed neurons. The lateral portions of the MGV show neurons forming parallel arrays oriented from dorsolateral to ventromedial, whereas in the more medial portions, the cell packing is organized in concentric circles (Llano and Sherman, 2008, 2009). These differences may correspond to the lateral ventral and ovoid nuclei of the MGV, respectively, described in other species but definitive evidence remains to be presented. The MGV also shows strong neuropil staining and moderate somatic staining for parvalbumin. The principal cells of the MGV are the bitufted neurons (Fig. 24.11), which have diametrically opposed dendritic fields that extend from the poles of elongated soma. These neurons are closely spaced and tend to be arranged in rows about 50 to 100 μm wide, with dendritic fields oriented from dorsolateral to ventromedial (Winer et al., 1999). The fibrodendritic laminae are hypothesized to correspond to the organized projection from the CIC, which underlies a tonotopic organization. The principal neurons are proposed to be glutamatergic and approximately 25% of the population may be GABAergic interneurons. Rodents (including mice) and bats, however, apparently lack GABAergic neurons (Winer and Larue, 1996).

The main source of inputs to the MGV is the ipsilateral CIC (Fig. 24.1). Projections from the IC to MGV appear to arise from both glutamatergic and GABAergic neurons (Bartlett and Smith, 1999). The main MGV projection to auditory cortex terminates mainly in layers III and IV of the primary auditory cortex (Fig. 24.1). The tonotopic organization of the projection is preserved in the primary fields.

The dorsal division of the MG possesses larger cell bodies, in particular, in the most dorsal and medial locations. MGD shows no obvious packing arrangement of neurons. The largest neurons in the medial portions of the MGD likely represent the suprageniculate nucleus (Llano and Sherman, 2008, 2009). The MGD shows strong somatic staining for calbindin and weak neuropil staining for parvalbumin (Fig. 24.11 and 24.12). Several cell types have been described in the MGD. Radiate cells are the most numerous with radially symmetric dendritic fields and a simple branching pattern. Tufted cells are also present in substantial numbers (Fig. 24.11). These cells tend to be organized in thin sheets, especially dorsolaterally, with dendritic arbors that extend from each pole (Winer et al., 1999). A secondary population of small stellate cells has also been recognized. Most of the MGD neurons respond to acoustic stimulation with a wide range of latencies, typically longer than MGV neurons, and exhibit broader frequency tuning. Tonotopic organization in the MGD is not apparent from recordings in any species.

The main sources of ascending auditory inputs to the MGD are the DCIC and LCIC (Fig. 24.1; Jones, 2007; Lee and Sherman, 2009; Malmierca, 2003). These inputs represent both glutamatergic and GABAergic neurons (Bartlett and Smith, 1999). The MGD mainly projects to the nonprimary (belt) areas of auditory cortex, where tonotopy is weak or absent (*v.i.*).

The medial division of the MG borders the MGV and MGD medially, extending from the rostral to caudal poles of the MG (Fig. 24.11 and 24.12). Although

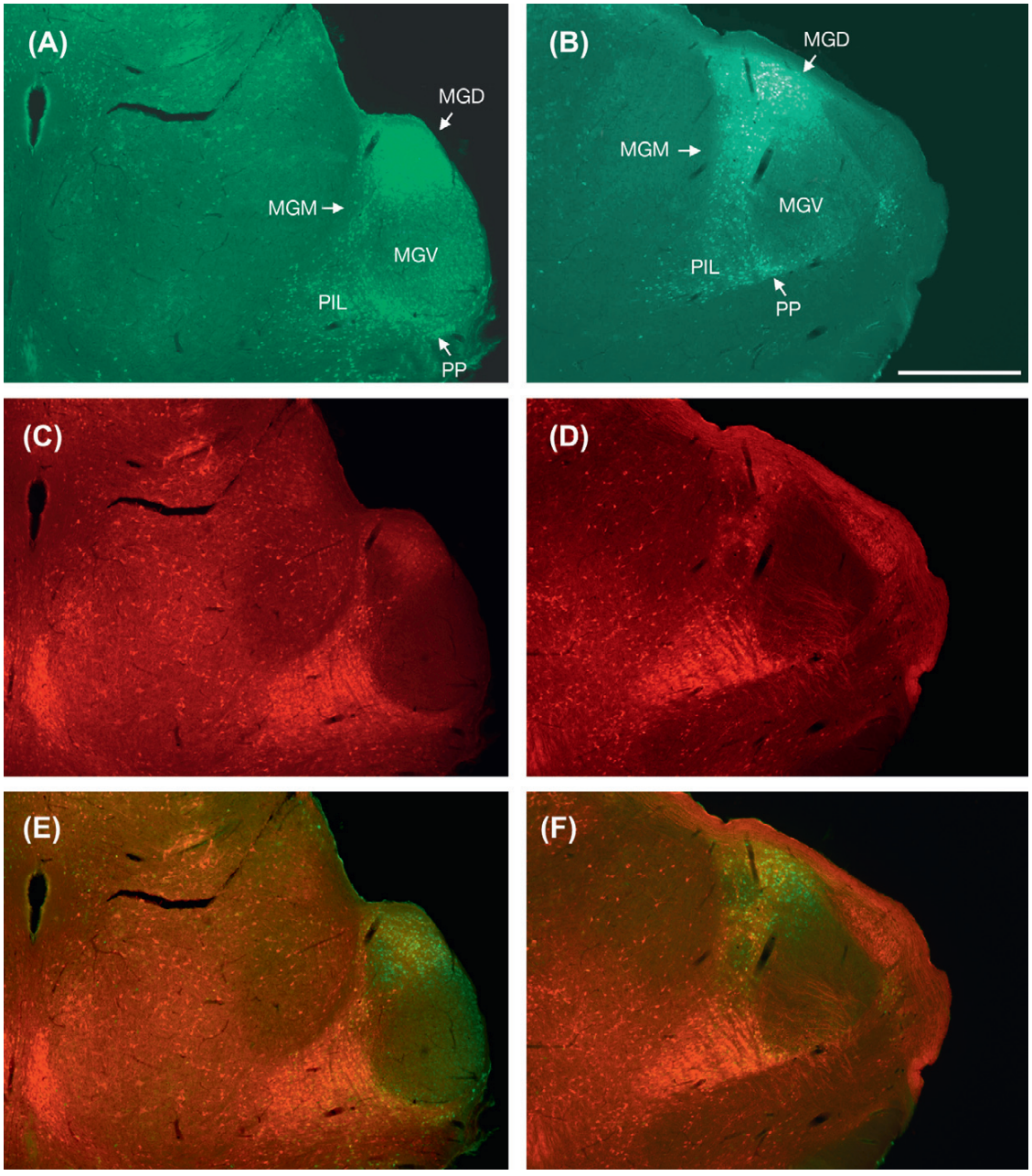

FIGURE 24.12 **Distribution of calbindin (CB) and calretinin (CR) areas at two different rostro-caudal levels of the MGB.** (A) and (B) Two sections from same mouse immunostained for CR, visualized with Alexafluor 594. (C) and (D) Identical sections from A and B, immunostained for CB, visualized with Cy-2. (E) Overlay images from A and C. (F) Overlay images from B and D. Scale bar = 500 μm. *Figure kindly provided by Dr. Daniel Llano, adapted from Lu et al., 2009.*

recognized as a single division, the MGM is rather heterogeneous with respect to cell types and connections. The MGM shows a loose packing arrangement, with some very large cells. Similar to the MGD, the MGM shows strong somatic staining for calbindin and weak neuropil staining for parvalbumin (Fig. 24.12; Llano and Sherman, 2008, 2009; Lu et al., 2009). The MGM contains the largest neurons of the MG and a variety of different types of cells have also been identified (Winer et al., 1999). Some neurons are calbindin-reactive and project mainly to cortical layers I and II, whereas others immunostain for calbindin and parvalbumin and project to the middle layers (Jones, 2007). Response properties in the MGM neurons are highly variable and consistent with the various classes of neurons populating the MGM. Some neurons are narrowly tuned to frequencies with short latencies, similar to MGV neurons, whereas others are broadly tuned and have longer latencies.

Inputs to the MGM include both auditory and nonauditory sources (Ryugo and Weinberger, 1978; Wepsic, 1966). The main auditory inputs arise from the CNC and ECIC, as well as the CN, SOC and VLL (Malmierca et al., 2002). The MGM also projects to the striatum and amygdala (LeDoux et al., 1985; Ryugo and Killackey, 1974). Non-auditory inputs include the deep layers of the superior colliculus and others somatosensory, vestibular, visual, and nociceptive stimuli (Jones, 2007).

In addition to the prototypical principal auditory thalamic nuclei, many other thalamic cells in higher-order nuclei project to layer 1 of the neocortex or to other subcortical structures, such as the basal ganglia or amygdala (Cheatwood et al., 2003). This projection pattern is particularly prevalent among neurons in the intralaminar and the adjacent 'paralaminar' nuclei (Herkenham, 1980), such as the suprageniculate, posterior intralaminar nucleus and the peripeduncular nucleus (Fig. 24.11 and 24.12; Clugnet et al., 1990; Ryugo and Killackey, 1974). The degree of this heterogeneity is reflected in different distributions of calcium-binding proteins (Lu et al., 2009).

THE AUDITORY CORTEX (AC)

The auditory cortex represents the site of termination of fibers ascending from the MG. In the ascending auditory pathway, species differences are the most apparent in the auditory cortex, in which the number of areas identified ranges from five in mice (Fig. 24.13) to over 30 in some studies of humans (Malmierca and Hackett, 2010; Stiebler et al., 1997; Winer, 1992). Species differences include the number of areas present, their relative position and arrangement, cell density, connections, and tonotopic organization.

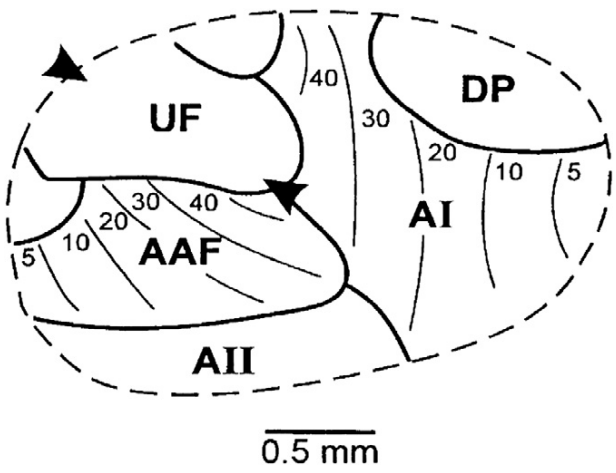

FIGURE 24.13 Electrophysiologically defined fields of the mouse AC are A1 and AAF with a clear tonotopy as indicated and AII and a dorsoposterior field (DP) without an obvious orderly frequency representation. The arrowheads in the UF indicate the approximate position of a line dividing the UF in a rostral and caudal part, whereby the latter might be regarded as belonging to AI. *adapted from Stiebler, 1997.*

In all mammals studied to date, a core koniocortex (granular cortex) with one or more complete and orderly representations of audible frequencies is found to be surrounded by a variable number of secondary or belt areas with less sharp frequency representation. The AC has been most extensively studied in the cat, where the auditory cortex comprises part of the anterior, medial, and posterior ectosylvian gyri, below the suprasylvian sulcus (Winer, 1992). Four tonotopically organized regions have been defined on the basis of responses to pure tone stimulation: primary auditory cortex, anterior auditory field, posterior auditory field, and ventroposterior auditory field. In these areas, there is a systematic change in the frequency representation along the cortical surface, where vertical sheets of similar frequencies are stacked, like slices of a loaf of bread, from low to high. The secondary auditory cortex and the temporal auditory area are situated ventral to the primary auditory area and show a less distinct frequency representation; that is, the neurons are not as sharply tuned, and the progressive change in frequency representation is not as regular. In the rat, several cortical maps have been proposed (Doron et al., 2002; Winer, 1992) but because of the lack of gross anatomical landmarks, like the neocortical sulci, a comparison of the various maps is difficult.

In the mouse, the AC is situated on the caudal half of the parietal cortex. Since the mouse cortex is smooth, reliable landmarks are missing. Nevertheless, Ehret and colleagues (Hofstetter and Ehret, 1992; Stiebler et al., 1997) have differentiated five auditory fields in the cortex (Fig. 24.13) on the basis of tonotopy, spontaneous activity, and the general characteristics of responses to tones, noise bursts, and frequency sweeps. These fields include the primary auditory field (AI), the anterior auditory field (AAF), the ultrasonic field (UF), the secondary auditory field (AII) and the dorsoposterior field (DP). AI and AAF are tonotopically organized and may constitute the primary or core auditory cortex. They are organized, as in other mammals, with a reversal of tonotopy across the high-frequency border between the two fields. The UF may be a continuation of AI and/or AAF into ultrasonic frequency sensitivities (Hofstetter and Ehret, 1992; Stiebler et al., 1997).

Except for a brief study by Cruikshank et al. (2001), detailed studies on the lamination and histological details of the mouse auditory cortex (Fig. 24.14) are lacking. In general, however, the mouse core areas (AI and AAF) seem to follow the general cytoarchitectural plan seen in other rodents such as the rat. AI is characterized

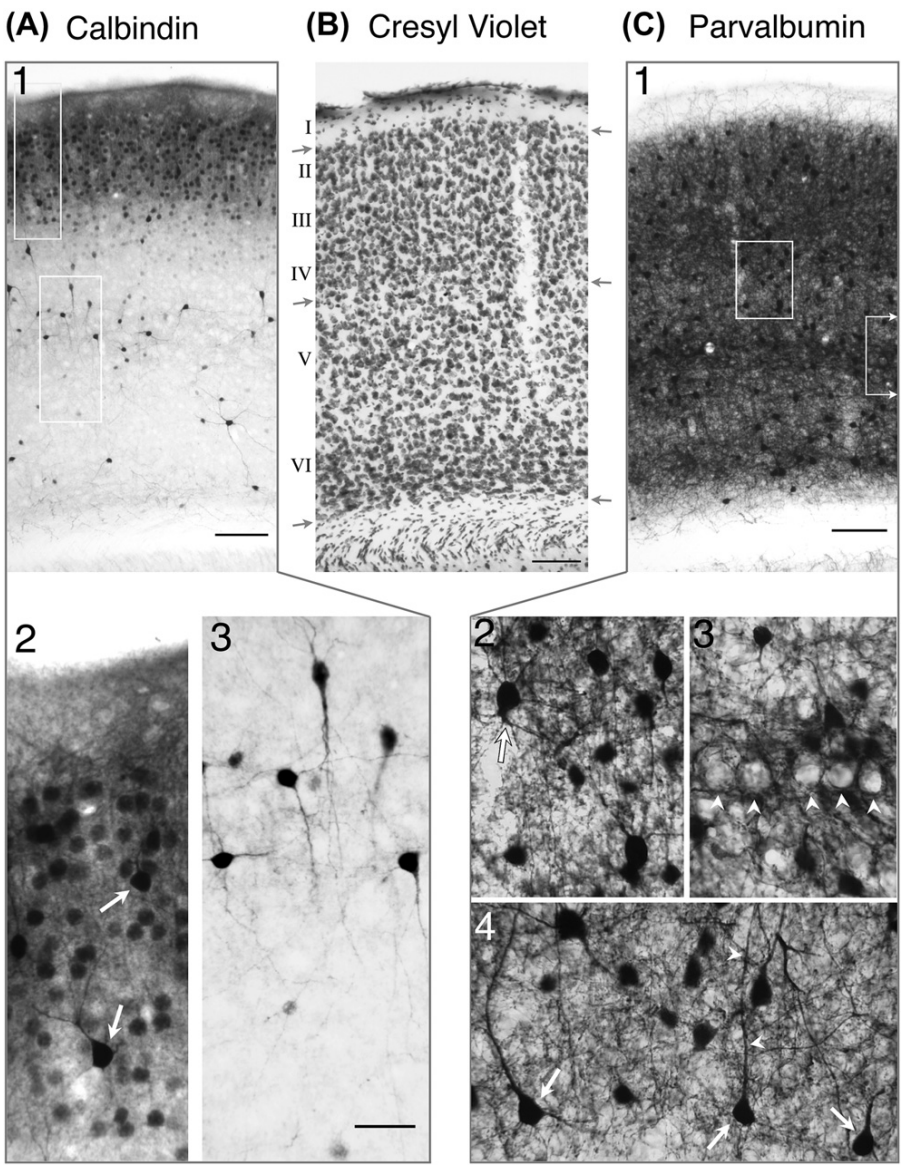

FIGURE 24.14 Laminar and cellular distributions of calbindin (CV) and parvalbumin (PV) in A1. Top panels illustrate laminar staining for CB (A1), Cresyl Violet (B) and PV (C1) of A1, obtained from the same three adjacent sections shown in Fig. 24.1. Gray arrows beside Nissl-stained image (B) point to approximate borders between layers I/II, layers IV/V, and layer VI/white matter. Roman numerals to the left of Nissl image are positioned at suggested centers of each layer. White rectangles in A1 and C1 indicate positions of higher power images presented in bottom panels (A2;3 and C2;3). A, CB immunoreactivity is concentrated in the three upper layers (A1;2). Arrows in A2 point to layer II/III non-pyramidal cells that appear darker and larger than the majority of moderately stained CB positive somata in upper layers. A3 shows a variety of non-pyramidal CB positive cells in layers IV and V. C, Intense PV immunoreactivity exists throughout layers II-VI, including both somata and processes (C1-4). The arrow in C2 points to a multipolar PV positive non-pyramidal cell in deep layer 4. Other non-pyramidal cells can also be seen in C2-4. The arrowheads in C3 point to 5 dense axonal arrangements, surrounding presumed unstained somata, within layer V. Note that about half of the image in C3 comes from outside the frame of C1 (indicated in C1). The arrows in C4 point to three PV positive pyramidal-like cells in AC layer VI that has conical somata and apical-like dendrites projecting toward the pia (pia toward top of page). The 'apical' dendrite of the middle cell is indicated by two arrowheads. Note that C4 comes from a younger mouse brain than C1-3. Scale bar in A3 equals 30 μm and applies to all 5 bottom panels. Scale bars in A1, B and C1 equal 100 μm. *Figure kindly provided by Dr. Raju Metherate; adapted from Cruikshank et al., 2001.*

by high cell density in a broad layer IV, dense myelination across laminae, and relatively high expression of several markers in the horizontal band involving layers III and IV (e.g., cytochrome oxidase, acetylcholinesterase, parvalbumin (Cruikshank et al., 2001; Kaas and Hackett, 2000). Several classes of pyramidal and non-pyramidal cells are distributed across the six layers of auditory cortex (Fig. 24.14; Winer, 1992). Pyramidal cells tend to be glutamatergic and are concentrated in layers III and V, whereas GABAergic cells are mainly nonpyramidal and account for about one-fourth of the neurons in most layers except layer I. Layer I has the lowest cell density (Fig. 24.14), where over 90% are small GABAergic neurons. Layer II contains both pyramidal and non-pyramidal neurons (Fig. 24.14). The smaller cells are located superficially in layer II, and the larger pyramidal cells predominate near the border with layer III. About one quarter of the nonpyramidal cells are GABAergic. Layer III is populated by several types of pyramidal and non-pyramidal cells (Fig. 24.14). The largest pyramidal cells are deeper in layer III at the border with layer IV. Their apical dendrites extend to layer I where they branch horizontally, while the basal dendrites spread widely within layers III and IV, contributing to the horizontal band involving layers III and IV. Smaller pyramidal cells populate the more superficial parts of layer III. The non-pyramidal cells of layer III include tufted, stellate, and multipolar neurons of various sizes, and tend to be GABAergic. Layer IV is mainly populated by small tufted cells, which have radially oriented somata and dendritic fields and have mainly local columnar projections (Fig. 24.14). Layer V contains

both pyramidal and nonpyramidal neurons. The somata of the conspicuous large pyramidal neurons located in V have apical dendrites that extend to layer I, with several branches along the way. The other pyramidal cells in layer V are smaller and more evenly distributed (Fig. 24.14). GABAergic cells in layer V are mainly multipolar and bipolar varieties. Layer VI has perhaps the widest variety of cell types. These include several classes of pyramidal cells, along with multipolar, bipolar, and horizontal cells (Fig. 24.14). Less than 20% of layer VI neurons are GABAergic.

The main source of ascending inputs to the core A1 and AAF are MGV and MGD, respectively (Fig. 24.1; Jones, 2007; Llano and Sherman, 2008; Winer et al., 2005). The thalamic input mostly terminates in layer IV. The organization of these connections is topographic, reflecting tonotopic organization within the MGV. MGM also projects to the core AC and moreover, it also projects broadly to all areas of auditory cortex. The intracortical connections of the core mainly include other areas of auditory cortex ipsilaterally, and sparse connections with areas beyond auditory cortex. Tonotopically-matched sites are more densely interconnected than non-matched sites (Lee et al., 2004; Lee and Winer, 2005); a feature that is likely to reflect an underlying organizational principle of the auditory cortex. Commissural connections with the contralateral AC in the opposite hemisphere are concentrated in the homotopic (matching) area, and most strongly link identical best-frequency representations in both hemispheres (Lee and Winer, 2008).

Layers V and VI represent the main source of descending projections to the thalamus and the main callosal projections include both pyramidal and non-pyramidal neurons in layers III and V. Therefore, Layers V and VI are of particular interest because their neurons form part of the corticofugal projection to the thalamus, midbrain, and pons as well as to the opposite hemisphere (Doucet et al., 2002; Games and Winer, 1988; Hefti and Smith, 2000; Llano and Sherman, 2009; Weedman et al., 1996; Weedman and Ryugo, 1996). Within layer V of the primary sensory cortex, including the AC two distinct types of pyramidal cells, 'intrinsically bursting' and 'regular spiking' have been distinguished on the basis of their correlated morphology and physiology (Hefti and Smith, 2000; Llano and Sherman, 2009; McCormick et al., 1985).

These two types of pyramidal cells are also present in A1 (Fig. 24.15), whose intrinsic electrical properties and local network inputs implicate a role of inhibition in shaping their responses (Hefti and Smith, 2000; Llano and Sherman, 2009; McCormick et al., 1985). Layer V corticothalamic neurons are large pyramidal cells, with a thick apical dendrite containing an apical tuft extending into layer 1. Most layer V corticothalamic neurons

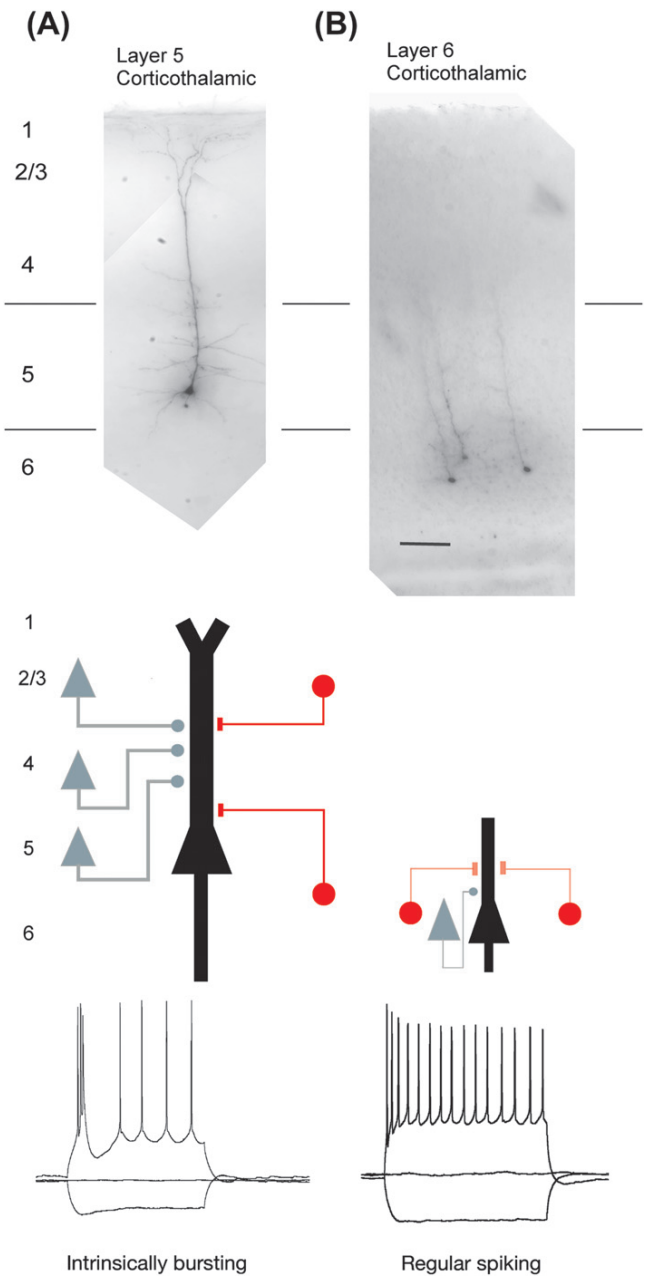

FIGURE 24.15 *Top panel*, examples of morphology of layer V and layer VI biocytin-filled corticothalamic neurons. Scale bar 100 μm; *Bottom panels*, proposed model of differences of synaptic input and response properties between auditory layer V and layer VI corticothalamic neurons. In Llano and Sherman model, layer V corticothalamic neurons receive excitatory input from neurons in layers II/III, IV, and V (gray) and GABAA-mediated inhibitory input mostly from lower layer V with a smaller contribution from layer II/III (red). In response to excitatory input, these neurons fire a burst of action potentials at low threshold. In contrast, layer VI corticothalamic neurons integrate excitatory input primarily from layer VI and receive inhibitory input from adjacent areas in layer VI. In response to excitatory input, these neurons fire a train of individual action potentials. *Figure kindly provided by Dr. Daniel Llano, adapted from Llano and Sherman, 2009.*

show bursting in response to depolarizing current pulses (Fig. 24.15), whereas layer VI corticothalamic neurons are small pyramidal neurons with short and thin apical dendrites that exhibit regular spiking in response to depolarizing current pulses (Fig. 24.15). Other layer V regular spiking neurons form part of the callosal pathway (Llano and Sherman, 2009). These authors have also demonstrated that photostimulation of layer V corticothalamic neurons integrate excitatory inputs over a significantly larger area and across more layers than do layer VI corticothalamic neurons, and that the patterns of GABAergic inhibition differ between these two cell types. The data of Llano and Sherman suggest that layer V and layer VI corticothalamic neurons receive unique sets of inputs and process them in different manners, supporting the hypothesis that layer-specific corticothalamic projections play distinct roles in information processing. In this context, it is noteworthy to mention that layer V corticothalamic neurons are drivers (Sherman and Guillery, 1998; 2002) that also relay a highly secure signal, in the form of a burst, to their subcortical targets. By contrast, layer VI neurons are modulators (Sherman and Guillery, 1998; 2002), which integrate information locally, and have spike train characteristics that are appropriate to modulate the excitability of their subcortical targets.

Areas that lie outside of the core region are often referred to as the non-lemniscal, or belt areas. These areas are anatomically and physiologically distinct from the core fields, and from one another. The number of belt fields is typically greater than the number of core fields, and they are generally less well-characterized, as research efforts have been focused on the core. Architectonically, each of the belt areas is difficult to identify; compared to the core region, cell density and myelination is generally reduced, as is the expression of cytochrome oxidase, acetylcholinesterase, and parvalbumin (Jones, 2003; Malmierca and Hackkett, 2010). In other words, there are no magic stains that cause one cortical region in the mouse to stand out unambiguously from another.

Aside from inputs from the core, the main source of projections to most of the belt areas is the MGD (Jones, 2007; Winer and Lee, 2007). Additional connections include the MGM and nuclei surrounding the MG (Fig. 24.1). In contrast to the core, areas in the belt and parabelt have widespread connections with areas outside of auditory cortex (Malmierca and Hackett, 2010), including projections to different areas of the temporal, frontal, and parietal lobes. This circumstance has been interpreted as evidence of functional segregation in the outputs of auditory cortex to different functional regions of the cortex (Rauschecker and Tian, 2000). In the mouse, the belt areas include the UF, AII and DP, all of which lack tonotopy and show complex response properties such as broad tuning curves, multiple best frequencies and selective response to frequency modulations.

THE DESCENDING AUDITORY PATHWAY

Parallel to the ascending pathways (Fig. 24.1), there are a series of descending projections extending from auditory cortex to the organ of Corti (Fig. 24.16–20). Descending pathways in the brain have been known since the end of the nineteenth century (Held, 1893) but until recently their significance was unappreciated, due to the focus on ascending pathways. The relays of this projection are also influenced by ascending fibers, and although there is some physiological evidence of inhibitory and facilitatory actions (e.g., Ryugo and Weinberger, 1976; Watanabe et al., 1966; Zhang et al., 1997), the functional role of these projections in audition is just starting to become apparent. The pioneering studies by Suga and associates using bats (e.g. Gao and Suga, 1998; 2000; Ma and Suga, 2004; 2007; Yan and Suga, 1998) and intriguingly, more recently in the mouse (Wu and Yan, 2007; Yan et al., 2005; Yan and Ehret, 2002), have started to disclose some of the details of the different functions of these descending projections.

The descending auditory system should be considered as both a descending chain (Fig. 24.16) and a series of regional feedback loops (e.g., (Fig. 24.17A; Warr, 1992). The descending chain is composed of three steps (Fig. 24.16). The first link in the chain is the AC that gives off four descending tracts: corticothalamic, corticotectal, corticopontine, and corticobulbar. The corticothalamic projection forms reciprocal and non-reciprocal connections between the AC and MG (Hofstetter and Ehret, 1992; Llano and Sherman, 2008; Winer, 2006). The corticotectal projection terminates in the IC (Faye-Lund, 1985; Herbert et al., 1991; Hofstetter and Ehret, 1992). The corticopontine projections originate in the auditory cortex and terminate in a topographic pattern that resembles that arising from somatosensory and visual cortices (Gimenez-Amaya, 1988; Perales et al., 2006). The corticobulbar projections terminate in and around the superior olivary nuclei (Mulders and Robertson, 2000; Feliciano and Potashner, 1995) and cochlear nucleus (Feliciano et al., 1995; Weedman and Ryugo, 1996; Weedman et al., 1996) in rats, and these have also been confirmed in mice and shown to form synapses on granule cell dendrites (Meltzer and Ryugo, 2006).

The second step consists of fibers arising from the IC (Fig. 24.16). These fibers constitute a colliculo-olivary and colliculo-cochlear nuclear projection. The colliculo-

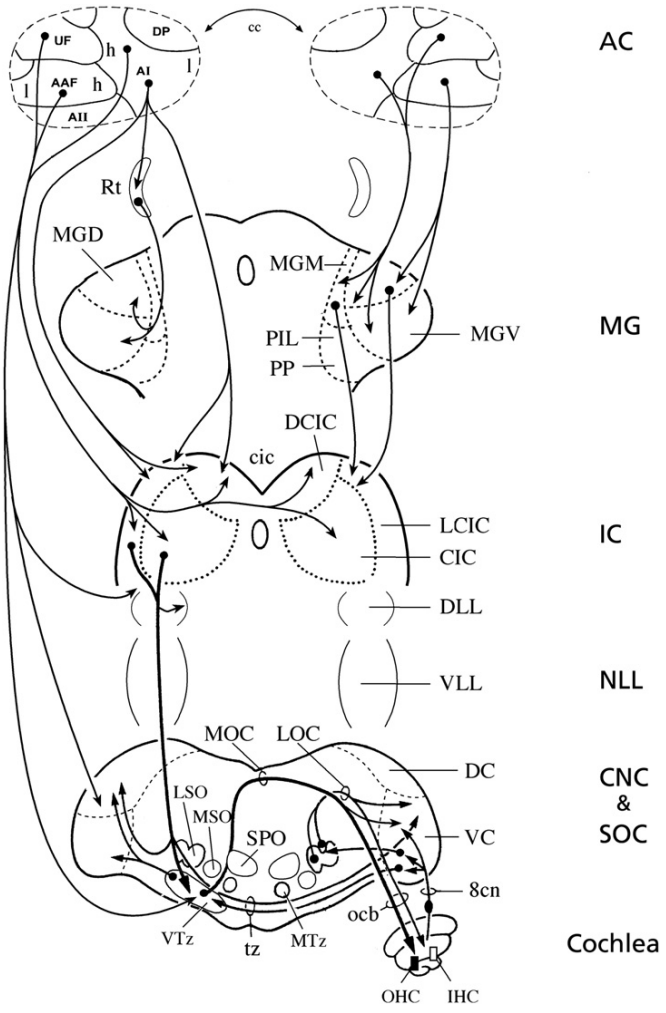

FIGURE 24.16 Descending auditory pathway of the rat. (Modified after Brodal, 1981, AC is from Stiebler et al., 1997.) For abbreviations see list.

olivary fibers arise from the LCIC and the ventral part of the CIC (Caicedo and Herbert, 1993; Faye-Lund, 1985; Vetter et al., 1993). The fibers terminate on the periolivary medial olivocochlear cells, which supply the OHCs, and probably on lateral olivocochlear cells which supply the IHCs (Feliciano and Potashner, 1995). Electrical stimulation of some IC sites produces a long-lasting (5–20 min) enhancement or suppression of compound action potentials without change in otoacoustic emissions. These novel cochlear effects have not been seen when activating MOC efferents, and so are attributed to the LOC system (Groff and Liberman, 2003). Thus, these may constitute a three-neuron pathway from the AC to the sensory cells.

The third step in the chain is the olivocochlear system (Figs. 24.19 and 24.20) that constitutes the efferent innervation of the cochlea, which consists of the MOC and LOC (see below). In addition, the series of feedback loops comprise cortical projections to subcortical nuclei that project back to cortex, directly or indirectly, allowing it to control its inputs from lower centers. Thus, there are mechanisms to modulate and/or 'gate' ascending auditory information at virtually every synaptic station in the pathway.

The Corticofugal Pathways

The mouse AC projects to a wide range of subcortical targets in the auditory pathway (Winer, 2006; Winer and Lee, 2007). The projections to the auditory thalamus and midbrain are the largest, but there are also the projections to subcollicular nuclei (Fig. 24.16), including nucleus sagulum, paraleminical regions, superior olivary complex, cochlear nuclear complex and pontine nuclei (Doucet et al., 2002, 2003; Feliciano and Potashner, 1995; Meltzer and Ryugo, 2006; Perales et al., 2006; Weedman and Ryugo, 1996). The AC also supplies the amygdala (Romanski and LeDoux, 1993), basal ganglia, striatum (Beneyto and Prieto, 2001), superior colliculus (Paula-Barbosa and Sousa-Pinto, 1973), and central gray (Winer et al., 1998), suggesting that the AC has important roles not only in auditory sensory processing but also in motor behavior, autonomic function, and state dependent responses (Winer, 2006).

In the auditory thalamus, The MGV receives the heaviest source of input from A1 and AAF, whereas the MGM receives the least and the MGD receives an intermediate amount. A prominent feature of the corticothalamic projection is its reciprocity; a cortical region projects to the same part of the thalamus from which it receives input. However there are also non-overlapping zones (Llano and Sherman, 2008). In the MG, there are two main types of synaptic terminals (I and II) arising from A1 and AAF (Fig. 24.16). Type I terminals are small (< 1 μm in long-axis diameter), associate with small caliber dendrites of the MGV and MGD and arise from the pyramidal cells of layer VI (Bartlett et al., 2000; Llano and Sherman, 2009). Type II terminals are large (>2 μm in long-axis diameter), mostly distributed in the MGD and occasionally in the MGM (Bartlett et al., 2000; Llano and Sherman, 2009) and arise from pyramidal neurons from layer V.

As mentioned above, reciprocity is a prominent feature of the corticothalamic projection. These connections could serve a feedback function, classically regarded as the primary role of corticothalamic projections (Fig. 24.17A). The non-reciprocal connections, however, may provide feedforward effects, such that a specific cortical region sends information to a distant or different cortical region via the thalamus. Thus, feedback and feedforward mechanisms can be viewed within a broader framework of cortico-thalamo-cortical loops that relate the pathways to axon morphology

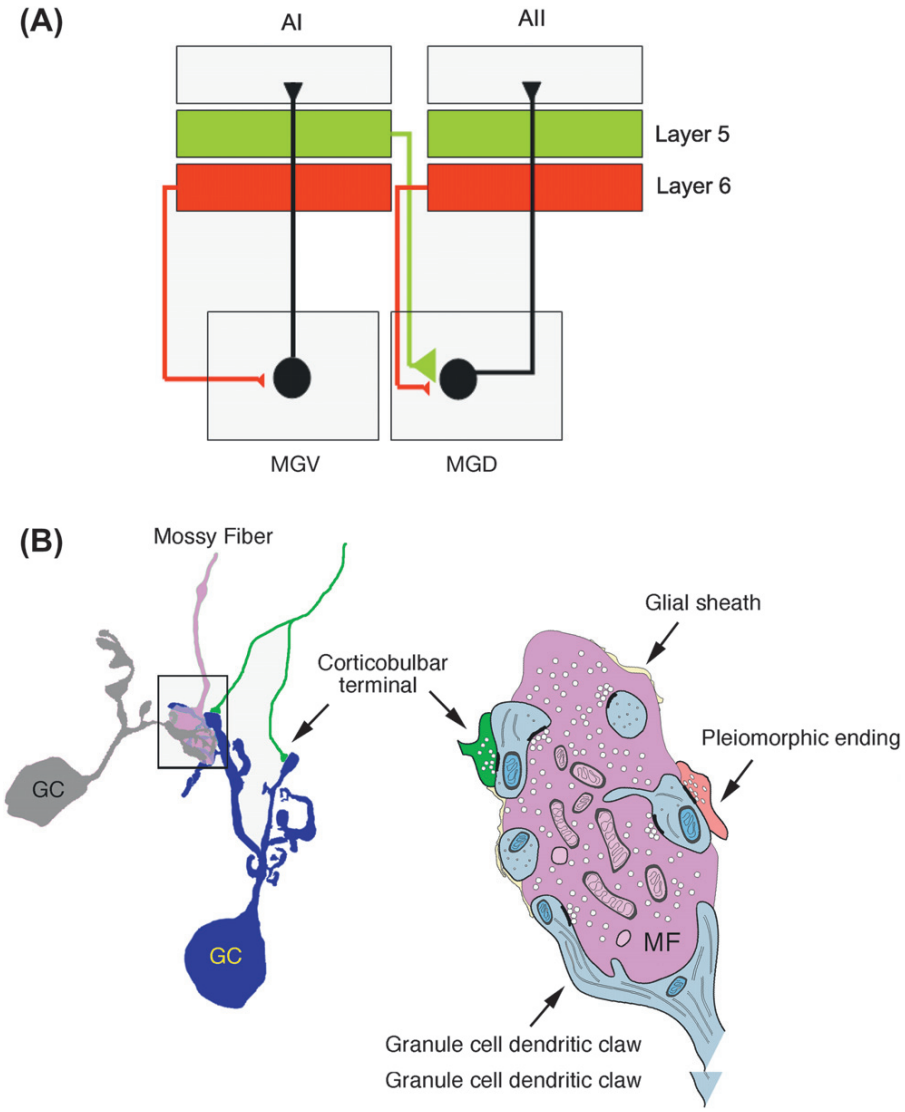

FIGURE 24.17 (A) Diagram illustrating a cortico-thalamocortical model of cortical processing. In this model, information reaches the lemniscal AC via a projection from the MGV to layer IV of either the AAF or the AI. From here, a layer 5 pyramidal projects to the MGD, where a thalamocortical relay cell projects to layer IV of the nonlemniscal AC (DP or AII). From the nonlemniscal AC, a layer VI projection is sent to the MGB, adhering to the principle that all thalamocortical projections, whether coming from the first or higher order thalamus, receive a modulator, reciprocal projection from layer VI. (Figure kindly provided by Dr. Daniel Llano, adapted from Llano and Sherman, 2008.) (B) Summary diagram of the synaptic glomerulus contributed to by mossy fibers, granule cell dendrites, and corticobulbar endings. The small size and remote location of the cortical terminals suggest that the postsynaptic effect is modulatory. (From Meltzer and Ryugo, 2006.)

and physiological effects on thalamic cells. Sherman and Guillery (1996) originally proposed the concept of 'drivers' and 'modulators' of thalamic neurons for the visual and somatosensory thalamus, but a recent study in the mouse has confirmed this idea for the auditory system (Llano and Sherman, 2008). According to their hypothesis, the type I terminals in MGV and MGD described above might play a modulatory role in the first-order thalamic nuclei, such that corticothalamic inputs converge with ascending inputs on thalamic neurons where the ascending inputs would drive these thalamic neurons and the cortical inputs would modulate them. In contrast, in 'higher order' thalamic nuclei such as the MGD, 'driver' inputs arise from the large type II terminals and interact with other ascending input from the IC (Fig. 24.17A). Direct visualization of actual synapses using electron microscopy, however, is required for validation of this idea and the 'other ascending inputs' need to be defined.

Although the corticofugal projections appear to be glutamatergic (Potashner et al., 1988), suggesting an excitatory function, electrical stimulation of the AC results in both excitatory and inhibitory effects on MG neurons (Ryugo and Weinberger, 1976; Watanabe et al., 1966; Wu and Yan, 2007). Since the AC also projects to the auditory sector of the reticular thalamic nucleus, which in turns projects to the MG, the AC can provide the MG with an inhibitory influence (Bartlett et al., 2000). The corticofugal projection, therefore, can modulate the MG responses to sound through a direct excitatory pathway and/or an indirect inhibitory pathway.

The first report on corticollicular projections was from the temporal cortex to the *corpora quadrigemina* in

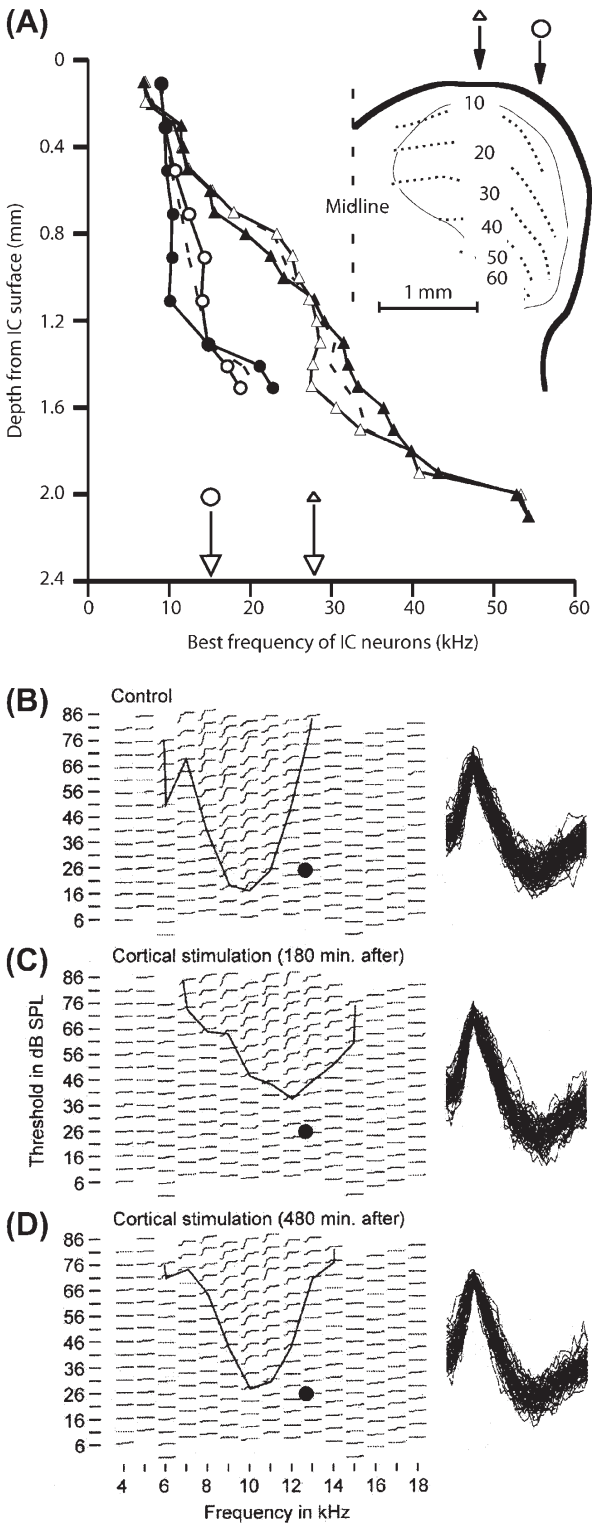

FIGURE 24.18 *Top panel*, BF of collicular neurons recorded in two separate penetrations through the CIC. Note that collicular BF increases systematically as a function of depth (circles and triangles). When the AC is stimulated electrically, the BF shift to the BF of the site at the AC (open arrows and opened circles and triangles, 3 hours after cortical stimulation). After 8 hours post-stimulation, the responses tend to return to the original control. Reproduced from Yan and Ehret, 2001 with permission). *Bottom panels*, example of a single frequency response area of a well-isolated neuron from the CIC before (A) and after cortical stimulation (B, 180 min. after and C, 480 min. after). The BF of the collicular neuron was 10 kHz and threshold was about 25 dB SPL. After cortical stimulation at 12.5 kHz (indicated by dots), the collicular neuron shifted its BF and threshold (B), and recovers about 8 hours later (C). Note that the spike waveform for this unit was unchanged through the 8 hours period. The excitatory frequency response area was significantly changed after cortical stimulation. (Reproduced from Yan et al. 2004.)

the primate by Thompson (1900). Since then, a number of studies have confirmed and extended the knowledge of this pathway in several species (reviewed in Malmierca and Ryugo, 2010) including the mouse (Hofstetter and Ehret, 1992). Most of these studies have emphasized that the AC innervates the collicular cortices only in a topographic fashion. However, studies in the rat (Beyerl, 1978; Saldana et al., 1996) demonstrated that A1 also projects into the CIC. The cellular origin of these projections is mostly the pyramidal cells in layer V and to a lesser extent in layer VI (Doucet et al., 2003).

Studies in guinea pigs have demonstrated the glutamatergic nature of this projection (Feliciano and Potashner, 1995). While this study suggests a purely excitatory corticollicular projection, electrical stimulation of the auditory cortex in the cat (Mitani et al., 1983), or its inactivation in the rat using tetrodotoxin (Nwabueze-Ogbo et al., 2002) produces not only excitatory but also inhibitory interactions in the IC neurons. Therefore, as with the MG, AC may modulate the processing of sounds in the IC through the activation of local inhibitory connections within the IC. Physiological studies have demonstrated that these descending projections may serve to sharpen and amplify ascending inputs of the same best frequency as the site of cortical activation (Gao and Suga, 1998; Gao and Suga, 2000; Yan et al., 2005; Yan and Ehret, 2001; Yan and Ehret, 2002; Yan and Zhang, 2005). This effect is called 'egocentric selection' (Zhang et al., 1997). Furthermore, the general shapes of frequency response areas are altered in the mouse (Fig. 24.18), meaning that AC influences spectral processing in the IC (Yan et al., 2005). Thus, a key role of the mammalian corticofugal system may be to modulate subcortical sensory maps in response to sensory experience (Yan and Suga, 1998).

Several studies have observed a direct neocortical projection to auditory brainstem nuclei (Feliciano and Potashner, 1995; Kuypers and Lawrence, 1967; Weedman et al., 1996; Weedman and Ryugo, 1996). These studies have demonstrated that A1 sends direct projections to regions surrounding the lateral lemniscus, including the nucleus sagulum ipsilaterally and bilaterally to SOC and CNC, namely the VTz, LSO, a narrow region that overlies the dorsal aspect of the SOC, the

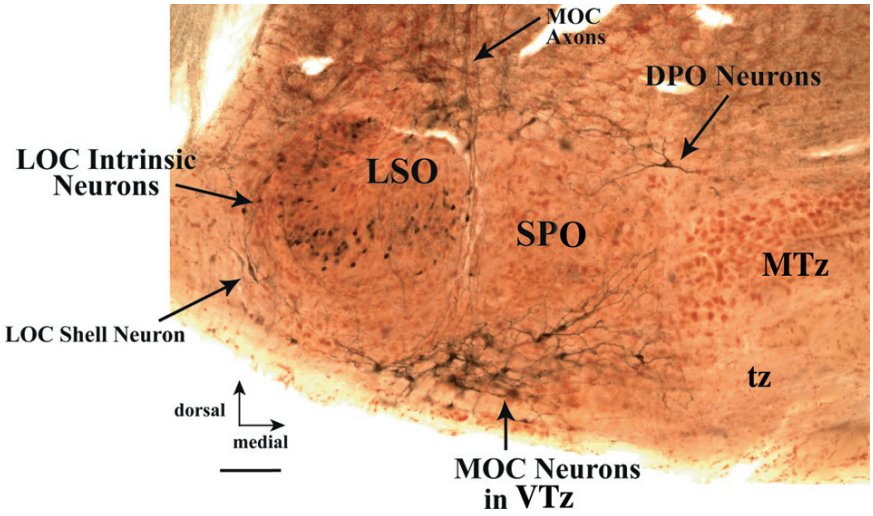

FIGURE 24.19 Dark AChE staining (black) in presumed OC neurons in the SOC in a photomicrograph of a transverse section through the left side of the mouse brainstem. Most MOC neurons are in the VTz and extend dendrites medially toward the trapezoid body (tz). A few stained neurons are located more dorsally, in the DPO, and extend dendrites in all directions. Stained MOC axons are visible projecting dorsally, which eventually form the OC bundle. More lightly stained presumed LOC neurons are seen within (intrinsic neurons) and on the margins of (shell neurons) the LSO. LOC dendrites and axons are not as well stained. Neutral Red counterstain. Scale bar 100 μm. *Figure kindly provided by Dr. M. Chris Brown, adapted from Brown and Levine, 2008.*

DC and to the granule cells domain in the VC (Fig. 24.16, 24.17B). Since this descending input terminates on the LSO, perhaps neurons of the LOC (at least in the shell, *v.i.*) are probably involved in more than just feedback loops to the cochlea. Before we focus our attention on the descending projections from the midbrain to the brainstem, we should cite reports on descending projections from the MG to the IC in several species (Senatorov and Hu, 2002). The projection originates in the MGM and MGD and terminates in the LCIC, suggesting a role in multisensory processing (Fig. 24.16; Kuwabara and Zook, 2000).

The Colliculofugal Pathways

Studies in the rat and guinea pig have shown that the IC provides descending projections to the LL, SOC and CNC (Fig. 24.16; Caicedo and Herbert, 1993; Faye-Lund, 1985; Malmierca et al., 1996; Vetter et al., 1993). The *colliculo-lemniscal* projections are largely confined to the dorsal nucleus, the sagulum, the horizontal cell group, and the perilemniscal zone (Caicedo and Herbert, 1993). The *colliculo-olivary* projections originate in the CIC and LCIC and terminate in band of terminals that extends from the RPO to the VTz (Caicedo and Herbert, 1993; Faye-Lund, 1985; Malmierca et al., 1996; Vetter et al., 1993). This projection is topographic and the terminal fibers overlap with the site of origin of the MOC (White and Warr, 1983), suggesting that the IC influences MOC neurons (Mulders and Robertson, 2005; Vetter et al., 1993). In fact, electrical stimulation of the IC produces an increase in the latency and a reduction in the amplitude of the auditory whole-nerve response as well as the temporal threshold shift that appears after the exposure to a loud noise. These effects are similar to those elicited by electrical stimulation of the MOC (Rajan, 1990). Finally, the *colliculo-cochlear nucleus* projection originates in the CIC and LCIC and targets the DC and granule cell domain of the VC (Caicedo and Herbert, 1993; Rajan, 1990), but the functional role of this projection it still unknown.

It should be mentioned that the IC also projects to non-traditional auditory nuclei, including the pontine nuclei, lateral paragigantocellular nucleus, gigantocellular reticular nucleus, ventrolateral tegmental nucleus and caudal pontine reticular nucleus (Caicedo and Herbert, 1993). As these nuclei also receive auditory projections they may play some role in acoustically

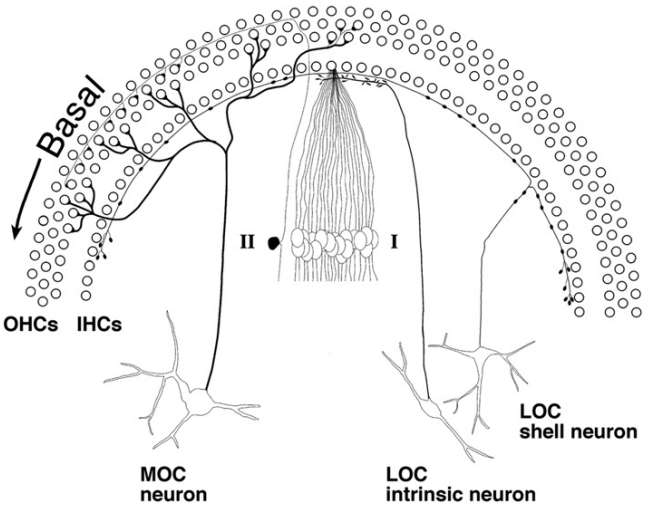

FIGURE 24.20 Scheme of the LOC and MOC neurons and their projections to the IHCs and OHCs respectively. Two types of LOC cells occur: intrinsic located inside the LSO and shell located in the margins of the LSO. Afferent fibers type I and type II projecting to the CNC are also represented. Note the convergence of type I onto single IHCs. *Figure kindly provided by Dr. Bruce Warr, adapted from Warr, 1992.*

elicited responses such as autonomic and auditory-motor behaviors (Caicedo and Herbert, 1993).

The Olivocochlear System

The olivocochlear bundle provides the organ of Corti with the efferent innervation (Rasmussen, 1940; 1946). It should be noted that the auditory-vestibular system appears unique among sensory systems because hair cell receptors receive direct projections from the brain (Robertson, 2009). In the auditory system, there are medial (MOC) and lateral (LOC) olivocochlear neurons (Figs. 24.3, 24.16, 24.19, 24.20; Warr, 1992; White and Warr, 1983). The MOC neurons are located medial and ventral within the SOC and project mainly to the contralateral cochlea, whereas the LOC neurons are located within or near the LSO and project to the ipsilateral cochlea (Brown and Levine, 2008; Campbell and Henson, 1988; Maison et al., 2003; Warr, 1992).

The MOC neurons (Figs. 24.3, 24.16, 24.19 and 24.20) innervate the OHCs using thick myelinated axons that terminate directly on the OHCs. Approximately 75% (Campbell and Henson, 1988; Maison et al., 2007; Warr, 1992; White and Warr, 1983) originate in the contralateral side and the reminder in the ipsilateral side (Brown and Levine, 2008; Wilson et al., 1991). MOC neurons (Figs. 24.19 and 24.20) have generally large cell bodies, are star- or triangle-shaped, and possess dendritic arbors that radiate, branch profusely, and taper (Fig. 24.19; Brown and Levine, 2008; Campbell and Henson, 1988; Maison et al., 2007). They are located in the VTz and constitute a neurochemically homogeneous population of cholinergic cells (Fig. 24.19; Brown and Levine, 2008; Campbell and Henson, 1988; Maison et al., 2007). They may receive descending input from the ipsilateral IC and ascending input bilaterally from the VC. It has also been suggested that some neurons in the dorsomedial periolivary region in the mouse may belong to the MOC (Brown and Levine, 2008).

The LOC neurons predominantly innervate the region beneath the IHCs on the ipsilateral side (Figs. 24.3, 24.16, 24.19 and 24.20; Brown et al., 1988; Campbell and Henson, 1988; Wilson et al., 1991). In rats, two distinct types of neurons form the LOC, *intrinsic* and *shell* neurons (Vetter and Mugnaini, 1992; Warr et al., 1997). They are also present in mouse (Fig. 24.19; Brown and Levine, 2008). All *intrinsic neurons* are small cells confined within the limits of the ipsilateral LSO. They possess disc-shaped dendritic arbors with thin, untapered dendrites and constitute about 85% of all LOC neurons (Fig. 24.19; Brown and Levine, 2008; Vetter and Mugnaini, 1992; Warr et al., 1997).

The intrinsic neurons probably receive the same input as the principal cells in the LSO. Some of them are GABAergic and the remainder are cholinergic and colocalize calcitonin gene-related peptide (Vetter et al., 1999; but see Maison et al., 2003). Their axons are thin and unmyelinated, travel relatively short distances in the inner spiral bundle, and terminate forming discrete arborizations with a focal, tonotopic organization (Warr et al., 1997; Wilson et al., 2001). Most *shell neurons* are distributed around the borders of the LSO (Fig. 24.19; Brown and Levine, 2003). They are large multipolar cells with thick and tapered dendrites, and constitute the remaining 15% of the LOC neurons (Fig. 24.19; Vetter and Mugnaini, 1992; Warr et al., 1997). Little is known about the source of the inputs they receive, although one source could be small cells of the cochlear nucleus cap (Ye et al., 2000). Only one third of these shell neurons are GABAergic, whereas the other two thirds are cholinergic but do not co-localize calcitonin gene-related peptide (Vetter et al., 1991; Maison et al., 2003). Their axons are thin and unmyelinated, travel long distances in the inner spiral bundle, and terminate as diffuse arborizations that are probably not tonotopic (Warr et al., 1997).

Physiological studies in several species have shown that MOC neurons are sharply tuned with a wide dynamic range. MOC neurons may enhance transduction or signal detection through an unmasking effect, thus regulating the slow motility of the OHCs and thereby the stiffness of the basilar membrane (Eggermont, 2001). MOC activity can also reduce temporary threshold shift by inhibiting cochlear sensitivity and thereby protect the inner ear from acoustic injury (Taranda et al., 2009).

The functional role of the LOC is still unclear. However several immunocytochemical studies have shown that these neurons contain neuroactive substances such as dopamine, serotonin, and opioid peptides (e.g., Safieddine et al., 1997; Safieddine and Eybalin, 1992), which speaks in favor of a modulatory effect on the IHCs afferents. More recently, Rajan (2000) has shown in cats that in background noise there is a conjoint activation of the MOC and LOC to protect the inner ear (by almost 30 dB) from loud sounds that otherwise would be exacerbated by the noise (Rajan, 2000). In summary, the olivocochlear system plays a critical role in maintaining the normal operating of the cochlea and may introduce non-linear dynamics (Eggermont, 2001) into the auditory system.

Acknowledgments

We are especially grateful for the work of our colleagues who made this review possible. We specially thank Drs. J.G.G. Borst, M.C. Brown; D. Furness, D. Llano; R. Metherate and W.B. Warr for proving us with beautiful original illustrations. The authors were supported by grants from the Spanish MEC (BFU2009-07286), EU (EUI2009-04083) and JCYL-UE (GR221) to MSM, and NIH grants DC00232 and DC04395, a grant from the New South Wales Office for Science & Medical Research, and a grant from the Australian NHMRC #1009482 to DKR.

ABBREVIATION LIST

Aq	Aqueduct (Sylvius)
AC	Auditory cortex
AMPA	α-amino-3-hydroxy-5-methyl-4-isoxazolepropionic acid
bic	Brachium of the inferior colliculus
C	Caudal
Cb	Cerebellum
cc	Corpus callosum
CIC	Central nucleus of the inferior colliculus
cic	Commissure of the inferior colliculus
cll	Commissure of the lateral lemniscus (Probst)
CNC	Cochlear nuclear complex
DAS	Dorsal acoustic stria
D	Dorsal
DC	Dorsal cochlear complex
DCIC	Dorsal cortex of the inferior colliculus
DLL	Dorsal nucleus of the lateral lemniscus
DPO	Dorsal periolivary region
EPSP	Excitatory postsynaptic potential
ECIC	External cortex of the inferior colliculus
EE	Excitatory-excitatory
EI	Excitatory-inhibitory
Ep	Ependyma
F	Flat neurons
FS	Fast spiking
GABA	γ-aminobutyric acid
GAD	Glutamic acid decarboxylase
GrC	Granule cell layer
h	High frequency region
IAS	Intermediate acoustic stria
IB	Intrinsically bursting
IC	Inferior colliculus
icp	Inferior cerebellar peduncle
IHC	Inner hair cell
IPSP	Inhibitory postsynaptic potential
l	Low frequency region
L	Lateral
LF	Less flat neurons
ll	Lateral lemniscus
LPO	Lateral periolivary zone
LVPO	Lateroventral periolivary zone
LOC	Lateral olivocochlear system
LR4V	Lateral recess of the fourth ventricle
LSO	Lateral superior olive
LTz	Lateral nucleus of the trapezoid body
M	Medial
MG	Medial geniculate body
MGD	Dorsal division of the medial geniculate body
MGM	Medial division of the medial geniculate body
MGV	Ventral division of the medial geniculate body
MOC	Medial olivocochlear system
MSO	Medial superior olive
MTz	Medial nucleus of the trapezoid body
MVPO	Medioventral periolivary zone
NLL	Nuclei of the lateral lemniscus
NMDA	*N*-methyl-D-aspartate
ocb	Olivocochlear bundle
OHC	Outer hair cells
PAG	Periaqueductal gray matter
PIL	Posterior intralaminar nucleus
PnC	Pontine reticular nucleus, caudalis
PO	Periolivary regions
PP	Peripeduncular nucleus
PSTH	Peristimulus histogram
R	Rostral
ReIC	Recess of the inferior colliculus
RS	Regular spiking
Rt	Auditory sector of the reticular thalamic nucleus
SC	Superior colliculus
SOC	Superior olivary complex
SpG	Spiral ganglion
sp5	Spinal trigeminal tract
SPO	Superior paraolivary nucleus
Tz	Nucleus of the trapezoid body
tz	Trapezoid body (ventral acoustic stria)
V	Ventral
VAS	Ventral acoustic stria
VC	Ventral cochlear complex
VCA	Anteroventral cochlear complex
VCP	Posteroventral cochlear complex
VLL	Ventral complex of the lateral lemniscus
VTT	Ventrotubercular tract
VTz	Ventral nucleus of the trapezoid body
4V	4^{th} ventricle
5	Trigeminal ganglion
7	Facial nucleus

8cn	Cochlear root of the vestibulocochlear nerve
8vn	Vestibular root of the vestibulocochlear nerve

References

Adams JC. Ascending projections to the inferior colliculus. *J Comp Neurol* 1979;183:519–538.

Adams JC. Cytology of periolivary cells and the organization of their projections in the cat. *J Comp Neurol* 1983;215:275–289.

Aitkin LM, Kenyon CE, Philpott P. The representation of the auditory and somatosensory systems in the external nucleus of the cat inferior colliculus. *J Comp Neurol* 1981;196:25–40.

Aitkin LM, Dickhaus H, Schult W, and Zimmermann M. External nucleus of inferior colliculus: auditory and spinal somatosensory afferents and their interactions. *J Neurophysiol* 1978;41:837–847.

Amann LC, Halene TB, Ehrlichman RS, et al. Chronic ketamine impairs fear conditioning and produces long-lasting reductions in auditory evoked potentials. *Neurobiol Dis* 2009;35,311–317.

Arnott RH, Wallace MN, Shackleton TM, and Palmer AR. Onset neurones in the anteroventral cochlear nucleus project to the dorsal cochlear nucleus. *J Assoc Res Otolaryngol* 2004;5:153–170.

Babalian AL, Ryugo DK, Rouiller EM. Discharge properties of identified cochlear nucleus neurons and auditory nerve fibers in response to repetitive electrical stimulation of the auditory nerve. *Exp Brain Res* 2003;153:452–460.

Bajo VM, Merchan MA, Lopez DE, and Rouiller EM. Neuronal morphology and efferent projections of the dorsal nucleus of the lateral lemniscus in the rat. *J Comp Neurol* 1993;334:241–262.

Banks MI, and Smith PH. Intracellular recordings from neurobiotin-labeled cells in brain slices of the rat medial nucleus of the trapezoid body. *J Neurosci* 1992;12:2819–2837.

Bartlett EL, and Smith PH. Anatomic, intrinsic, and synaptic properties of dorsal and ventral division neurons in rat medial geniculate body. *J Neurophysiol* 1999;81:1999–2016.

Bartlett EL, Stark JM, Guillery RW, and Smith PH. Comparison of the fine structure of cortical and collicular terminals in the rat medial geniculate body. *Neuroscience* 2000;100:811–828.

Beneyto M, and Prieto JJ. Connections of the auditory cortex with the claustrum and the endopiriform nucleus in the cat. *Brain Res Bull* 2001;54:485–498.

Berglund AM, Benson TE, and Brown MC. Synapses from labeled type II axons in the mouse cochlear nucleus. *Hear Res* 1996;94:31–46.

Berglund AM, and Brown MC. Central trajectories of type II spiral ganglion cells from various cochlear regions in mice. *Hear Res* 1994;75:121–130.

Berglund AM, and Ryugo DK. Hair cell innervation by spiral ganglion neurons in the mouse. *J Comp Neurol* 1987;255:560–570.

Beyerl BD. Afferent projections to the central nucleus of the inferior colliculus in the rat. *Brain Res* 1978;145:209–223.

Blackstad TW, Osen KK, and Mugnaini E. Pyramidal neurones of the dorsal cochlear nucleus: a Golgi and computer reconstruction study in cat. *Neuroscience* 1984;13:827–854.

Bosher SK, and Warren RL. Observations on the electrochemistry of the cochlear endolymph of the rat: a quantitative study of its electrical potential and ionic composition as determined by means of flame spectrophotometry. *Proc R Soc Lond B Biol Sci* 1968;171: 227–247.

Brown MC, and Benson TE. Transneuronal labeling of cochlear nucleus neurons by HRP-labeled auditory nerve fibers and olivocochlear branches in mice. *J Comp Neurol* 1992;321:645–665.

Brown MC, Berglund AM, Kiang NY, and Ryugo DK. Central trajectories of type II spiral ganglion neurons. *J Comp Neurol* 1988;278:581–590.

Brown MC, and Ledwith JV, III. Projections of thin (type-II) and thick (type-I) auditory-nerve fibers into the cochlear nucleus of the mouse. *Hear Res* 1990;49:105–118.

Brown MC, and Levine JL. Dendrites of medial olivocochlear neurons in mouse. *Neuroscience* 2008;154:147–159.

Brown MC, and Liu TS. Fos-like immunoreactivity in central auditory neurons of the mouse. *J Comp Neurol* 1995;357:85–97.

Brown MC, Pierce S, and Berglund AM. Cochlear-nucleus branches of thick (medial) olivocochlear fibers in the mouse: a cochleotopic projection. *J Comp Neurol* 1991;303:300–315.

Caicedo A, and Herbert H. Topography of descending projections from the inferior colliculus to auditory brainstem nuclei in the rat. *J Comp Neurol* 1993;328:377–392.

Campbell JP, and Henson MM. Olivocochlear neurons in the brainstem of the mouse. *Hear Res* 1988;35:271–274.

Cant NB. The fine structure of two types of stellate cells in the anterior division of the anteroventral cochlear nucleus of the cat. *Neuroscience* 1981;6:2643–2655.

Cant NB. Identification of cell types in the anteroventral cochlear nucleus that project to the inferior colliculus. *Neurosci Lett* 1982;32:241–246.

Cant NB, and Benson CG. Parallel auditory pathways: projection patterns of the different neuronal populations in the dorsal and ventral cochlear nuclei. *Brain Res Bull* 2003;60:457–474.

Casseday JH, Fremouw T, and Covey E. The inferior colliculus. A hub for the central audiotory system. In: Oertel, D., Popper, A.N., and Fay, R.R. Eds. New York: Springer *Handbook of Auditory Research*, Springer; 2002.

Cheatwood JL, Reep RL, and Corwin JV. The associative striatum: cortical and thalamic projections to the dorsocentral striatum in rats. *Brain Res* 2003;968:1–14.

Chen L, Kelly JB, and Wu SH. The commissure of probst as a source of GABAergic inhibition. *Hear Res* 1999;138:106–114.

Clugnet MC, LeDoux JE, and Morrison SF. Unit responses evoked in the amygdala and striatum by electrical stimulation of the medial geniculate body. *J Neurosci* 1990;10:1055–1061.

Covey E. The monaural nucleus of the lateral lemniscus, parallel pathways from the cochelar nucleus to midbrain. In Merchán, M, Juiz J, Godfrey D A, Muganini E. Eds. *The mammalian cochlear nuclei, organization and Function*. New York :Plenunm Press; 1993:321–334.

Covey E, Kauer JA, and Casseday JH. Whole-cell patch-clamp recording reveals subthreshold sound-evoked postsynaptic currents in the inferior colliculus of awake bats. *J Neurosci* 1996;16:3009–3018.

Cruikshank SJ, Killackey HP, and Metherate R. Parvalbumin and calbindin are differentially distributed within primary and secondary subregions of the mouse auditory forebrain. *Neuroscience* 2001;105:553–569.

Dallos P. The active cochlea. *J Neurosci* 1992;12:4575–4585.

Dehmel S, Kopp-Scheinpflug C, Dorrscheidt GJ, and Rubsamen R. Electrophysiological characterization of the superior paraolivary nucleus in the Mongolian gerbil. *Hear Res* 2002;172:18–36.

Doron NN, LeDoux JE, and Semple MN. Redefining the tonotopic core of rat auditory cortex: physiological evidence for a posterior field. *J Comp Neurol* 2002;453:345–360.

Doucet JR, Molavi DL, and Ryugo DK. The source of corticocollicular and corticobulbar projections in area Te1 of the rat. *Exp Brain Res* 2003;153:461–466.

Doucet JR, Rose L, and Ryugo DK. The cellular origin of corticofugal projections to the superior olivary complex in the rat. *Brain Res* 2002;925:28–41.

Doucet JR, Ross AT, Gillespie MB, and Ryugo DK. Glycine immunoreactivity of multipolar neurons in the ventral cochlear nucleus which project to the dorsal cochlear nucleus. *J Comp Neurol* 1999;408:515–531.

Doucet JR, and Ryugo DK. Projections from the ventral cochlear nucleus to the dorsal cochlear nucleus in rats. *J Comp Neurol* 1997;385:245–264.

Doucet JR, Ryugo DK. Axonal pathways to the lateral superior olive labeled with biotinylated dextran amine injections in the dorsal cochlear nucleus of rats. *J Comp Neurol* 2003;461:452–465.

Echteler SM, Fay RR, and Popper AN. Structure of the mammalian cochlea, In: Fay RR and Popper AN Eds. *Comparative Hearing, Mammals*. Berlin:Springer-Verlag; 1994.

Edeline JM. Learning-induced physiological plasticity in the thalamo-cortical sensory systems: a critical evaluation of receptive field plasticity, map changes and their potential mechanisms. *Prog Neurobiol* 1999;57:165–224.

Edeline JM. The thalamo-cortical auditory receptive fields: regulation by the states of vigilance, learning and the neuromodulatory systems. *Exp Brain Res* 2003;153:554–572.

Eggermont JJ. Between sound and perception: reviewing the search for a neural code. *Hear Res* 2001;157:1–42.

Egorova M, and Ehret G. Tonotopy and inhibition in the midbrain inferior colliculus shape spectral resolution of sounds in neural critical bands. *Eur J Neurosci* 2008;28:675–692.

Egorova M, Ehret G, Vartanian I, and Esser KH. Frequency response areas of neurons in the mouse inferior colliculus. I Threshold and tuning characteristics *Exp Brain Res* 2001;140:145–161.

Egorova M, Vartanyan I, and Ehret G. Frequency response areas of mouse inferior colliculus neurons: II. Critical bands *Neuroreport* 2006;17:1783–1786.

Egorova MA, Vartanyan IA, and Ehret G. Neural critical bands and inhibition in the auditory midbrain of the house mouse (Mus domesticus). *Dokl Biol Sci* 2002;382:5–7.

Ehret G. Critical bands and filter characteristics in the ear of the housemouse (Mus musculus). *Biol Cybern* 1976a;24,35–42.

Ehret G. Temporal auditory summation for pure tones and white noise in the house mouse (Mus musculus). *J Acoust Soc Am* 1976b;59:1421–1433.

Ehret G. Stiffness gradient along the basilar membrane as a basis for spatial frequency analysis within the cochlea. *J Acoust Soc Am* 1978;64:1723–1726.

Ehret G. Quantitative analysis of nerve fibre densities in the cochlea of the house mouse (Mus musculus). *J Comp Neurol* 1979;183:73–88.

Ehret G, Egorova M, Hage SR, and Muller BA. Spatial map of frequency tuning-curve shapes in the mouse inferior colliculus. *Neuroreport* 2003;14:1365–1369.

Ehret G, and Moffat AJM. Inferior colliculus of the house mouse. IIsingle-unit response to tones, noise and tone-noise combinations as a function of sound intensity. *J Comp Phyiol A* 1985a;156:619–635.

Ehret G, and Moffat AJM. Inferior colliculus of the house mouse. III Response probabilities and thresholds of single units to synthetized mouse calls compared to tone and noise bursts. *J Comp Phyiol A* 1985b;156:637–644.

Ehret G, and Schmid C. Reproductive cycle-dependent plasticity of perception of acoustic meaning in mice. *Physiol Behav* 2009;96:428–433.

Ehrlichman RS, Luminais SN, White SL, et al. Neuregulin 1 transgenic mice display reduced mismatch negativity, contextual fear conditioning and social interactions. *Brain Res* 2009;1294:116–127.

Engström H. On the double innervation of the sensory epithelia of the inner ear. *Acta Otolaryngol* 1958;49:109–118.

Faye-Lund H. The neocortical projection to the inferior colliculus in the albino rat. *Anat Embryol (Berl)* 1985;173:53–70.

Faye-Lund H, and Osen KK. Anatomy of the inferior colliculus in rat. *Anat Embryol (Berl)* 1985;171:1–20.

Fekete DM, Rouiller EM, Liberman MC, and Ryugo DK. The central projections of intracellularly labeled auditory nerve fibers in cats. *J Comp Neurol* 1984;229:432–450.

Feliciano M, and Potashner SJ. Evidence for a glutamatergic pathway from the guinea pig auditory cortex to the inferior colliculus. *J Neurochem* 1995;65:1348–1357.

Feliciano M, Saldana E, and Mugnaini E. Direct projection from the rat primary auditory neocrotex to the nucleus sagulum, paralemniscal regions, superior olivary complex and cochlear nuclei. *Aud Neureosci* 1995;1:287–308.

Felix RA, and Portfors CV. Excitatory, inhibitory and facilitatory frequency response areas in the inferior colliculus of hearing impaired mice. *Hear Res* 2007;228:212–229.

Fichtel I, and Ehret G. Perception and recognition discriminated in the mouse auditory cortex by c-Fos labeling. *Neuroreport* 1999;10:2341–2345.

Floris A, Diño M, Jacobowitz DM, Mugnaini E. The unipolar brush cells of the rat cerebellar cortex and cochlear nucleus are calretinin-positive: A study by light and electron microscopic immunocyto-chemistry. *Anat Embryol* 1994;189:495–520.

Francis HW, Rivas A, Lehar M, and Ryugo DK. Two types of afferent terminals innervate cochlear inner hair cells in C57BL/6J mice. *Brain Res* 2004;1016:182–194.

Friedland DR, Pongstaporn T, Doucet JR, and Ryugo DK. Ultrastructural examination of the somatic innervation of ventrotubercular cells in the rat. *J Comp Neurol* 2003;459:77–89.

Galindo-Leon EE, Lin FG, and Liu RC. Inhibitory plasticity in a lateral band improves cortical detection of natural vocalizations. *Neuron* 2009;62:705–716.

Games KD, and Winer JA. Layer V in rat auditory cortex: projections to the inferior colliculus and contralateral cortex. *Hear Res* 1988;34:1–25.

Gao E, and Suga N. Experience-dependent plasticity in the auditory cortex and the inferior colliculus of bats: role of the corticofugal system. *Proc Natl Acad Sci USA* 2000;97:8081–8086.

Gao E, and Suga N. Experience-dependent corticofugal adjustment of midbrain frequency map in bat auditory system. *Proc Natl Acad Sci USA* 1998;95:12663–12670.

Geis HR, and Borst JG. Intracellular responses of neurons in the mouse inferior colliculus to sinusoidal amplitude-modulated tones. *J Neurophysiol* 2009;101:2002–2016.

Giménez-Amaya JM. Afferent connections to the pontine nuclei from the cortex of the anterior ectosylvian sulcus in the cat. *Neurosci Lett* 1988;85:29–34.

Gonzalez Hernandez TH, Meyer G, and Ferres-Torres R. The commissural interconnections of the inferior colliculus in the albino mouse. *Brain Res* 1986;368:268–276.

Groff JA, and Liberman MC. Modulation of cochlear afferent response by the lateral olivocochlear system: activation via electrical stimulation of the inferior colliculus. *J Neurophysiol* 2003;90:3178–3200.

Guinan Jr JJ, Norris BE, Guinan SS. Single auditory units in the superior olivary complex. II: Locations of unit categories and tonotopic organization 1972;4:147–166.

Guinan Jr JJ, Li RY-S. Signal processing in brainstem auditory neurons which receive giant endings (calyces of Held) in the medial nucleus of the trapezoid body of the cat. *Hear Res* 1990;49:321–334.

Haenggeli CA, Pongstaporn T, Doucet JR, and Ryugo DK. Projections from the spinal trigeminal nucleus to the cochlear nucleus in the rat. *J Comp Neurol* 2005;484:191–205.

Hage SR, and Ehret G. Mapping responses to frequency sweeps and tones in the inferior colliculus of house mice. *Eur J Neurosci* 2003;18:2301–2312.

Harrison JM, and Warr WB. A study of the cochlear nuclei and ascending auditory pathways of the medulla. *J Comp Neurol* 1962;119:341–379.

Harrison JM, Warr WB, and Irving RE. Second order neurons in the acoustic nerve. *Science* 1962;138:893–895.

He J. Corticofugal modulation of the auditory thalamus. *Exp Brain Res* 2003;153:579–590.

He J, and Hu B. Differential distribution of burst and single-spike responses in auditory thalamus. *J Neurophysiol* 2002;88:2152–2156.
Heffner RS, Koay G, and Heffner HE. Audiograms of five species of rodents: implications for the evolution of hearing and the perception of pitch. *Hear Res* 2001;157:138–152.
Hefti BJ, and Smith PH. Anatomy, physiology, and synaptic responses of rat layer V auditory cortical cells and effects of intracellular GABA(A) blockade. *J Neurophysiol* 2000;83:2626–2638.
Held, H., 1893. Die centralem Bahnen des Nervus acusticus bei der Katz. *Arch Anat Abtheil* 15, 190–271.
Herbert H, Aschoff A, and Ostwald J. Topography of projections from the auditory cortex to the inferior colliculus in the rat. *J Comp Neurol* 1991;304:103–122.
Herkenham M. Laminar organization of thalamic projections to the rat neocortex. *Science* 1980;207:532–535.
Hernandez O, Rees A, and Malmierca MS. A GABAergic component in the commissure of the inferior colliculus in rat. *Neuroreport* 2006;17:1611–1614.
Herrnberger B, Kempf S, and Ehret G. Basic maps in the auditory midbrain. *Biol Cybern* 2002;87:231–240.
Hofstetter KM, and Ehret G. The auditory cortex of the mouse: connections of the ultrasonic field. *J Comp Neurol* 1992;323:370–386.
Hu B. Cellular basis of temporal synaptic signalling: an *in vitro* electrophysiological study in rat auditory thalamus. *J Physiol* 1995;483: (Pt 1),167–182.
Hu B. Functional organization of lemniscal and nonlemniscal auditory thalamus. *Exp Brain Res* 2003;153:543–549.
Ito M, van AB, and Kelly JB. Sound localization after transection of the commissure of Probst in the albino rat. *J Neurophysiol* 1996;76:3493–3502.
Iwahori N. A Golgi study on the dorsal nucleus of the lateral lemniscus in the mouse. *Neurosci Res* 1986;3:196–212.
Jeffress LA. A place theory of sound localization. *J Comp Physiol Psychol* 1948;1,35–39.
Johnstone BM, and Sellick PM. Dynamic changes in cochlear potentials and endolymph concentrations. *J Otolaryngol Soc Aust* 1972;3:317–319.
Jones EG. Chemically defined parallel pathways in the monkey auditory system 2003. *Ann N Y Acad Sci* 1999,218–233.
Jones EG. The Thalamus. Cambridge University Press, Cambridge 2007
Joris PX, Smith PH, and Yin TC. Coincidence detection in the auditory system: 50 years after Jeffress. *Neuron* 1998;21:1235–1238.
Kaas JH, and Hackett TA. Subdivisions of auditory cortex and processing streams in primates. *Proc Natl Acad Sci USA* 2000;97: 11793–11799.
Kanold PO, and Young ED. Proprioceptive information from the pinna provides somatosensory input to cat dorsal cochlear nucleus. *J Neurosci* 2001;21:7848–7858.
Kelly JB, Van Adel BA, and Ito M. Anatomical projections of the nuclei of the lateral lemmiscus in the albino rat (*Rattus norvegicus*). *J Comp Neurol* 2009;512:573–793.
Kelly JB and Caspry DM Pharmacology of the inferior colliculus. In Winer JA and Schreiner CE Eds. *The inferior colliculus.* New York: Springer; 2005:248–281.
Kelly JB, and Kidd SA. NMDA and AMPA receptors in the dorsal nucleus of the lateral lemniscus shape binaural responses in rat inferior colliculus. *J Neurophysiol* 2000;83:1403–1414.
Kelly JB, Li L, and van AB. Sound localization after kainic acid lesions of the dorsal nucleus of the lateral lemniscus in the albino rat. *Behav Neurosci* 1996;110:1445–1455.
Kiang NYS, Rho JM, Northrop CC, Liberman MC, and Ryugo DK. Hair-cell innervation by spiral ganglion cells in adult cats. *Science* 1982;217:175–177.
Kimura RS. The ultrastructure of the organ of Corti. *Int Rev Cytol* 1975;42:173–222.
King AJ, Jiang ZD, and Moore DR. Auditory brainstem projections to the ferret superior colliculus: anatomical contribution to the neural coding of sound azimuth. *J Comp Neurol* 1998;390:342–365.
Koay G, Heffner R, and Heffner H. Behavioral audiograms of homozygous med(*J*) mutant mice with sodium channel deficiency and unaffected controls. *Hear Res* 2002;171:111–118.
Kopp-Scheinpflug C, Fuchs K, Lippe WR, Tempel BL, and Rubsamen R. Decreased temporal precision of auditory signaling in Kcna1-null mice: an electrophysiological study in vivo. *J Neurosci* 2003;23:9199–9207.
Kopp-Scheinpflug C, Tolnai S, Malmierca MS, and Rubsamen R. The medial nucleus of the trapezoid body: comparative physiology. *Neuroscience* 2008;154:160–170.
Kulesza RJ, Jr Kadner A, and Berrebi AS. Distinct roles for glycine and GABA in shaping the response properties of neurons in the superior paraolivary nucleus of the rat. *J Neurophysiol* 2007;97:1610–1620.
Kuwabara N, and Zook JM. Geniculo-collicular descending projections in the gerbil. *Brain Res* 2000;878:79–87.
Kuwada S, Batra R, Yin TC, Oliver DL, Haberly LB, and Stanford TR. Intracellular recordings in response to monaural and binaural stimulation of neurons in the inferior colliculus of the cat. *J Neurosci* 1997;17:7565–7581.
Kuypers HG, and Lawrence DG. Cortical projections to the red nucleus and the brain stem in the Rhesus monkey. *Brain Res* 1967;4:151–188.
LeBeau FEN, Malmierca MS, and Rees A. Iontophoresis in vivo demonstrates a key role for GABAA- and glycinergic inhibition in shaping frequency response areas in the inferior colliculus of guinea pig. *J Neurosci* 2001;21,7303–7312.
LeDoux JE, Sakaguchi A, Iwata J, and Reis DJ. Auditory emotional memories: establishment by projections from the medial geniculate nucleus to the posterior neostriatum and/or dorsal amygdala. *Ann N Y Acad Sci* 1985;444:463–464.
Lee CC, Schreiner CE, Imaizumi K, and Winer JA. Tonotopic and heterotopic projection systems in physiologically defined auditory cortex. *Neuroscience* 2004;128:871–887.
Lee CC, and Sherman SM. Topography and physiology of ascending streams in the auditory tectothalamic pathway. *Proc Natl Acad Sci USA* 2009
Lee CC, and Winer JA. Connections of cat auditory cortex: II. Commissural system *J Comp Neurol* 2008;507:1901–1919.
Lee CC, and Winer JA. Principles governing auditory cortex connections. *Cereb Cortex* 2005;15:1804–1814.
Li L, and Kelly JB. Inhibitory influence of the dorsal nucleus of the lateral lemniscus on binaural responses in the rat's inferior colliculus. *J Neurosci* 1992;12:4530–4539.
Llano DA, and Sherman SM. Evidence for nonreciprocal organization of the mouse auditory thalamocortical-corticothalamic projection systems. *J Comp Neurol* 2008;507:1209–1227.
Llano DA, and Sherman SM. Differences in intrinsic properties and local network connectivity of identified layer 5 and layer 6 adult mouse auditory corticothalamic neurons support a dual corticothalamic projection hypothesis. *Cereb Cortex* 2009;19:2810–2826.
Loftus WC, Malmierca MS, Bishop DC, and Oliver DL. The cytoarchitecture of the inferior colliculus revisited: a common organization of the lateral cortex in rat and cat. *Neuroscience* 2008;154:196–205.
Lopez DE, Saldana E, Nodal FR, Merchan MA, and Warr WB. Projections of cochlear root neurons, sentinels of the rat auditory pathway. *J Comp Neurol* 1999;415:160–174.
Lorente de Nó, R. Anatomy of the eight nerve. III General plan of structure of the primary cochlear nuclei. *Laryngoscope* 1933;43:327–350.
Lorente de Nó, R. *The primary acoustic nuclei.* New York :Raven Press; 1981

Lu E, Llano DA, and Sherman SM. Different distributions of calbindin and calretinin immunostaining across the medial and dorsal divisions of the mouse medial geniculate body. *Hear Res* 2009;257:16–23.

Ma X, and Suga N. Lateral inhibition for center-surround reorganization of the frequency map of bat auditory cortex. *J Neurophysiol* 2004;92:3192–3199.

Ma X, and Suga N. Multiparametric corticofugal modulation of collicular duration-tuned neurons: modulation in the amplitude domain. *J Neurophysiol* 2007;97:3722–3730.

Maison SF, Adams JC, and Liberman MC. Olivocochlear innervation in the mouse: immunocytochemical maps, crossed versus uncrossed contributions, and transmitter colocalization. *J Comp Neurol* 2003;455:406–416.

Maison SF, Vetter DE, and Liberman MC. A novel effect of cochlear efferents: in vivo response enhancement does not require alpha9 cholinergic receptors. *J Neurophysiol* 2007;97:3269–3278.

Malmierca MS. The structure and physiology of the rat auditory system: an overview. *Int Rev Neurobiol* 2003;56:147–211.

Malmierca MS, Blackstad TW, Osen KK, Karagulle T, and Molowny RL. The central nucleus of the inferior colliculus in rat: a Golgi and computer reconstruction study of neuronal and laminar structure. *J Comp Neurol* 1993;333:1–27.

Malmierca MS, Cristaudo S, Perez-Gonzalez D, and Covey E. Stimulus-specific adaptation in the inferior colliculus of the anesthetized rat. *J Neurosci* 2009;29:5483–5493.

Malmierca M.S. and Hackett T. Structural Organization of the ascending audiotory pathway. In Palmer AR and Rees A Eds. Auditory Brain OUP Handbook. Oxford: Oxford University Press; 2010. In press.

Malmierca MS, Hernandez O, Falconi A, Lopez-Poveda EA, Merchan M, and Rees A. The commissure of the inferior colliculus shapes frequency response areas in rat: an in vivo study using reversible blockade with microinjection of kynurenic acid. *Exp Brain Res* 2003;153:522–529.

Malmierca MS, Le Beau FE, and Rees A. The topographical organization of descending projections from the central nucleus of the inferior colliculus in guinea pig. *Hear Res* 1996;93:167–180.

Malmierca MS, Merchan MA. Auditory system. In Paxinos G, Ed. *The rat nervous system.* San Diego: Academic Press; 2004:997–1082

Malmierca MS, Merchan MA, Henkel CK, and Oliver DL. Direct projections from cochlear nuclear complex to auditory thalamus in the rat. *J Neurosci* 2002;22:10891–10897.

Malmierca MS, Rees A, Le Beau FE, and Bjaalie JG. Laminar organization of frequency-defined local axons within and between the inferior colliculi of the guinea pig. *J Comp Neurol* 1995;357:124–144.

Malmierca MS, and Ryugo DK. Cortical descending projections to auditory midbrain and brainstem. In Winer JA and Schreiner CE Eds. *The Auditory Cortex*. New York: Springer; 2010.

Malmierca MS, Hernandez O, and Rees A. Intercollicular commissural projections modulate neuronal responses in the inferior colliculus. *Eur J Neurosci* 2005a;21:2701–2710.

Malmierca MS, Saint Marie RL, Merchan MA, and Oliver DL. Laminar inputs from dorsal cochlear nucleus and ventral cochlear nucleus to the central nucleus of the inferior colliculus: two patterns of convergence. *Neuroscience* 2005b;136:883–894.

Markin VS, and Hudspeth AJ. Gating-spring models of mechanoelectrical transduction by hair cells of the internal ear. *Annu Rev Biophys Biomol Struct* 1995;24:59–83.

Masterton B, Thompson GC, Bechtold JK, and RoBards MJ. Neuroanatomical basis of binaural phase-difference analysis for sound localization: a comparative study. *J Comp Physiol Psychol* 1975;89:379–386.

May BJ, Prosen CA, Weiss D, and Vetter D. Behavioral investigation of some possible effects of the central olivocochlear pathways in transgenic mice. *Hear Res* 2002;171:142–157.

McCormick DA, Connors BW, Lighthall JW, and Prince DA. Comparative electrophysiology of pyramidal and sparsely spiny stellate neurons of the neocortex. *J Neurophysiol* 1985;54:782–806.

McMullen NT, Velenovsky DS, Holmes MG. Auditory thalamic organization: cellular slabs, dendritic arbors and tectothalamic axons underlying the frequency map. *Neuroscience* 2005;136: 927–943.

Meininger V, Pol D, and Derer P. The inferior colliculus of the mouse. A Nissl and Golgi study *Neuroscience* 1986;17:1159–1179.

Meltzer NE, and Ryugo DK. Projections from auditory cortex to cochlear nucleus: A comparative analysis of rat and mouse. *Anat Rec A Discov Mol Cell Evol Biol* 2006;288:397–408.

Merchan MA, and Berbel P. Anatomy of the ventral nucleus of the lateral lemniscus in rats: a nucleus with a concentric laminar organization. *J Comp Neurol* 1996;372:245–263.

Merchan MA, Collia F, Lopez DE, and Saldana E. Morphology of cochlear root neurons in the rat. *J Neurocytol* 1988;17:711–725.

Mikaelian DO. Development and degeneration of hearing in the C57/b16 mouse: relation of electrophysiologic responses from the round window and cochlear nucleus to cochlear anatomy and behavioral responses. *Laryngoscope* 1979;89:1–15.

Mitani A, Shimokouchi M, and Nomura S. Effects of stimulation of the primary auditory cortex upon colliculogeniculate neurons in the inferior colliculus of the cat. *Neurosci Lett* 1983;42:185–189.

Moore JK, and Osen KK. The cochlear nuclei in man. *Am J Anat* 1979;154:393–418.

Moore JK, Osen KK, Storm-Mathisen J, and Ottersen OP. gamma-Aminobutyric acid and glycine in the baboon cochlear nuclei: an immunocytochemical colocalization study with reference to interspecies differences in inhibitory systems. *J Comp Neurol* 1996;369:497–519.

Moore MJ, and Caspary DM. Strychnine blocks binaural inhibition in lateral superior olivary neurons. *J Neurosci* 1983;3:237–242.

Morest DK. Auditory neurons of the brain stem. *Adv Otorhinolaryngol* 1973;20:337–356.

Morest DK, and Oliver DL. The neuronal architecture of the inferior colliculus in the cat: defining the functional anatomy of the auditory midbrain. *J Comp Neurol* 1984;222:209–236.

Mugnaini E, Osen KK, Dahl AL, Friedrich VL, Jr and Korte G. Fine structure of granule cells and related interneurons (termed Golgi cells) in the cochlear nuclear complex of cat, rat and mouse. *J Neurocytol* 1980a;9:537–570.

Mugnaini E, Warr WB, and Osen KK. Distribution and light microscopic features of granule cells in the cochlear nuclei of cat, rat, and mouse. *J Comp Neurol* 1980b;191:581–606.

Mulders WH, and Robertson D. Diverse responses of single auditory afferent fibres to electrical stimulation of the inferior colliculus in guinea-pig. *Exp Brain Res* 2005;160:235–244.

Mulders WH, and Robertson D. Evidence for direct cortical innervation of medical olivocochlear newones in rats. *Hear Res* 2000;144:65–72.

Nayagam DA, Clarey JC, and Paolini AG. Intracellular responses and morphology of rat ventral complex of the lateral lemniscus neurons in vivo. *J Comp Neurol* 2006;498:295–315.

Newlands SD, and Perachio AA. Central projections of the vestibular nerve: a review and single fiber study in the Mongolian gerbil. *Brain Res Bull* 2003;60:475–495.

Nobili R, Mammano F, and Ashmore J. How well do we understand the cochlea? *Trends Neurosci*. 1998;21:159–167.

Nodal FR, and Lopez DE. Direct input from cochlear root neurons to pontine reticulospinal neurons in albino rat. *J Comp Neurol* 2003;460:80–93.

Nwabueze-Ogbo FC, Popelar J, and Syka J. Changes in the acoustically evoked activity in the inferior colliculus of the rat after

functional ablation of the auditory cortex. *Physiol Res* 2002;51 Suppl 1,S95–S104.
Oertel D, and Wu SH. Morphology and physiology of cells in slice preparations of the dorsal cochlear nucleus of mice. *J Comp Neurol* 1989;283:228–247.
Oertel D, Wu SH, Garb MW, and Dizack C. Morphology and physiology of cells in slice preparations of the posteroventral cochlear nucleus of mice. *J Comp Neurol* 1990;295:136–154.
Oertel D, and Young ED. What's a cerebellar circuit doing in the auditory system? *Trends Neurosci* 2004;27:104–110.
Ohlrogge M, Doucet JR, and Ryugo DK. Projections of the pontine nuclei to the cochlear nucleus in rats. *J Comp Neurol* 2001;436:290–303.
Oliver DL. Neuronal organization of the inferior colliculus. In Winer JA and Schreiner CE Eds. *The Auditory Cortex*. New York :Springer; 2005:69–114.
Oliver DL, and Morest DK. The central nucleus of the inferior colliculus in the cat. *J Comp Neurol* 1984;222:237–264.
Ollo C, and Schwartz IR. The superior olivary complex in C57BL/6 mice. *Am J Anat* 1979;155:349–373.
Osen KK. Cytoarchitecture of the cochlear nuclei in the cat. *J Comp Neurol* 1969;136:453–484.
Osen KK, Lopez DE, Slyngstad TA, Ottersen OP, and Storm-Mathisen *J*. GABA-like and glycine-like immunoreactivities of the cochlear root nucleus in rat. *J Neurocytol* 1991;20:17–25.
Osen KK, Mugnaini E, Dahl AL, and Christiansen AH. Histochemical localization of acetylcholinesterase in the cochlear and superior olivary nuclei. A reappraisal with emphasis on the cochlear granule cell system. *Arch Ital Biol* 1984;122:169–212.
Osen, K.K., Ottersen, O.P., and Storm-Mathisen, *J*., Colocalization of glicine-like and GABA-like inmunoreactivities, a semiquantitative study of individual neurons in the dorsal cochlear nucleus of cat. In. Ottersen OP and Storm-Mathisen J. Eds. *Glycine Neurotransmission.* Chichester: Wiley; 1990:417–451.
Osen KK, Storm-Mathisen *J*, Ottersen OP, and Dihle B. Glutamate is concentrated in and released from parallel fiber terminals in the dorsal cochlear nucleus: a quantitative immunocytochemical analysis in guinea pig. *J Comp Neurol* 1995;357:482–500.
Ota Y, Oliver DL, and Dolan DF. Frequency-specific effects on cochlear responses during activation of the inferior colliculus in the Guinea pig. *J Neurophysiol* 2004;91:2185–2193.
Palmer AR, Wallace MN, Arnott RH, and Shackleton TM. Morphology of physiologically characterised ventral cochlear nucleus stellate cells. *Exp Brain Res* 2003;153:418–426.
Paula-Barbosa MM, and Sousa-Pinto A. Auditory cortical projections to the superior colliculus in the cat. *Brain Res* 1973;50:47–61.
Perales M, Winer JA, and Prieto JJ. Focal projections of cat auditory cortex to the pontine nuclei. *J Comp Neurol* 2006;497:959–980.
Perez-Gonzalez D, Malmierca MS, and Covey E. Novelty detector neurons in the mammalian auditory midbrain. *Eur J Neurosci* 2005;22:2879–2885.
Peruzzi D, Bartlett E, Smith PH, and Oliver DL. A monosynaptic GABAergic input from the inferior colliculus to the medial geniculate body in rat. *J Neurosci* 1997;17:3766–3777.
Portfors CV, and Felix RA. Spectral integration in the inferior colliculus of the CBA/CaJ mouse. *Neuroscience* 2005;136:1159–1170.
Portfors CV, and Roberts PD. Temporal and frequency characteristics of cartwheel cells in the dorsal cochlear nucleus of the awake mouse. *J Neurophysiol* 2007;98:744–756.
Portfors CV, Roberts PD, and Jonson K. Over-representation of species-specific vocalizations in the awake mouse inferior colliculus. *Neuroscience* 2009;162:486–500.
Potashner SJ, Dymczyk L, and Deangelis MM. D-aspartate uptake and release in the guinea pig spinal cord after partial ablation of the cerebral cortex. *J Neurochem* 1988;50:103–111.
Prosen CA, Bath KG, Vetter DE, and May BJ. Behavioral assessments of auditory sensitivity in transgenic mice. *J Neurosci Methods* 2000;97:59–67.
Rajan R. Electrical stimulation of the inferior colliculus at low rates protects the cochlea from auditory desensitization. *Brain Res* 1990;506:192–204.
Rajan, R. Centrifugal pathways protect hearing sensitivity at the cochlea in noisy environments that exacerbate the damage induced by loud sound. *J Neurosci* 2000;20:6684–6693.
Ramón y Cajal S. *Histología del Sistema Nervioso del Hombre y los Vertebrados*. Imprenta N. Moya., Madrid; 1904
Ramón y Cajal S. *Histologie du système nerveux de l'homme et des vértébrates.* Trans Azoulay L. Maloine, Paris (reprinted in 1972 by Consejo Superior de Investigaciones Científicas, CSIC. Madrid); 1909
Rasmusen GL. The olivary peduncle and other fiber projections of the superior olivary complex. *J Comp Neurol* 1946;84:61–74.
Rasmusen GL. Studies of the VIIIth cranial nerve of man. Laryngoscope 1940;50:67–83.
Rauschecker JP, and Tian B. Mechanisms and streams for processing of "what" and "where" in auditory cortex. *Proc Natl Acad Sci* USA 2000;97:11800–11806.
Reetz G, and Ehret G. Inputs from three brainstem sources to identified neurons of the mouse inferior colliculus slice. *Brain Res* 1999;816:527–543.
Reimer K. Simultaneous demonstration of Fos–like immunoreactivity and 2-deoxy-glucose uptake in the inferior colliculus of the mouse. *Brain Res* 1993;616:339–343.
Rhode WS. Cochlear mechanics. *Annu Rev Physiol* 1984;46:231–246.
Rhode WS. Vertical cell responses to sound in cat dorsal cochlear nucleus. *J Neurophysiol* 1999;82:1019–1032.
Riquelme R, Saldana E, Osen KK, Ottersen OP, and Merchan MA. Colocalization of GABA and glycine in the ventral nucleus of the lateral lemniscus in rat: an in situ hybridization and semiquantitative immunocytochemical study. *J Comp Neurol* 2001;432:409–424.
RoBards MJ. Somatic neurons in the brainstem and neocortex projecting to the external nucleus of the inferior colliculus: anatomical study in the opossum. *J Comp Neurol* 1979;184:547–566.
Robertson, D. Centrifugal control in mammalian hearing. *Clin Exp Pharmacol Physiol* 2009;36,603–611.
Romanski LM, and LeDoux JE. Information cascade from primary auditory cortex to the amygdala: corticocortical and corticoamygdaloid projections of temporal cortex in the rat. *Cereb Cortex* 1993;3:515–532.
Rosenbluth J. The fine structure of acoustic ganglia in the rat. *J Cell Biol* 1962;12:329–359.
Rubio ME, Gudsnuk KA, Smith Y, and Ryugo DK. Revealing the molecular layer of the primate dorsal cochlear nucleus. *Neuroscience* 2008;154:99–113.
Russell IJ. Origin of the receptor potential in inner hair cells of the mammalian cochlea-–evidence for Davis' theory. *Nature* 1983;301:334–336.
Ryugo DK. Projections of low spontaneous rate, high threshold auditory nerve fibers to the small cell cap of the cochlear nucleus in cats. *Neuroscience* 2008;154:114–126.
Ryugo, D.K., The auditory nerve, Peripheral innervation, cell body morphology, and central projections. In: Webster DB, Popper AN, and Fay RR. Eds. *The Mammalian Auditory Pathway, Neuroanatomy.* Berlin: Springer-Verlag; 1992:23–65.
Ryugo DK, and Killackey HP. Differential telencephalic projections of the medial and ventral divisions of the medial geniculate body of the rat. *Brain Res* 1974;82:173–177.

Ryugo DK, May SK. The projections of intracellularly labeled auditory nerve fibers to the dorsal cochlear nucleus of cats. *J Comp Neurol* 1993;329:20–35.

Ryugo DK, and Parks TN. Primary innervation of the avian and mammalian cochlear nucleus. *Brain Res Bull* 2003;60:435–456.

Ryugo DK, and Weinberger NM. Corticofugal modulation of the medial geniculate body. *Exp Neurol* 1976;51:377–391.

Ryugo DK, and Weinberger NM. Differential plasticity of morphologically distinct neuron populations in the medical geniculate body of the cat during classical conditioning. *Behav Biol* 1978;22:275–301.

Ryugo DK, and Willard FH. The dorsal cochlear nucleus of the mouse: a light microscopic analysis of neurons that project to the inferior colliculus. *J Comp Neurol* 1985;242:381–396.

Ryugo DK, Willard FH, and Fekete DM. Differential afferent projections to the inferior colliculus from the cochlear nucleus in the albino mouse. *Brain Res* 1981;210:342–349.

Safieddine S, and Eybalin M. Triple Immunofluorescence Evidence for the Coexistence of Acetylcholine, Enkephalins and Calcitonin Gene-related Peptide Within Efferent (Olivocochlear) Neurons of Rats and Guinea-pigs. *Eur J Neurosci* 1992;4:981–992.

Safieddine S, Prior AM, and Eybalin M. Choline acetyltransferase, glutamate decarboxylase, tyrosine hydroxylase, calcitonin gene-related peptide and opioid peptides coexist in lateral efferent neurons of rat and guinea-pig. *Eur J Neurosci* 1997;9:356–367.

Saint Marie RL, and Baker RA. Neurotransmitter-specific uptake and retrograde transport of [3H]glycine from the inferior colliculus by ipsilateral projections of the superior olivary complex and nuclei of the lateral lemniscus. *Brain Res* 1990;524:244–253.

Saint Marie RL, Ostapoff EM, Morest DK, and Wenthold RJ. Glycine-immunoreactive projection of the cat lateral superior olive: possible role in midbrain ear dominance. *J Comp Neurol* 1989;279:382–396.

Saldana E, Feliciano M, and Mugnaini E. Distribution of descending projections from primary auditory neocortex to inferior colliculus mimics the topography of intracollicular projections. *J Comp Neurol* 1996;371:15–40.

Saldana E, and Merchan MA. Intrinsic and commissural connections of the rat inferior colliculus. *J Comp Neurol* 1992;319:417–437.

Scheibel ME, and Scheibel AB. Neuropil organization in the superior olive of the cat. *Exp Neurol* 1974;43:339–348.

Schofield BR. Superior paraolivary nucleus in the pigmented guinea pig: separate classes of neurons project to the inferior colliculus and the cochlear nucleus. *J Comp Neurol* 1991;312:68–76.

Senatorov VV, and Hu B. Extracortical descending projections to the rat inferior colliculus. *Neuroscience* 2002;115:243–250.

Sherman SM, and Guillery RW. Functional organization of thalamocortical relays. *J Neurophysiol* 1996;76:1367–1395.

Sherman SM, and Guillery RW. On the actions that one nerve cell can have on another: distinguishing "drivers" from "modulators". *Proc Natl Acad Sci USA* 1998;95:7121–7126.

Sherman SM, and Guillery RW. The role of the thalamus in the flow of information to the cortex. *Philos Trans R Soc Lond B Biol Sci* 2002;357:1695–1708.

Shneiderman A, and Henkel CK. Banding of lateral superior olivary nucleus afferents in the inferior colliculus: a possible substrate for sensory integration. *J Comp Neurol* 1987;266:519–534.

Sinex DG, Lopez DE, and Warr WB. Electrophysiological responses of cochlear root neurons. *Hear Res* 2001;158:28–38.

Sivaramakrishnan S, and Oliver DL. Distinct K currents result in physiologically distinct cell types in the inferior colliculus of the rat. *J Neurosci* 2001;21:2861–2877.

Sivaramakrishnan S, and Oliver DL. Neuronal responses to lemniscal stimulation in laminar brain slices of the inferior colliculus. *J Assoc Res Otolaryngol* 2006;7:1–14.

Slepecky, N.B., Structure of the mammalian cochlea. In: Dallos, P.P.A.N.a.F.R.R. Ed. *The cochlea: Springer Handbook of Auditory Research.* New York: Springer Verlag; 1996:44–129.

Smith PH. Structural and functional differences distinguish principal from nonprincipal cells in the guinea pig MSO slice. *J Neurophysiol* 1995;73:1653–1667.

Smith PH, and Rhode WS. Structural and functional properties distinguish two types of multipolar cells in the ventral cochlear nucleus. *J Comp Neurol* 1989;282:595–616.

Spangler KM, Warr WB, and Henkel CK. The projections of principal cells of the medial nucleus of the trapezoid body in the cat. *J Comp Neurol* 1985;238:249–262.

Spirou GA, May BJ, Wright DD, and Ryugo DK. Frequency organization of the dorsal cochlear nucleus in cats. *J Comp Neurol* 1993;329:36–52.

Spoendlin H. The innervation of the organ of Corti. *J Laryngol Otol* 1967;81:717–738.

Spoendlin H. Innervation densities of the cochlea. *Acta Otolaryngol* 1972;73:235–248.

Steel KP. Inherited hearing defects in mice. *Annu Rev Genet* 1995;29:675–701.

Stiebler I, and Ehret G. Inferior colliculus of the house mouse. I A quantitative study of tonotopic organization, frequency representation, and tone-threshold distribution *J Comp Neurol* 1985;238:65–76.

Stiebler I, Neulist R, Fichtel I, and Ehret G. The auditory cortex of the house mouse: left-right differences, tonotopic organization and quantitative analysis of frequency representation. *J Comp Physiol A* 1997;181:559–571.

Stotler WA. An experimental study of the cells and connections of the superior olivary complex of the cat. *J Comp Neurol* 1953;98:401–432.

Tan ML, and Borst JG. Comparison of responses of neurons in the mouse inferior colliculus to current injections, tones of different durations, and sinusoidal amplitude-modulated tones. *J Neurophysiol* 2007;98:454–466.

Tan ML, Theeuwes HP, Feenstra L, and Borst JG. Membrane properties and firing patterns of inferior colliculus neurons: an in vivo patch-clamp study in rodents. *J Neurophysiol* 2007;98:443–453.

Taranda J, Maison SF, Ballestero JA, et al. A point mutation in the hair cell nicotinic cholinergic receptor prolongs cochlear inhibition and enhances noise protection. *PLoS Biol* 7, e18;2009

Thompson AM, and Schofield BR. Afferent projections of the superior olivary complex. Microsc *Res Tech* 2000;51:330–354.

Vetter DE, and Mugnaini E. Distribution and dendritic features of three groups of rat olivocochlear neurons. A study with two retrograde cholera toxin tracers. *Anat Embryol (Berl)* 1992;185:1–16.

Vetter DE, Saldana E, and Mugnaini E. Input from the inferior colliculus to medial olivocochlear neurons in the rat: a double label study with PHA-L and cholera toxin. *Hear Res* 1993;70:173–186.

Volman SF, and Konishi M. Comparative physiology of sound localization in four species of owls. *Brain Behav Evol* 1990;36:196–215.

von Bèkèsy G. *Experiments in Hearing*. New York: McGraw-Hill; 1960.

Warr, W.B., Organization of olivocochlear efferent systems in mammals. In: Webster, D.B.P.A.N.F.R.R. Ed. The Mammalian Auditory Pathway, Neuroanatomy. Berlin: Springer-Verlag; 1992: 410–448.

Warr WB, and Beck JE. Multiple projections from the ventral nucleus of the trapezoid body in the rat. *Hear Res* 1996;93:83–101.

Warr WB, Boche JB, and Neely ST. Efferent innervation of the inner hair cell region: origins and terminations of two lateral olivocochlear systems. *Hear Res* 1997;108:89–111.

Warr WB, and Guinan JJ, Jr. Efferent innervation of the organ of corti: two separate systems. *Brain Res* 1979;173:152–155.

Watanabe T, Yanagisawa K, Kanzaki J, and Katsuki Y. Cortical efferent flow influencing unit responses of medial geniculate body to sound stimulation. *Exp Brain Res* 1966;2:302–317.

Webster DB, Trune DR. Cochlear nuclear complex of mice. *Am J Anat* 1982;163:103–130.

Weedman DL, Pongstaporn T, and Ryugo DK. Ultrastructural study of the granule cell domain of the cochlear nucleus in rats: mossy fiber endings and their targets. *J Comp Neurol* 1996;369:345–360.

Weedman DL, and Ryugo DK. Projections from auditory cortex to the cochlear nucleus in rats: synapses on granule cell dendrites. *J Comp Neurol* 1996;371:311–324.

Wepsic JG. Multimodal sensory activation of cells in the magnocellular medial geniculate nucleus. *Exp Neurol* 1966;15:299–318.

White JS, and Warr WB. The dual origins of the olivocochlear bundle in the albino rat. *J Comp Neurol* 1983;219:203–214.

Wickesberg RE, and Oertel D. Tonotopic projection from the dorsal to the anteroventral cochlear nucleus of mice. *J Comp Neurol* 1988;268:389–399.

Willard, F.H. and Ryugo, D.K., Anatomy of the central auditory system. In: Willott, JF Ed. *The Auditory Psychobiology of the Mouse*. Springfield, IL:Charles C. Thomas Publishers; 1983:201–304.

Willott JF. *The Auditory Psychobiology of the Mouse*. Springfield, IL:Charles C. Thomas Publishers; 1983

Willott JF. Effects of aging, hearing loss, and anatomical location on thresholds of inferior colliculus neurons in C57BL/6 and CBA mice. *J europhysiol* 1986;56:391–408.

Willott JF, Hnath CT, and Lister JJ. Modulation of presbycusis: current status and future directions. *Audiol Neurootol* 2001;6:231–249.

Wilson JL, Henson MM, and Henson OW, Jr. Course and distribution of efferent fibers in the cochlea of the mouse. *Hear Res* 1991;55:98–108.

Winer JA. Decoding the auditory corticofugal systems. *Hear Res* 2006;212:1–8.

Winer, JA, The functional architecture of the medial geniculate body and the primary auditory cortex. In: Webster, D.B.P.A.N.F.R.R. Ed. *The Mammalian Auditory Pathway, Neuroanatomy.* Berlin: Springer-Verlag; 1992:222–409.

Winer JA, Kelly JB, and Larue DT. Neural architecture of the rat medial geniculate body. *Hear Res* 1999;130:19–41.

Winer JA, and Larue DT. Evolution of GABAergic circuitry in the mammalian medial geniculate body. *Proc Natl Acad Sci USA* 1996;93:3083–3087.

Winer JA, Larue DT, Diehl JJ, and Hefti BJ. Auditory cortical projections to the cat inferior colliculus. *J Comp Neurol* 1998;400:147–174.

Winer JA, and Lee CC. The distributed auditory cortex. *Hear Res* 2007;229:3–13.

Winer JA, Miller LM, Lee CC, and Schreiner CE. Auditory thalamocortical transformation: structure and function. *Trends Neurosci* 2005;28:255–263.

Wright DD, and Ryugo DK. Mossy fiber projections from the cuneate nucleus to the cochlear nucleus in the rat. *J Comp Neurol* 1996;365:159–172.

Wu SH. Physiological properties of neurons in the ventral nucleus of the lateral lemniscus of the rat: intrinsic membrane properties and synaptic responses. *J Neurophysiol* 1999;81:2862–2874.

Wu SH, and Kelly JB. *In vitro* brain slice studies of the rat's dorsal nucleus of the lateral lemniscus. I Membrane and synaptic response properties. *J Neurophysiol* 1995b;73:780–793.

Wu SH, and Kelly JB. *In vitro* brain slice studies of the rat's dorsal nucleus of the lateral lemniscus. II Physiological properties of biocytin-labeled neurons. *J Neurophysiol* 1995c;73:794–809.

Wu SH, and Kelly JB. *In vitro* brain slice studies of the rat's dorsal nucleus of the lateral lemniscus. III synaptic pharmacology. *J Neurophysiol* 1996;75:1271–1282.

Wu SH, and Kelly JB. Binaural interaction in the lateral superior olive: time difference sensitivity studied in mouse brain slice. *J Neurophysiol* 1992a;68:1151–1159.

Wu SH, and Kelly JB. NMDA, non-NMDA and glycine receptors mediate binaural interaction in the lateral superior olive: physiological evidence from mouse brain slice. *Neurosci Lett* 1992b;134:257–260.

Wu SH, and Kelly JB. Synaptic pharmacology of the superior olivary complex studied in mouse brain slice. *J Neurosci* 1992c;12:3084–3097.

Wu SH, and Kelly JB. Response of neurons in the lateral superior olive and medial nucleus of the trapezoid body to repetitive stimulation: intracellular and extracellular recordings from mouse brain slice. *Hear Res* 1993;68:189–201.

Wu SH, and Kelly JB. Physiological evidence for ipsilateral inhibition in the lateral superior olive: synaptic responses in mouse brain slice. *Hear Res* 1994;73:57–64.

Wu SH, and Kelly JB. *In vitro* brain slice studies of the rat's dorsal nucleus of the lateral lemniscus. I Membrane and synaptic response properties *J Neurophysiol* 1995a;73:780–793.

Wu Y, and Yan J. Modulation of the receptive fields of midbrain neurons elicited by thalamic electrical stimulation through corticofugal feedback. *J Neurosci* 2007;27:10651–10658.

Yan J, and Ehret G. Corticofugal reorganization of the midbrain tonotopic map in mice. *Neuroreport* 2001;12:3313–3316.

Yan J, and Ehret G. Corticofugal modulation of midbrain sound processing in the house mouse. *Eur J Neurosci* 2002;16:119–128.

Yan J, and Zhang Y. Sound-guided shaping of the receptive field in the mouse auditory cortex by basal forebrain activation. *Eur J Neurosci* 2005;21:563–576.

Yan J, Zhang Y, and Ehret G. Corticofugal shaping of frequency tuning curves in the central nucleus of the inferior colliculus of mice. *J Neurophysiol* 2004;93:71–83.

Yan W, and Suga N. Corticofugal modulation of the midbrain frequency map in the bat auditory system. *Nat Neurosci* 1998;1:54–58.

Ye Y, Machado DG, and Kim DO. Projection of the marginal shell of the anteroventral cochlear nucleus to olivocochlear neurons in the cat. *J Comp Neurol* 2000;420:127–138.

Young ED, Robert JM, and Shofner WP. Regularity and latency of units in ventral cochlear nucleus: implications for unit classification and generation of response properties. *J Neurophysiol* 1988a;60:1–29.

Young, E.D., Shofner, W.P., White, J.A., Robert, J.M., and Voigh H., Response properties of cochlear nucleus neurons in relationship to physiological mechanisms. In: Edelman, G.M.G.W.E.a.C.W.M. Ed. *Auditory Function. Neurobiological Bases of Hearing.* New York: Wiley; 1988b:277–312.

Zhan X, and Ryugo DK. Projections of the lateral reticular nucleus to the cochlear nucleus in rats. *J Comp Neurol* 2007;504:583–598.

Zhang DX, Li L, Kelly JB, and Wu SH. GABAergic projections from the lateral lemniscus to the inferior colliculus of the rat. *Hear Res* 1998;117:1–12.

Zhang Y, Suga N, and Yan J. Corticofugal modulation of frequency processing in bat auditory system. *Nature* 1997;387:900–903.

Zhao M, and Wu SH. Morphology and physiology of neurons in the ventral nucleus of the lateral lemniscus in rat brain slices. *J Comp Neurol* 2001;433:255–271.

Zhou J, Nannapaneni N, and Shore S. Vesicular glutamate transporters 1 and 2 are differentially associated with auditory nerve and spinal trigeminal inputs to the cochlear nucleus. *J comp Neurol* 2007;500:777–787.

Zhou J, and Shore S. Convergence of spinal trigeminal and cochlear nucleus projections in the inferior colliculus of the guinea pig. *J Comp Neurol* 2006;495:100–112.

Zook JM, and Casseday JH. Cytoarchitecture of auditory system in lower brainstem of the mustache bat, Pteronotus parnellii. *J Comp Neurol* 1982;207:1–13.

Zook JM, and Casseday JH. Projections from the cochlear nuclei in the mustache bat, Pteronotus parnellii. *J Comp Neurol* 1985;237:307–324.

Zook JM, and Casseday JH. Convergence of ascending pathways at the inferior colliculus of the mustache bat, Pteronotus parnellii. *J Comp Neurol* 1987;261:347–361.